

Doctoral thesis

Doctoral theses at NTNU, 2021:351

Jorge Mendoza Espinosa

Integrated design and maintenance of deteriorating structural systems

NTNU
Norwegian University of Science and Technology
Thesis for the Degree of
Philosophiae Doctor
Faculty of Engineering
Department of Structural Engineering



Norwegian University of
Science and Technology

Jorge Mendoza Espinosa

Integrated design and maintenance of deteriorating structural systems

Thesis for the Degree of Philosophiae Doctor

Trondheim, November 2021

Norwegian University of Science and Technology
Faculty of Engineering
Department of Structural Engineering



Norwegian University of
Science and Technology

NTNU

Norwegian University of Science and Technology

Thesis for the Degree of Philosophiae Doctor

Faculty of Engineering

Department of Structural Engineering

© Jorge Mendoza Espinosa

ISBN 978-82-326-6608-9 (printed ver.)

ISBN 978-82-326-6954-7 (electronic ver.)

ISSN 1503-8181 (printed ver.)

ISSN 2703-8084 (online ver.)

Doctoral theses at NTNU, 2021:351

Printed by NTNU Grafisk senter

Preface

This doctoral dissertation is submitted in partial fulfilment of the requirements of the degree of Philosophiae Doctor (Ph.D.) at the Faculty of Engineering of the Norwegian University of Science and Technology (NTNU). The research was conducted at the Department of Structural Engineering at NTNU in Trondheim, Norway.

The project was funded by the Department of Structural Engineering at NTNU. The project started in November 2017 and the thesis was submitted in September 2021. In addition to the conducted research, the funding included one-year worth of teaching assistance activities. This time was spread over the first three years (2017-2020) and it was dedicated to the assistance in the lecturing of two courses, TKT4196 - Aspects of structural safety and TBA4125 - Prosjektering, and to the co-supervision of four MSc projects and three MSc theses.

The main supervisor of my doctoral studies was Jochen Köhler and the co-supervisor was Michael Muskulus. Both supervisors are professors at NTNU, Trondheim.

This doctoral dissertation is a collection of scientific papers. This means that the main research outcomes have been published or submitted for publication in peer-reviewed scientific journals and the dissertation guides the interested reader through the context and research methodology of the conducted investigations.

Jorge Mendoza Espinosa
Norwegian University of Science and Technology
Trondheim, September 9th, 2021

Abstract

Large structural systems such as bridges and offshore structures are subject to deterioration processes during their service life. Specifically, fatigue and corrosion are of major concern. To ensure that the structures are operated within acceptable safety levels, actions to mitigate the risks associated with deterioration need to be conducted throughout their life cycle. Examples of mitigation actions are to increase the reliability of the deterioration-sensitive components at design (e.g., by increasing their resisting cross-section area), to choose more robust structural configurations to minimise the consequences of deterioration, and to repair structural components based on identified damage. Generally, the optimal mitigation strategy will be a combination of several mitigation measures. The limited societal budgets and the increasing environmental concerns demand an efficient use of the construction materials. To efficiently manage the large portfolios of existing and planned infrastructure systems, the decisions made throughout the life cycle of the structures need to be optimised within a common framework.

The aim of this thesis is to improve the design basis of mitigation strategies for structural systems. Structural reliability methods are used to assess the effect of the mitigation measures on structural safety. At the design phase, the effect of future inspections and monitoring on the system reliability can be estimated by integrating over possible outcomes using prior information. Similarly, one can perform the same integration at any stage of the service life based on information updated with obtained data. Reliability- and risk-based design are applied to the assessment of the optimal mitigation strategies at the system level. System-level design is of particular relevance for the present research, because aspects such as spatial dependence of the deterioration processes or structural redundancy have a strong effect on the system reliability and the value of the information that can be obtained.

A framework for simultaneously assessing optimal design and inspection strategies is developed. This framework is then applied to the investigation of how the optimal mitigation strategy varies as a function of system redundancy and size. These results aim at generalising decision rules for the standardisation of mitigation strategies. Moreover, a novel method for assessing system reliability bounds of multimember offshore structures subject to extreme environmental loads and high-cycle fatigue is developed. This method is applied to the assessment of the reliability associated with existing system-level design methodologies and the evaluation of system effects, such as fatigue dependence and progressive collapse. In addition to the developed theoretical frameworks, the articles include several examples of applications, specifically on the design of monopile support structures for offshore wind turbines subject to fatigue and extreme environmental loads, and on the design, reassessment and inspection planning of mooring systems affected by combined fatigue and pitting corrosion.

Acknowledgements

I want to begin by acknowledging my supervisor Jochen Köhler, for the many inspiring discussions we had on structural reliability, sustainability and the philosophy of design, and for being persistent in the dissemination of a sound foundation for structural safety and uncertainty quantification. I acknowledge the support provided by my co-supervisor Michael Muskulus too. His capacity and willingness to share his knowledge and his efforts in building a wind energy research community in Trondheim are much appreciated.

I would like to appreciate the Engineering Risk Analysis group at the Technical University of Munich, for warmly hosting me for two months. Particularly, I would like to thank Daniel Straub and Elizabeth Bismut for the many discussions and shared knowledge during and after my stay, which positively and significantly improved this work. Also, I would like to acknowledge the COST action project TU1402 and their organisers for providing the funding for my stay in Munich and for fostering many fruitful projects, collaborations, and discussions around the emerging topic of value of information analysis of structural health monitoring. I also want to take the chance to thank John D. Sørensen and Jannie J. Nielsen, from Aalborg University, for being open to collaborate and share their experience with me, and Per J. Haagenzen, prof. emeritus at NTNU, for introducing me to the challenges of corroded mooring chains.

My colleagues at the department of Structural Engineering are also very much appreciated for creating a nice and friendly working environment, in which one could find advice when needed and relax and have fun when needed even more.

Finally, I would like to appreciate the people closer to me: my family, my friends (both here and in Spain) and Tuna. My family, for supporting me during all my formative years and motivating me to keep learning. My friends, for their little interest in my research and their great interest in life, which allows one to put things into perspective. Tuna, for sharing these wonderful years and patiently putting up with me during all the stressful periods.

Jorge Mendoza Espinosa
Norwegian University of Science and Technology
Trondheim, September 9th, 2021

Table of Contents

	Page
Preface	i
Abstract	iii
Acknowledgements	v
List of publications	xi
List of Abbreviations	xiii
Chapter 1. Introduction	1
1. Context and motivation	1
2. Objectives and scope	3
3. Organisation of the thesis	3
4. Perspectives of structural design	4
4.1 Prescriptive design	4
4.2 Goal-oriented design	6
5. Life-cycle structural assessment	7
5.1 Prior, posterior and preposterior decision analysis	7
5.2 System reliability	14
Chapter 2. Conclusions	23
1. Main findings and highlights	23
1.1 Paper I: Risk-based Fatigue Design Considering Inspections and Maintenance	23
1.2 Paper II: Optimal life-cycle mitigation of fatigue failure risk for structural systems	23
1.3 Paper III: Structural reliability analysis of offshore jackets for system- level fatigue design	24

1.4	Paper IV: Analysis of fatigue test data of retrieved mooring chain links subject to pitting corrosion	25
1.5	Paper V: Value of information of in situ inspections of mooring lines	25
1.6	Paper VI: Risk-based Design of an Offshore Wind Turbine using Vol Analysis	26
2.	General conclusions	26
2.1	Integrated life-cycle decisions	26
2.2	System-level design	27
3.	Future outlook	28
3.1	Standardisation of integrated life-cycle mitigation	28
3.2	Mitigation of human error effects	29
3.3	Fatigue design of bottom-fixed offshore structures	29
3.4	Design and integrity management of mooring systems subject to fatigue and pitting corrosion	31
	References	33
	Appended papers	43
	Paper I	45
	Paper II	61
	Paper III	93
	Paper IV	127
	Paper V	159
	Paper VI	175

List of publications

Publications appended to the thesis

Paper I: Mendoza, J., E. Bismut, D. Straub, and J. Köhler (2020). “Risk-based Fatigue Design Considering Inspections and Maintenance”. In: *ASCE ASME J Risk Uncertain Eng Syst A Civ Eng* 7.1., pp. 04020055. DOI: 10.1061/AJRUA6.0001104.

Paper II: Mendoza, J., E. Bismut, D. Straub, and J. Köhler (2021). “Optimal life-cycle mitigation of fatigue failure risk for structural systems”. Submitted for publication to peer-reviewed journal.

Paper III: Mendoza, J., J.S. Nielsen, J.D. Sørensen, and J. Köhler (2021). “Structural reliability analysis of offshore jackets for system-level fatigue design”. Submitted for publication to peer-reviewed journal.

Paper IV: Mendoza, J., P. Haagenen, and J. Köhler (2021). “Analysis of fatigue test data of retrieved mooring chain links subject to pitting corrosion”. Submitted for publication to peer-reviewed journal.

Paper V: Mendoza, J., J. Paglia, J. Eidsvik, and J. Köhler (2021). “Value of information of in situ inspections of mooring lines”. In: *Proceedings of the Institution of Mechanical Engineers, Part O: Journal of Risk and Reliability* 235.4, pp. 556–567. DOI: 10.1177/1748006X20987404.

Paper VI: Mendoza, J., and J. Köhler (2019). “Risk-based Design of an Offshore Wind Turbine using VoI Analysis”. In: *13th International Conference on Applications of Statistics and Probability in Civil Engineering, ICASP13*, Seoul, Republic of Korea.

Publications not appended to the thesis

Mendoza, J., and J. Köhler (2019). “Value of site-specific information for the design of offshore wind farms”. In: *Towards a Resilient Built Environment - Risk and Asset Management, IABSE Symposium*, Guimarães, Portugal.

Mendoza, J., J. Köhler, E. Bismut, and D. Straub (2019). “Integrated Life-cycle Decision Framework for Structural Systems”. In: *Enabling Intelligent Life-cycle Health Management for Industry Internet of Things (IIOT). Proceedings of the Twelfth International Workshop on Structural Health Monitoring*, Stanford, USA, pp. 1496–1503.

List of Abbreviations

3D	=	Three-dimensional
ALS	=	Accidental Limit State
BN	=	Bayesian Network
BUS	=	Bayesian Updating with Structural reliability methods
CPT	=	Cone Penetration Test
CVPI	=	Conditional Value of Perfect Information
EDS	=	Equivalent Daniels System
EVPI	=	Expected Value of Perfect Information
FDF	=	Fatigue Design Factor
FE	=	Finite Element
FORM	=	First-Order Reliability Method
GDP	=	Gross Domestic Product
HSE	=	Health and Safety Executive
ID	=	Influence Diagram
I&M	=	Inspections and Maintenance
ISO	=	International Organization for Standardization
MCMC	=	Markov Chain Monte Carlo
MDP	=	Markov Decision Process
O&M	=	Operation and Maintenance
OWT	=	Offshore Wind Turbine
PDF	=	Probability Density Function
POD	=	Probability of Detection
POMDP	=	Partially Observable Markov Decision Process
PPV	=	Preposterior Value
PV	=	Prior Value
RAC	=	Risk Acceptance Criterion
RBI	=	Risk-based Inspection
RIF	=	Residual Influence Factor
SEI	=	Single Element Importance
SLS	=	Serviceability Limit State
SORM	=	Second-Order Reliability Method
SRA	=	Structural Reliability Analysis
ULS	=	Ultimate Limit State
VOI	=	Value Of Information

Chapter 1. Introduction

1. Context and motivation

The large structures that are built to support offshore and civil infrastructure play a crucial role in society. Their purpose is to safely enable a variety of services in sectors such as energy production, transportation, water management and communications. The design, construction, and operation and maintenance (O&M) of large structural systems demand large economic commitments. Specifically, public infrastructure requires in the order of 2 – 8% of a country’s gross domestic product (GDP) (Athenosy et al. 2017; Congressional Budget Office 2017; Kalaitzidakis and Kalyvitis 2005). Moreover, the environmental impacts associated with civil engineering infrastructure are diverse and significant (Kupolati 2010). It is estimated that the building materials are responsible for 3 – 8% of the global greenhouse emissions, with steel and concrete being the major contributors (Walker-Morison et al. 2007). Therefore, the performance of large structural systems is to be judged in accordance with safety, environmental and economic considerations, with the economic criterion encompassing their life-cycle costs and the direct and indirect revenue streams of the infrastructure that they support.

Structures such as bridges and offshore structures are exposed to rough environments that favour deterioration processes. Specially, corrosion and fatigue are of major concern. The deterioration of these structures leads to safety hazards, and to large costs associated with mitigating these hazards. In particular, fatigue has been identified as one of the main causes of partial failure or total collapse of railway bridges (Byers et al. 1997), bottom-fixed offshore structures (Almar-Naess et al. 1984; Vårdal et al. 1999) and offshore mooring systems (Fontaine et al. 2014; Gordon et al. 2014). The costs of safely operating and maintaining structures constitute a large part of their life-cycle expenditures. For instance, 25–30% of the life-cycle costs of offshore wind energy is dedicated to O&M (Miedema 2012), of which maintenance costs constitute around 38% (Lagerveld et al. 2014). Furthermore, around 21 – 49% of the total expenditure for public infrastructure is associated with O&M (Kalaitzidakis and Kalyvitis 2005; Rioja 2013).

The ageing of the built environment is reaching a state of maturity in developed countries (Beck 2003). As a reference, the ratio of the number of highway bridges being retrofitted or reconstructed to newly constructed ones increased from being 7% during the 1950s, to being 13% during the 1970s and 24% during the 2000s, see Figure 1 (FHWA

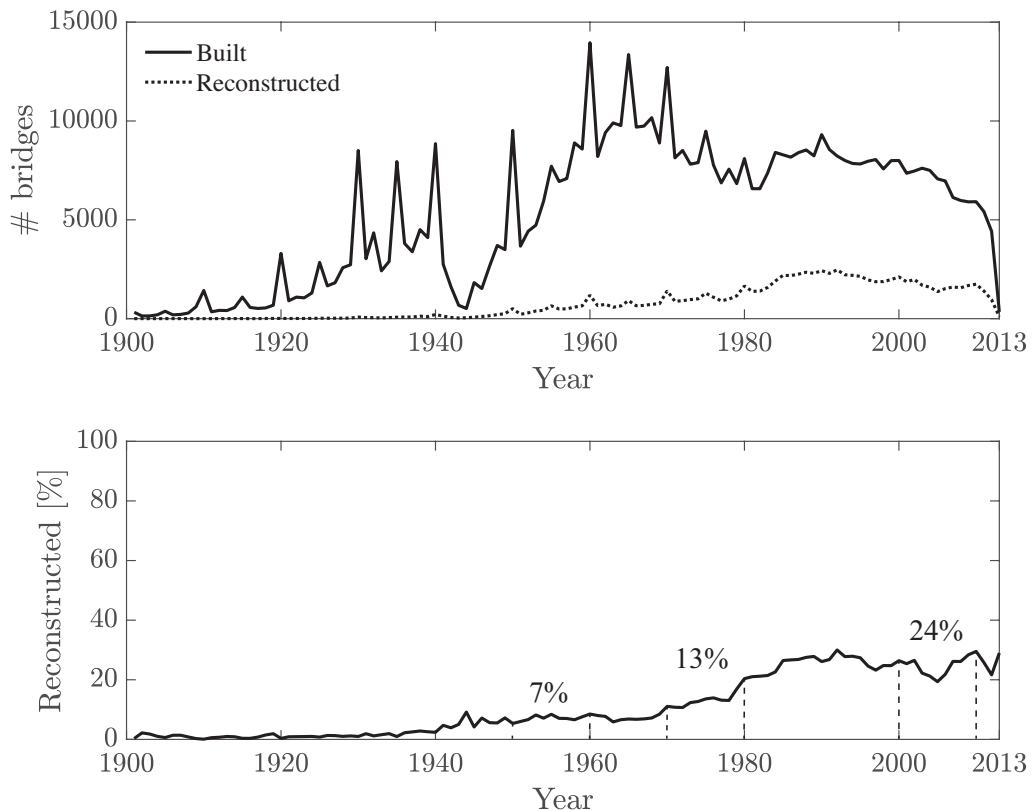


Figure 1: Historical data of constructed and reconstructed bridges in the USA per year from 1901 to 2013. The upper figure shows the raw data, and the lower figure shows the percentage of reconstructed over newly built bridges. Data is gathered from the database of the US Department of Transportation (FHWA 2020).

2020). Moreover, the number of structurally deficient bridges is roughly half of the total portfolio in Europe (Daly 2000), and more than 40% of the bridges in the USA are at least 50 years old (ASCE 2021). As a consequence, the cost associated with the integrity management of existing infrastructure is increasing its share of the total expenditure in public infrastructure (ASCE 2021).

The maturation of the built environment comes with new challenges. As a response, the civil engineering profession is increasing its focus on topics such as structural reassessment (Melchers and Jeffrey 2008; Schneider 2020; Straub et al. 2020), life extension (Beck 2003; Solland et al. 2011; Ziegler 2018; Nielsen et al. 2021), and inspection and monitoring optimisation (Straub 2004; Dong and Frangopol 2015; Lotsberg et al. 2016; Soliman et al. 2016; Luque and Straub 2019). Typically, these topics have been addressed in isolation; that is, little emphasis has been placed on accounting for the interrelationships between the decisions made at the different phases of the structure’s life (Mendoza et al. 2020). These interrelations should nonetheless be considered to further optimise the decisions made during the structural life cycle.

2. Objectives and scope

The present thesis contributes to the state-of-the-art of the analysis and design of deteriorating structural systems. The focus is on (i) the joint planning of design and inspections and maintenance (I&M) mitigation measures, and (ii) structural reliability analysis and design at the system level. The inclusion of these aspects into the design process is aimed at more efficiently mitigating the risks associated with deterioration and more fairly assessing the safety level of deteriorating structures.

The joint planning of design and I&M measures, referred to as the planning of a life-cycle mitigation strategy within this thesis, allows to find an optimal balance between the economic commitments dedicated to deterioration mitigation during the design and O&M phases of a structure. The search of optimal mitigation strategies will be investigated regarding two objectives: achieving a target safety level with minimum costs and minimising the expected life-cycle costs.

The consideration of system effects is particularly important in the context of deterioration. As a structure degrades, the consequences of component failures depend on the reserve capacity of the deteriorated structural system. Furthermore, the probability of occurrence of a given deterioration state depends on the statistical dependence of the simultaneously occurring deterioration processes. This thesis addresses the implications of system effects on the design of mitigation strategies.

Although many of the conclusions drawn from the present investigations can be extended to different deterioration mechanisms, the focus is primarily on fatigue deterioration. The scope of the assessment of the reliability of structural systems is here mainly constrained to ultimate limit states (ULS) at the system level, including limit states for deterioration failure at the component level. Accidental limit states (ALS) and serviceability limit states (SLS) are assumed to be separately accounted for. Furthermore, human error is not considered in this thesis. Nevertheless, a discussion on why and how to incorporate human error mitigation is presented in Section 3 of the next chapter.

3. Organisation of the thesis

This thesis is written as a collection of articles. As such, the thesis contains a number of appended articles (six in this case), and a number of introductory chapters. The current chapter serves the purpose of introducing the research questions addressed in this thesis, going through the context and motivation of the research, and the main theoretical background and tools. The next chapter presents a summary of the main research findings and suggests future lines of research that can be taken to continue the present work.

The core of the conducted research is presented through the appended papers. Papers I, II and III elaborate on the developed frameworks for assessing life-cycle fatigue mitigation of structural systems. Papers IV and V focus on the life-cycle assessment of mooring systems subject to combined fatigue and pitting corrosion. At last, Paper VI presents a case study of the application of value of information (VOI) analysis to support

decisions on site-specific information acquisition of soil-stiffness data for the design of offshore wind turbine (OWT) support structures.

4. Perspectives of structural design

The design of structural systems is inherently a problem of decision-making under uncertainty. The uncertainties in the problem originate from lack of knowledge and fundamental randomness of the involved variables and natural phenomena. Structural design can be addressed in several ways. Four levels are typically used in the literature to categorise structural design based on the level of detail of the probabilistic modelling (Thoft-Cristensen and Baker 2012; Melchers and Beck 2018). Level I encompasses the semi-probabilistic approaches, such as the popular partial safety factor method. Levels II and III consist of the reliability-based methods. Level IV corresponds to risk-based methods. The levels I to III methods differentiate from the level IV methods in that the safety level is prescribed as opposed to being an optimisation variable. In other words, the optimisation of the safety level is conducted outside of the design process for the levels I to III approaches, whereas it is a performance variable to be optimised for the level IV approaches. For this reason, the levels I to III approaches are designated prescriptive and the level IV approaches are designated performance-based or goal-oriented. An overview of both design perspectives is presented in this section.

4.1. Prescriptive design

Civil and offshore structures are generally designed following prescriptive regulations, codes and standards. These documents state a set of rules that a design must comply with. These rules explicitly include safety performance indicators, such as reliability indices and partial safety factors, and performance parameters, such as material strengths and geometrical parameters. Prescriptive regulations are formulated so that they can be applied in a broad range of design situations. In order to do so, systems are synthesised into categories by reducing the degrees of freedom of the system representation and ensuring safety margins that are large enough to accommodate for this generalisation. Typically, different safety levels are prescribed depending on the consequences of component failure and the relative cost of the safety measures. The generalisations associated with the categorisation are useful to simplify the process of structural design but are a burden for the structure-specific optimisation (Bergström 2017; Baravalle and Köhler 2019). Next, semi-probabilistic and reliability-based approaches are introduced.

4.1.1. Semi-probabilistic approaches

The semi-probabilistic approach is the most used approach in practice. It represents a simplified decision support under uncertainty. Random variables are represented by deterministic design values. Design values are computed using safety factors and characteristic values, which are given percentiles of the probabilistic distribution of the random

variables of interest. The design values are prescribed in combination with design equations, load cases and load combination factors, conforming what is known as a safety format. The parameters of a given safety format are determined by code calibration, which is performed by a combination of reliability- and risk-based optimisation, fitting and expert judgement (ISO 2015; Baravalle and Köhler 2019). In Europe, the predominant semi-probabilistic format is the *partial safety factor method*, which is standardised in the Eurocode 0 (CEN 2002).

The use of semi-probabilistic approaches is justified for the design of typical structures for which large experience exists and that will be exposed to normal operating and environmental conditions (Faber 2015). Furthermore, its applicability is restricted to structures whose consequences of failure are deemed sufficiently low, e.g., consequence classes 1, 2 or 3 in ISO 2394 (ISO 2015).

4.1.2. *Reliability-based approaches*

In reliability-based approaches, the goal is to find designs whose associated nominal probability of failure is close to and above a given target value. Structural reliability analysis (SRA) can be used to assess the nominal probability of failure of a system. In SRA, failure events, i.e., events associated with adverse consequences, are defined by limit state functions. The consequences of the failure events are not explicitly considered, but implicitly accounted for by the chosen target probability of failure. Thus, decisions can still not be made following cost-optimisation for case-specific situations at this level of probabilistic modelling (Baravalle and Köhler 2019). In other words, safety is established as a constraint, similarly as in level I. Therefore, even though the uncertainties associated with the system representation are explicitly addressed, reliability-based methodologies belong to the prescriptive regulation methodologies.

A limitation of this framework is that the assessment of the structural reliability is subjective to the designer. The probability of failure of a structure resulting from SRA is not an intrinsic characteristic of a structure, but of the model that is used to map the existing knowledge about the structure. Furthermore, civil and offshore structures are unique in most cases. Thus, an empirical, frequentistic treatment of the failure rate is not generally possible. Consequently, probabilities are better characterised as a *degree of belief*, which depends on the available information and the way this information is treated and employed (Pearl 1988). In principle, the assessment of the probability of failure can only be objective when no further information could be retrieved about the decision at hand, which is not a scenario that is faced in practice. By employing the degree-of-belief definition of probability, the validity of comparing two alternatives is constrained to how similar the models are to each other (Ditlevsen 1983; Melchers and Beck 2018). Therefore, the prescription of absolute target reliabilities without the standardisation of probabilistic modelling might lack some sound foundations. Although this limitation is present for the design in case-specific situations, the approach regains its meaning from a societal point of view, where the estimation biases average out over the large number of applications (JCSS 2001).

4.2. Goal-oriented design

As opposed to prescriptive methodologies, goal-oriented or performance-based design states the goals to be met without limiting the ways in which this can be achieved (Guedes et al. 2009). The name *goal-oriented design* is typically used in the marine sector, whereas the term *performance-based design* is more commonly used in building and civil engineering (Foliente 2000), being possible to trace it back to US NBS (1925). In goal-oriented approaches, safety is typically addressed using Level IV, i.e., risk-based methodologies.

Goal-oriented design can be used to enhance the design space, i.e., the abstract domain that contains the design possibilities that adequately address the design objectives (Coyne et al. 1990). According to Guedes et al. (2009), this can be used, among others, for (a) justifying the use of larger safety margins; (b) certifying solutions with reduced costs, i.e., safety equivalence; or (c) assessing new innovative solutions, i.e., prototypes. Moreover, goal-oriented design can be used in situations that lay outside the scope of standardised design. For instance, the reassessment of existing structures and the planning of O&M strategies are often not suitable within the prescriptive framework.

Challenges in the implementation of goal-oriented and performance-based methodologies are reported in Bakens et al. (2005). The principal difficulties for the general adoption of these methods are the more complex communication between the stakeholders in comparison with prescriptive methods and the technical complexities of the methods. Moreover, goal-oriented approaches suppose a challenge for standardisation, which discourages engineers from adopting them, as the legal responsibilities are partially transferred from the standards and regulation institutions to the engineers and engineering companies.

4.2.1. Risk-based design

Structural reliability analysis deals uniquely with safety considerations based on the notion of the probability of failure. Therefore, SRA cannot be directly used to balance the trade-off between safety and the costs of safety. Risk-based methodologies avoid the latter limitation in the following manner. Failure events at the component and system level can be identified. The consequences of these events can be quantified and combined with structural reliability metrics into the concept of risk. Metrics to quantify the possible consequences are often economic in nature, since it is then possible to directly combine them with the mitigation costs, such as the construction costs, inspection and monitoring costs and repair costs, in order to support decisions. Nevertheless, other aspects and attributes can be mapped into a common metric, often called utility. The risk of failure can be used to compute the expected utility (or equivalently the expected cost) associated with a decision. Utility theory and rational decision theory can be used to rank decisions (Neumann and Morgenstern 1966), as it is explained in more detail in Section 5.1.

Extensive literature exists on risk-based methodologies for the management of the different decision scenarios during the structural life cycle. Despite the fruitful develop-

ment of risk-based design methodologies in the research context, little implementation into civil engineering design applications exists. As mentioned above, it is nonetheless common practice to apply risk-based methods to the code-calibration of the widely used semi-probabilistic design methods, see e.g., (Madsen et al. 2006; Ditlevsen and Madsen 1996). Moreover, increasing attention is paid to risk-based design in the naval sector (Guedes et al. 2009). Among other reasons, this may be due to the demands of the naval industry for new solutions that are suitable for the arctic environment, which is an area where little experience exists (Bergström et al. 2016). In the civil engineering context, risk-based design has found new applicability for the optimum planning of systems of infrastructures (Faber and Stewart 2003) and the pursuit of designs with enhanced resilience and robustness to natural disasters (Faber et al. 2017). The use of risk-based methodologies for the optimisation of the I&M planning is receiving growing attention during the last two decades (Straub 2004; Straub and Faber 2005; Moan and Song 2000; Luque and Straub 2016; Schneider et al. 2017; Luque and Straub 2019). This is probably related to a combination of the increasing demand for cost reduction from the infrastructure operators and the increase in the computational capacity of personal computers.

4.2.2. Safety in risk-based design

Optimal risk-based design is typically performed from the operator's point of view. Since parts of the risks are taken over by additional stakeholders such as the infrastructure users and society as a whole, risk acceptance criteria (RAC) are needed to ensure sufficient safety according to the societal preferences. RAC can be included as an active constraint into the risk-based optimisation (Papalambros and Wilde 2000). Examples of RAC are the FN-curves (Farmer 1967), the risk matrix (Duijm 2015) and the Life Quality Index (Nathwani et al. 1997). The latter criterion provides a consistent framework for the optimal management of the societal resources, based on the societal willingness to pay and the marginal life saving costs (Fischer et al. 2013).

5. Life-cycle structural assessment

This section presents the theoretical background for the life-cycle assessment of structural systems. Here, structural systems are understood as a combination of limit state functions or failure modes. In practical applications, structural systems are idealised by considering a limited number of failure modes, which are chosen such that the estimation of the structural reliability is meaningful for decision making. First, the theoretical decision framework to assess design, inspection and maintenance actions is introduced. After that, the modelling and assessment of the reliability of structural systems is presented.

5.1. Prior, posterior and preposterior decision analysis

The theoretical foundation for decision making in civil engineering has traditionally built upon the Bayesian decision framework originally presented in Raiffa and Schlaifer

(1961). Bayesian decision analysis distinguishes between prior, posterior and preposterior decision analyses. In this section, these three types of decision analyses are addressed in relation to the topics of the thesis. For a more thorough introduction to Bayesian decision theory in civil engineering, the reader is referred to Benjamin and Cornell (2014), which is the classical reference on this matter.

Let Θ represent the uncertain *state of nature*, \mathbf{a} be a predefined set of possible actions that can be taken to probabilistically affect Θ , and $u(a, \theta)$ be the utility associated with state θ and action a . For instance, in the context of maintenance, Θ could represent the deterioration condition of a component, a could include choices such as to “repair” or “not repair” the component, and $u(a, \theta)$ could be the sum of the costs¹ associated with action a and the economic consequences of θ . The *prior* and *posterior* decision analyses deal with the problem of choosing the best alternative among \mathbf{a} . The best or optimal action a_{opt} is identified as the one that maximises the expected utility.

$$a_{opt} = \arg \max_{a \in \mathbf{a}} \{\mathbb{E}_{\Theta}[u(a, \theta)]\}. \quad (1)$$

In the prior decision analysis, the probabilistic representation of Θ includes only prior information. In this analysis, the maximum expected utility receives the name of prior value (PV), i.e.,

$$PV = \max_{a \in \mathbf{a}} \{\mathbb{E}_{\Theta}[u(a, \theta)]\} = \max_{a \in \mathbf{a}} \left\{ \int_{\Theta} u(a, \theta) f_{\Theta}(\theta) d\theta \right\}, \quad (2)$$

where $f_{\Theta}(\theta)$ is the prior probability density function (PDF) of Θ .

If new information z is taken into account to build a posterior model of Θ using Bayesian updating, the analysis is then known as posterior decision analysis, and the maximum expected utility receives the name of posterior value. Bayesian updating is explained below in Section 5.2.2. The only difference between the prior and posterior analyses is the probabilistic model of Θ . Because it is not always clear what constitutes prior information, the difference between both analyses is not clear-cut. In any case, this difference is inconsequential for the applications in this thesis. The prior and posterior decision analyses can be illustrated with a decision tree such as the one shown in Figure 2. By convention, choices are represented with squares and random outcomes or chances are represented with circles in the decision tree.

Bayesian decision analysis can be extended to include decisions on information acquisition. This type of analysis is the so-called *preposterior decision analysis* and is illustrated with a decision tree in Figure 3. The preposterior value (PPV) associated with an information acquisition strategy e , denoted PPV_e , is given by

$$PPV_e = \mathbb{E}_{z_e} \left[\max_{a \in \mathbf{a}} \{\mathbb{E}_{\Theta|z_e}[u(\theta, a)|z_e]\} \right] = \int_{z_e} \max_{a \in \mathbf{a}} \{\mathbb{E}_{\Theta|z_e}[u(\theta, a)|z_e]\} f_{z_e}(z_e) dz_e, \quad (3)$$

where z_e is a random variable representing the information potentially obtained with strategy e and $f_{z_e}(z_e)$ is the PDF of the inspection outcomes. Since the decision is made

¹Since utilities are to be maximised, costs or losses are here expressed with negative values.

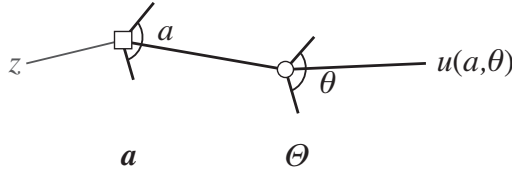


Figure 2: Decision tree of the prior and posterior decision analyses. Z = acquired data; \mathbf{a} = actions; Θ = state of nature; u = utility function. Unlike the prior analysis, the posterior analysis uses information z to update the belief in the state of nature Θ and inform the choice of the action a .

prior to acquiring any information, the PDF of Z_e can only be expressed using prior information about the state of nature Θ and the likelihood of the inspection technique e :

$$f_{Z_e}(z_e) = \mathbb{E}_{\Theta}[f_{Z_e}(z_e|\theta)] = \int_{\Theta} L(z_e|\theta)f_{\Theta}(\theta)d\theta, \quad (4)$$

where $L(z_e|\theta)$ is the likelihood function of e .

The preposterior value is nothing more than the expected posterior value. In other words, before information is acquired, the best strategy for gathering information can be obtained by integrating over inspection outcomes, whose probabilistic model is built using available knowledge, i.e., prior information. Note that in the case of e being the strategy of not acquiring any further information, the preposterior value PPV_e coincides with the prior value PV . According to the preposterior decision analysis, the optimal experiment or inspection is computed as:

$$e_{opt} = \arg \max_{e \in \mathbf{e}} \{PPV_e\}. \quad (5)$$

Since the preposterior decision analysis only considers prior information, the appropriate modelling of the prior knowledge is of particular importance. Prior probabilistic models of the state of nature are typically developed using available information about the load and resistance parameters and physics-based models for prediction. Bayesian decision analysis constitutes a generic framework for optimum decision making throughout the life cycle of a structure. Next, it is shown how the presented framework can be adapted to address different decision scenarios and thereby arrive at an integrated design framework.

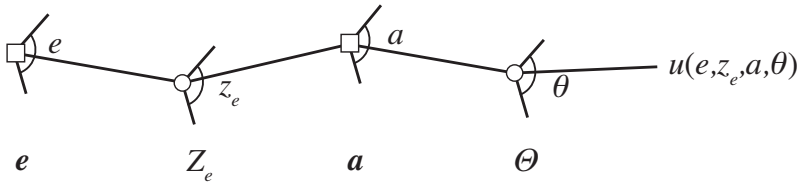


Figure 3: Decision tree of the preposterior decision analysis. \mathbf{e} = information acquisition choices; Z_e = random inspection outcome associated with inspection choice e ; \mathbf{a} = actions; Θ = state of nature; u = utility function.

5.1.1. Value of information analysis

Acquiring information comes with a cost. Therefore, information should only be acquired when its value outweighs its costs. Value of information analysis deals with this particular type of decisions (Thöns 2018). The VOI of an inspection strategy e can be computed as

$$\text{VOI}_e = \text{PPV}_e - \text{PV}, \quad (6)$$

where the prior value PV is given in Eq. (2) and the preposterior value of strategy e PPV_e is computed according to Eq. (3).

The VOI is strictly positive if the obtained information is unbiased and if one single decision maker participates in the decision. In other words, *information cannot hurt* under those assumptions. However, when there is a sequence of decisions made by different decision makers, e.g., the owner and the manager of a structure, the VOI can in fact be negative (Verzobio et al. 2021).

The computation of the VOI in practical situations can be computationally demanding due to the double expectation in Eq. (3). Often, only approximations are applicable. Existing approximations are of two types: computational approximations of the integrals in Eq. (3), or simplifications of the level of detail of the decision problem. One can of course make use of both kinds of approximations in a given application. Examples of the first kind of approximation are the use of linear and quadratic Laplace and Gaussian approximations (Eidsvik et al. 2015), sampling-based methods (Pozzi and Der Kiureghian 2011; Straub 2014), or approximate inference techniques for Bayesian Networks (Nielsen and Jensen 2009; Darwiche 2009). The second kind of approximation mainly comprises heuristic search, where the space of explored decisions is reduced (Bismut et al. 2017; Eidsvik et al. 2018). Moreover, in some occasions, simpler notions such as the conditional value of perfect information (CVPI) or the expected value of perfect information (EVPI) can help guiding decisions (Straub 2004). The CVPI is the value of information that would be obtained if perfect information about the state of nature would be available:

$$\text{CVPI}(\theta) = \max_{a \in \mathcal{A}} u(a, \theta) - \text{PV}. \quad (7)$$

The EVPI is the value of information that would be obtained should the measuring device acquires information without error. The EVPI is obtained from the CVPI by integrating over Θ :

$$\text{EVPI} = \mathbb{E}_{\Theta}[\text{CVPI}(\theta)] = \int_{\Theta} \text{CVPI}(\theta) f_{\Theta}(\theta) d\theta. \quad (8)$$

5.1.2. Sequential risk-based inspection planning

The preposterior decision analysis can be applied to plan optimal inspections, in which case it is called risk-based inspection (RBI) planning. The decision tree in Figure 3 could be directly applied to decide whether to inspect or not, or how to inspect, at a given point in time. In the context of integrity management, the focus is, however, on prescriptive inspection planning. Prescriptive inspection planning involves planning when and where

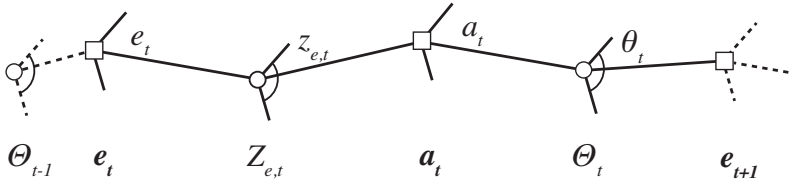


Figure 4: Sequential decision analysis for inspection planning. e_t = information acquisition choices at time t ; $Z_{e,t}$ = random inspection outcome associated with inspection choice e_t ; a_t = maintenance action choices at time t ; Θ_t = state of nature at time t .

to inspect or monitor a particular structure during its service life. In this case, a number of subsequent inspection campaigns are to be planned. Usually, the period over which inspections are to be planned is discretized into time steps of say, a year. Figure 4 shows a time slice of the sequential RBI planning decision tree.

Structural deterioration can in some occasions be well represented by the *Markov property*. The Markov property is satisfied when the past has no influence on the future given that the present is known. In other words, if the state of nature is observed at a given point in time, what happened prior to that time does not affect the prediction of the future state of nature. Based on the Markov property, deterioration can be modelled as a *Markov process*. A *Markov decision process* (MDP) consists in finding the optimal inspection policy of a Markov process. Generally, the information that can be retrieved from a system is imperfect and the MDP is then generalised to a *partially observable Markov decision process* (POMDP).

An intuitive way to represent a POMDP is with a *Bayesian Network* (BN) (Nielsen 2013). A BN is a probabilistic model in which the dependency structure between random variables is explicitly represented by a directed acyclic graph. BNs were formally introduced in Pearl (1988), and have been widely developed in the field of artificial intelligence (Russell and Norvig 2013). A BN is composed by *chance nodes*, which model random variables and are represented by circles, and *directed links* (also called *arcs*), which model the relation between the chance nodes. Although it is not a requisite of BNs, the arcs are here understood to point from cause to effect. When decisions are also represented in the BN, it is often referred to as an *Influence Diagram* (ID), although the term BN is indifferently used here. An ID also contains *Choice nodes*, modelling the possible decision alternatives and represented by squares and *utility nodes*, which model consequences or costs and are represented by diamonds. The principles of BNs are not presented here in detail; the interested reader is referred to Nielsen and Jensen (2009). Figure 5 shows a BN representing a simple POMDP. BNs in which the Markov property holds are often called *dynamic Bayesian Networks* (Straub 2009). It is noted that the relation between the outcome Z_t and the structural state E_t can rarely be established directly. Therefore, additional random variables are often included to model measurable indicators d_t of the deterioration condition, e.g., the crack depth in the case of fatigue deterioration. This is shown below in Figure 6.

Based on the Markov property, recursive dynamic programming algorithms can be used to efficiently solve a MDP (Dasgupta et al. 2008). In a POMDP, the structural

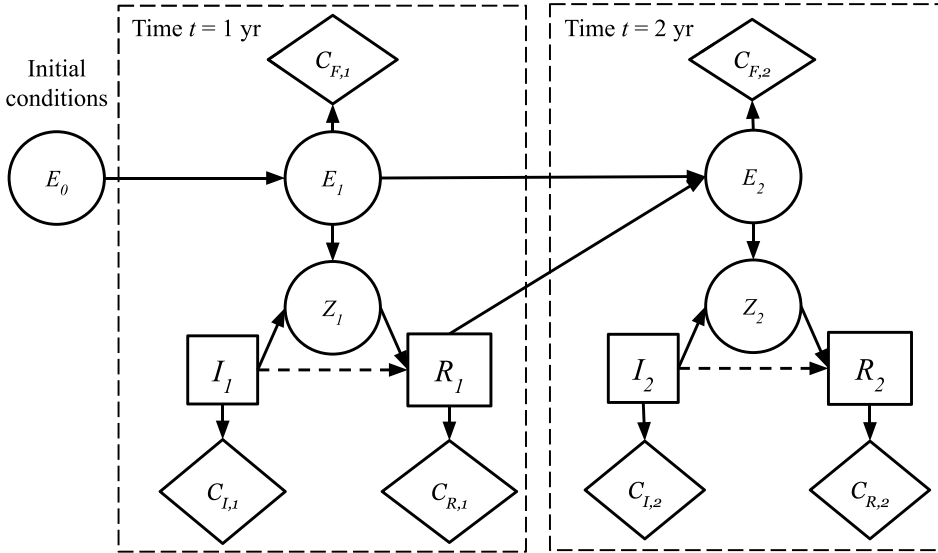


Figure 5: Bayesian Network representation of a partially observable Markov decision process (POMDP) for a single component system. E_t = structural state of the component at time t , e.g., failed or not failed; I_t = inspection decisions at time t , usually to inspect or not to inspect; R_t = repair actions at time t , usually to repair or not to repair; Z_t = inspection outcome at time t ; and $C_{I,t}$, $C_{R,t}$ and $C_{F,t}$ are the inspection costs, the repair costs and the failure cost at time t , respectively.

state is not known with certainty, but represented with a probabilistic distribution. The Markov property is then only applicable to a realisation of the structural state, and dynamic programming techniques need to be conducted for all possible states. The complexity of the POMDP was demonstrated to be PSPACE-complete (Papadimitriou and Tsitsiklis 1987). Hence, the exact solution is computationally intractable (Kochenderfer 2015; Russell and Norvig 2013). Reasonable approximations can be achieved by discretizing the state variables and evaluating the expected utilities at a number of grid points (Nielsen and Sørensen 2012). Another limitation of MDP and POMDP is that the Markov property does not generally hold in structural engineering problems, because of the time-invariant uncertainties associated with the parameters of the deterioration models (Straub 2009; Nielsen 2013). Straub (2009) proposes an extended BN model, similar to the one shown in Figure 6, in which time-variant and time-invariant parameters are separately modelled. This BN can be used to represent most deterioration models, taking advantage of the Markov property.

Another approach to solving the sequential inspection planning problem is to apply heuristic search, which is aimed at finding a good enough solution based on approximations of the decision problem. Close-to-optimum solutions were found in Bismut et al. (2017), where the decisions were parametrized by the fixed-interval between inspections, the failure probability threshold and a prioritisation index as proxy of the value of information that is expected to be gained by inspecting a component.

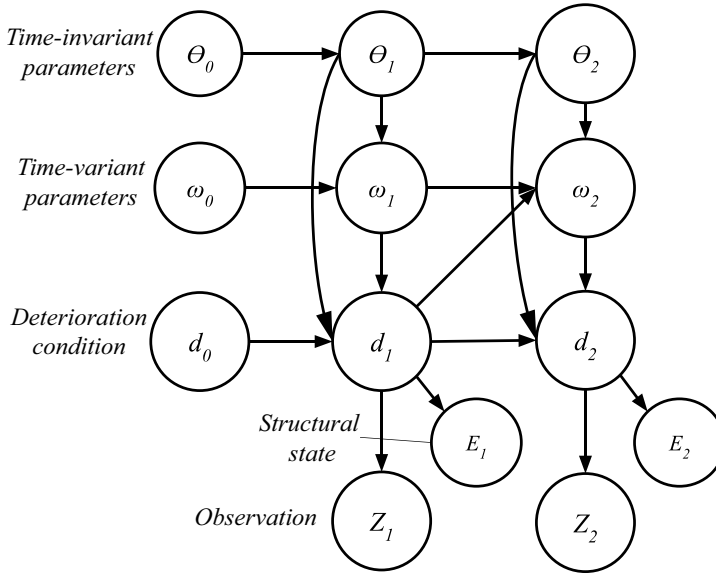


Figure 6: Bayesian Network representation of a deterioration process, explicitly modelling time-invariant parameters. Adapted from Straub (2009).

Further optimisation of the I&M strategic planning can be achieved with adaptive planning, i.e., updating the I&M plan after the retrieval of information (Yang and Frangopol 2021). An algorithm for adapting the optimum policy search upon observations of the deterioration history of the structure is presented in Bismut and Straub (2021). Memarzadeh et al. (2014) proposed a machine-learning algorithm to learn the deterioration process function of the POMDP using the acquired information from inspections. When conducting adaptive planning, additional indirect costs related to having a less regular or “unpredictable” planning and the complexity of the maintenance agreements that are made up-front with subcontractors need to be considered.

5.1.3. Integrated design and inspection planning

Simultaneously optimising design and inspection planning decisions is also a sequential decision problem. Given a design specification, inspection planning can be optimised following the risk-based inspection planning framework presented above. In this case, the available knowledge that exists is generic statistical information about the load and resistance parameters and physical and semi-empirical models for prediction of the performance of the structure as a function of the design specifications. Figure 7 shows a generic decision tree for integrated design and inspection planning. For simplicity, the part of the decision tree concerned with inspection planning is not represented as a sequential decision process in this figure. Generically, this part of the decision tree would be represented as in Figure 4.

In the context of integrated design and inspection planning, a structural design encompasses every specification that has an effect on the deterioration process. However,

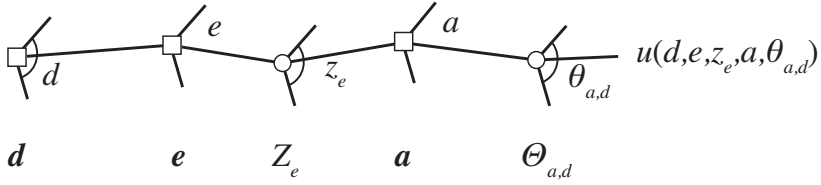


Figure 7: Preposterior decision analysis for combined design and inspection planning optimisation. \mathbf{d} = design choices; \mathbf{e} = inspection choice; Z_e = uncertain inspection outcome associated with inspection choice \mathbf{e} ; \mathbf{a} = maintenance choices; and $\Theta_{a,d}$ = state of nature associated with design \mathbf{d} and maintenance choice \mathbf{a} ; u = utility function.

this definition of design would require exploring an enormous design space. Therefore, the space of potential designs often need to be reduced. An option is to divide structural design into various steps, decoupling the designs of structural components that are mainly driven by the deterioration process and the ones that are dominated by other limit states, such as extreme load or serviceability limit states. For instance, for multimember offshore structures, the notion of hot spot or fatigue sensitive detail can aid in simplifying the design process. When deterioration has little effect on the structural response during most of the process, it may be possible to design the hot spots separately from the structural configuration. This is the case for high-cycle fatigue, in which crack initiation occupies a long period of the service life of a component, while crack growth and fatigue failure occur within a relatively short time span. In this way, structural configurations can be designed based on experience and the consideration of ULS, SLS and ALS, whereas the hot spots can be optimised for fatigue. Nonetheless, the structural configuration affects the redundancy and robustness of the structure and, thereby, affects the optimal fatigue design of the hot spots. Consequently, both design steps should still be performed iteratively.

The solution of the decision problem of integrated design and I&M planning is only optimal at the design point in time. When new information becomes available at a given point in time of the service life of the structure, the originally prescribed inspection plan will not be optimal in general. In principle, adaptive policy planning should be performed every time new information about the system becomes available (Madsen and Sørensen 1990; Moan 2018).

5.2. System reliability

Structural reliability analysis deals with the assessment of the probability of failure of a structural system, denoted $P_{f,sys}$. In SRA, a structural system is described by a set of basic random variables $\mathbf{X} = \{X_1, X_2, \dots, X_v\}$, whose knowledge is gathered by the joint PDF $f_{\mathbf{X}}(\mathbf{x})$, and a limit state function g , which may be a combination (unions and intersections) of limit state functions g_1, g_2, \dots, g_f . A limit state function g_i is a function such that $g_i(\mathbf{X}) \leq 0$ defines failure and $g_i(\mathbf{X}) > 0$ defines survival of a particular failure mode i . Thereby, $g(\mathbf{X}) \leq 0$ defines failure of the structural system. In the general case, g is a function of \mathbf{X} and time t , constituting the time-variant reliability problem. When

the limit state function is not a function of time, the problem is simplified to the so-called time-invariant reliability problem. The time-invariant reliability problem consists of solving the following equation:

$$p_{f,sys} = \Pr(F_{sys}) = \Pr(g(\mathbf{X}) \leq 0) = \int_{g(\mathbf{X}) \leq 0} f_{\mathbf{X}}(\mathbf{x}) d\mathbf{x}. \quad (9)$$

There exist many methods for efficiently solving this equation. Among these methods, commonly employed ones include the first-order reliability method (FORM) (Hasofer and Lind 1973), the second-order reliability method (SORM) (Hasofer and Lind 1974), importance sampling Monte Carlo simulation methods (Kurtz and Song 2013; Papaioannou et al. 2016; Papaioannou et al. 2019), subset simulation (Au and Beck 2001), and sampling methods enriched with surrogate models such as active learning with Kriging (Echard et al. 2011).

Unfortunately, deteriorating systems can rarely be modelled as time-invariant. Therefore, the reliability of systems subject to deterioration is to be assessed based on time-variant reliability analysis, which is introduced hereafter.

5.2.1. Time-variant reliability of deteriorating structures

The focus is here on assessing the reliability of a structure that is subject to deterioration. At a given point in time t of the service life of the structure, the point-in-time failure event $F_{sys}^*(t)$ is defined as

$$F_{sys}^*(t) = g(\mathbf{X}, t) \leq 0. \quad (10)$$

Based on this failure event, the point-in-time probability of failure $\Pr(F^*(t))$ is defined as

$$\Pr(F_{sys}^*(t)) = \Pr(g(\mathbf{X}, t) \leq 0). \quad (11)$$

Solving Eq. (11) is analogous to solving the time-invariant reliability problem, which, as already discussed, can be efficiently dealt with by employing existing methods. Nevertheless, the point-in-time failure probability is not directly meaningful for the design and integrity management of structures (Straub et al. 2020). The reason being that this failure probability does not account for the fact that the system may have failed prior to time t . Instead, the cumulative failure event $F(t)$ should be regarded:

$$F_{sys}(t) = \min_{\tau \in [0, t]} \{g(\mathbf{X}, \tau)\} \leq 0. \quad (12)$$

Based on this failure event, the probability of failure up to time t , also known as the cumulative probability of failure $P_{f,cum}(t)$, can be computed as

$$P_{f,cum}(t) = \Pr(F_{sys}(t)) = \Pr\left[\min_{\tau \in [0, t]} \{g(\mathbf{X}, \tau)\} \leq 0\right]. \quad (13)$$

In its general form, the computation of $P_{f,cum}(t)$ from Eq. (13) is the solution of a

first-passage problem, see Madsen et al. (2006) and Melchers and Beck (2018), among others. Methods to address the first-passage problem have been developed in the literature (Beck 2003; Beck and Melchers 2004). Often, the application of these methods is computationally expensive (Straub 2004). As an alternative, Straub et al. (2020) propose to express the cumulative failure event in Eq. (12) as a series of time-invariant failure events such as the one in Eq. (10). To apply this principle, time is to be discretized into time intervals. That is, time up to time t is divided into the m intervals $[t_0, t_1], [t_1, t_2], \dots, [t_i, t_{i+1}], \dots, [t_{m-1}, t]$. Intervals of one year is often a convenient choice. Similarly as for the point-in-time failure event and failure probability, the interval failure event $F_{sys,j}^*$ is defined as

$$F_{sys,j}^* = \min_{\tau \in (t_{j-1}, t_j]} \{g(\mathbf{X}, \tau)\} \leq 0, \quad (14)$$

and the interval probability of failure as

$$\Pr(F_{sys,j}^*) = \Pr(\min_{\tau \in (t_{j-1}, t_j]} \{g(\mathbf{X}, \tau)\} \leq 0). \quad (15)$$

In its general form, solving Eq. (15) still requires to solve a first-passage problem. Nevertheless, the problem can be simplified to a time-invariant reliability problem when one load dominates, in which case the dominating load can be modelled by its extreme value distribution (Straub et al. 2020). The cumulative failure probability $P_{f,cum}$ of the time-discretized problem is computed as the probability of the union of interval failure events up to time t :

$$P_{f,cum} = \Pr(F_{sys}(t)) = \Pr(F_{sys,1}^* \cup F_{sys,2}^* \cup \dots \cup F_{sys,t}^*), \quad (16)$$

which corresponds to a series system. Provided that the extreme loads at different years are mutually independent, the following bounds are available in the literature (Ditlevsen 1979):

$$\max_{j \in [1, m]} \Pr(F_{sys,j}^*) \leq P_{f,cum} \leq 1 - \prod_{j=1}^t [1 - \Pr(F_j^*)]. \quad (17)$$

In the applications found in this thesis, the cumulative probability of system failure has been often approximated by the upper bound in Eq. (17), due to the fact that it provides a better estimate when the probability of failure is dominated by uncertainties in loads (Straub et al. 2020).

The described approach for solving the time-variant reliability problem proposed in Straub et al. (2020) can be broadly applied to study deteriorating systems. Particularly, the approach is valid for situations in which load and resistance variables can be modelled independently from each other or for which system failure is given by a monotonically increasing damage function reaching a threshold. Whereas these assumptions are not generally satisfied for systems subject to low-cycle fatigue, they are typically applicable to high-cycle fatigue (Madsen et al. 2006).

The application of the time-variant failure probability estimates to risk- and reliability-based design is reviewed next. To perform a risk-based design such as the prior, posterior

or preposterior decision analyses described earlier, one needs to estimate the expected consequences of failure, also known as the *failure risk*. The failure risk R_F is the expected cost of failure. It is computed as

$$R_F(t) = \sum_{\tau=t_1}^t c_F \cdot e^{-\gamma\tau} \cdot P_{f,yr}(\tau) d\tau, \quad (18)$$

where c_F is the cost of failure, $e^{-\gamma\tau}$ is the discounting function with discount rate γ , and $P_{f,yr}(\tau)$ is the annual probability of failure at time τ . The annual failure probability is readily obtained from the cumulative probability of failure, which is defined in Eq. (16) and potentially estimated through the bounds in Eq. (17), as:

$$P_{f,yr}(t_j) = P_{f,cum}(t_{j+1}) - P_{f,cum}(t_j). \quad (19)$$

In reliability-based design, a design is considered safe enough if its probability of failure is below a given target value. Typically, design standards (ISO 2015; CEN 2002) and guidelines (JCSS 2001) provide target annual probabilities of failure $P_{f,yr}^T$, or analogously, target annual reliability indices β_{yr}^T . Note that both quantities are related through the expression $\beta_{yr}^T = -\Phi^{-1}(P_{f,yr}^T)$, with Φ being the standard normal cumulative distribution function. Thus, a design d is satisfactory from a safety point of view if

$$P_{f,yr}(d) \leq P_{f,yr}^T \quad (20)$$

at all times during service life.

For deteriorating systems, the annual probability of failure defined in Eq. (19) is not generally fitted to assess Eq. (20). The reason for this is that this estimate of the annual probability of failure is not necessarily monotonically increasing with time, even if no inspections are conducted. For the purpose of assessing Eq. (20), a better estimate of the failure probability is the hazard rate. The hazard rate at time t , denoted $h(t)$, is defined as the annual probability of failure at time t conditional on the structure having survived up to that time:

$$h(t) = \frac{P_{f,yr}(t)}{1 - P_{f,cum}(t)} \quad (21)$$

The difference between $P_{f,yr}(t)$ and $h(t)$ is illustrated in Figure 8 for two mitigation designs, which are assumed to be applied to the same structural configuration, it being associated with a given reliability in the intact state. As time progresses, the structure associated with Design 1 deteriorates faster than the one with Design 2. As a consequence, the difference between the annual probability of failure and the hazard rate of Design 1 increases faster than for Design 2. It can be seen that using the annual probability of failure for Design 1 would lead to the wrong conclusion that the structure is safe enough. In fact, if one would carelessly just take the estimates of $P_{f,yr}(t)$ at time t_m , they would conclude that Design 1 is safer than Design 2.

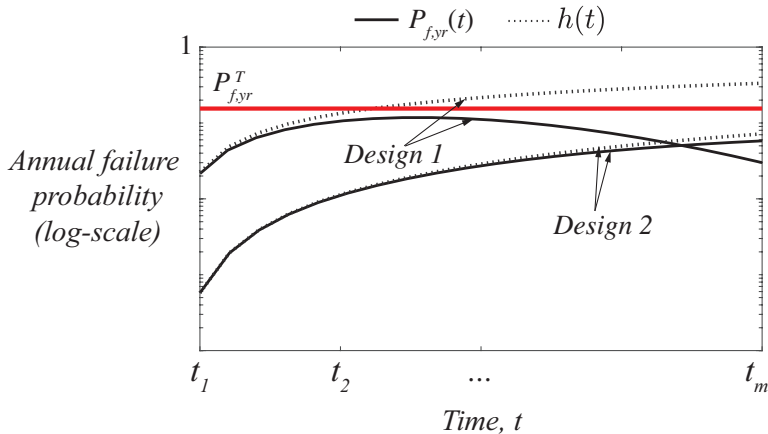


Figure 8: Reliability-based design of deteriorating system using an annual target probability of failure $P_{f,yr}^T$. The figure illustrates the difference between the annual probability of failure $P_{f,yr}(t)$ and the hazard rate $h(t)$.

5.2.2. Reliability updating

The posterior and preposterior decision analysis rely on the concept of Bayesian updating to compute how new data \mathbf{z} affects the system representation. Before acquiring the data, the basic random variables of the system are characterised by the prior PDF $f_{\mathbf{X}}(\mathbf{x})$. Once the data is gathered, the system can be better represented by the conditional distribution $f_{\mathbf{X}|\mathbf{Z}}(\mathbf{x}|\mathbf{z})$. The conditional distribution $f_{\mathbf{X}|\mathbf{Z}}(\mathbf{x}|\mathbf{z})$ can be computed from the prior distribution $f_{\mathbf{X}}(\mathbf{x})$ and the likelihood function of the data acquisition technique $L(\mathbf{x}|\mathbf{z})$ by applying Bayes' rule:

$$f_{\mathbf{X}|\mathbf{Z}}(\mathbf{x}|\mathbf{z}) = \frac{L(\mathbf{z}|\mathbf{x})f_{\mathbf{X}}(\mathbf{x})}{\int_{\mathbf{X}} L(\mathbf{z}|\mathbf{x})f_{\mathbf{X}}(\mathbf{x})d\mathbf{x}}, \quad (22)$$

Computing the posterior distribution $f_{\mathbf{X}|\mathbf{Z}}(\mathbf{x}|\mathbf{z})$ from Eq. (22) is in general computationally demanding. Several methods exist for this task. For SRA, the main approaches are sampling methods based on Markov chain Monte Carlo (MCMC) (Beck and Au 2002), Bayesian updating with structural reliability methods (BUS) (Straub 2011; Straub and Papaioannou 2014), and Bayesian Networks (Nielsen and Jensen 2009).

Generically, the likelihood function $L(\mathbf{x}|\mathbf{z})$ is defined as

$$L(\mathbf{x}|\mathbf{z}) \propto \Pr(\mathbf{z}|\mathbf{X} = \mathbf{x}). \quad (23)$$

That is, the likelihood function is proportional to the probability of observing \mathbf{z} given that the parameters \mathbf{X} realise as \mathbf{x} , thereby relating the observations with the model of the system. In structural reliability problems, mechanical models are used to predict \mathbf{X} . Let $h(\mathbf{X})$ be an unbiased prediction model of \mathbf{X} . An observation z_i of a continuous variable is related to $h(\mathbf{X})$ by an equation of the form $z_i + f(h(\mathbf{X})) = 0$. The likelihood function can be related to the mechanical models of the system depending on the type

of information. Information can be classified into two types: equality and inequality information (Madsen et al. 2006).

- *Equality information:* Two types of relations between the observation z_i and the mechanical model $h(\mathbf{X})$ are often encountered for equality information: additive and multiplicative error models (Straub and Papaioannou 2014). For additive error models, an observation z_i is deviated from the prediction $h(\mathbf{x})$ by an amount ε_i , i.e., $z_i = h(\mathbf{x}) + \varepsilon_i$. In this case, the likelihood function of the observation can be expressed as

$$L_i(\mathbf{x}) = f_{\varepsilon_i}(z_i - h(\mathbf{x})). \quad (24)$$

If the deviation ε_i is multiplicative, i.e., $z_i = h(\mathbf{x}) \cdot \varepsilon_i$, the likelihood is then expressed as

$$L_i(\mathbf{x}) = f_{\varepsilon_i}\left(\frac{z_i}{h(\mathbf{x})}\right). \quad (25)$$

Examples of equality information are the measurements of a fatigue crack depth or of the cross-section reduction due to corrosion.

- *Inequality information:* Formally, a model outcome $h(\mathbf{x})$ can be found for inequality information such that the observation is defined as

$$Z_i = [\mathbf{x} \in \mathbb{R}^n : h(\mathbf{x}) \leq 0], \quad (26)$$

after Straub and Papaioannou (2014). The likelihood function is expressed as

$$L_i(\mathbf{x}) = \Pr(Z_i | \mathbf{X} = \mathbf{x}) = \Pr[h(\mathbf{x}) \leq 0]. \quad (27)$$

Note that when information is perfect, the likelihood is binary.

Examples of tests that lead to this type of information are proof-loading tests (which indicate whether a structure survives a certain load), inspections for failed components, and inspections for the absence or not of cracks. For instance, different techniques to detect cracks are characterised by a probability of detection (POD) curve, which indicates the probability of detecting a crack with depth a :

$$L_i(a) = \Pr(Z_i > 0 | A = a) = \text{POD}(a) = 1 - \exp\left(-\frac{a}{\xi}\right), \quad (28)$$

where ξ is a parameter that depends on the inspection technique and $Z_i > 0$ indicates detection of a crack.

Typically, the observations can be assumed to be statistically independent, in which case the likelihood function is given by

$$L(\mathbf{x}) = \prod_{i=1}^m L_i(\mathbf{x}). \quad (29)$$

5.2.3. System effects

Steel bridges and offshore structures usually contain a large number of structural components, which are subject to deterioration processes. The deterioration of these components is generally influenced by several factors. For instance, the fatigue deterioration of steel components is caused by cyclic loading and is influenced by the quality of steel, the quality and geometry of the welding and so on. Some of these causes of deterioration are often common to, or statistically dependent among, the components of a given system. Consequently, the deterioration processes happening at the different components are generally statistically dependent too (Vrouwenvelder 2004; Malioka 2009; Maljaars and Vrouwenvelder 2014; Zhang and Collette 2021). System effects is here understood as the joint effect of the deterioration processes within a system.

The statistical dependence among deterioration processes affects the structural reliability of a system. This is illustrated in Figure 9, where the system reliability index β_{sys} is plotted along the vertical axis and the horizontal axis represents the pair-wise correlation coefficient among the linearized deterioration limit states of the components, denoted ρ_M . For purely parallel systems, the system reliability reduces with increasing correlation, whereas for purely series systems, correlation increases the reliability. For mixed systems, the reliability typically reduces with increasing correlation within a broad range of ρ_M and increases with ρ_M for high correlation values (ca. $\rho_M = 0.9$ in the case shown in the figure). Nevertheless, these high correlation values are unlikely to be found in practical situations. Redundant truss systems and offshore jacket structures are examples of mixed systems. For redundant systems (either parallel or mixed), it is crucial to take the statistical dependence of the deterioration processes into account so that their reliability is not overestimated.

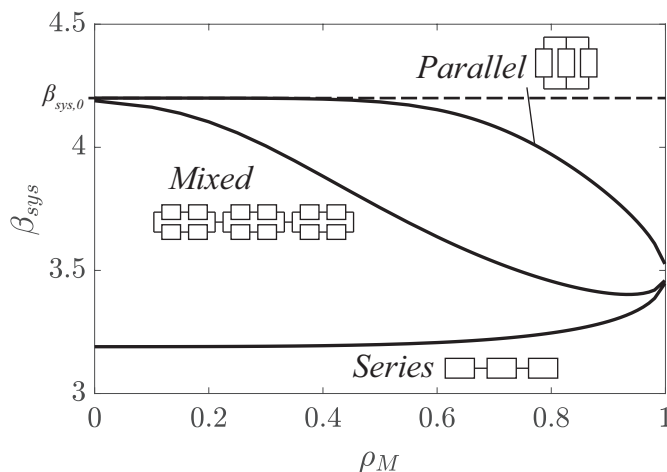


Figure 9: System reliability index β_{sys} as a function of the pair-wise correlation coefficient among components' safety margins ρ_M for three types of system: a purely parallel, a purely series and a mixed system. The intact reliability index is set to $\beta_{sys,0} = 4.2$ and the components' reliability indices to $\beta_C = 3.5$.

Structural redundancy is typically measured by what happens to the system should a component fail. For instance, the International Organization for Standardization (ISO) employs the residual influence factor (RIF) to measure redundancy (ISO 2020). The RIF, denoted RIF_i when related to a given component i , is defined as:

$$\text{RIF}_i = \frac{R_{m,Fi}}{R_{m,0}}, \quad (30)$$

where $R_{m,0}$ is the mean resistance of the intact system and $R_{m,Fi}$ is the mean resistance of the system given failure of only component i .

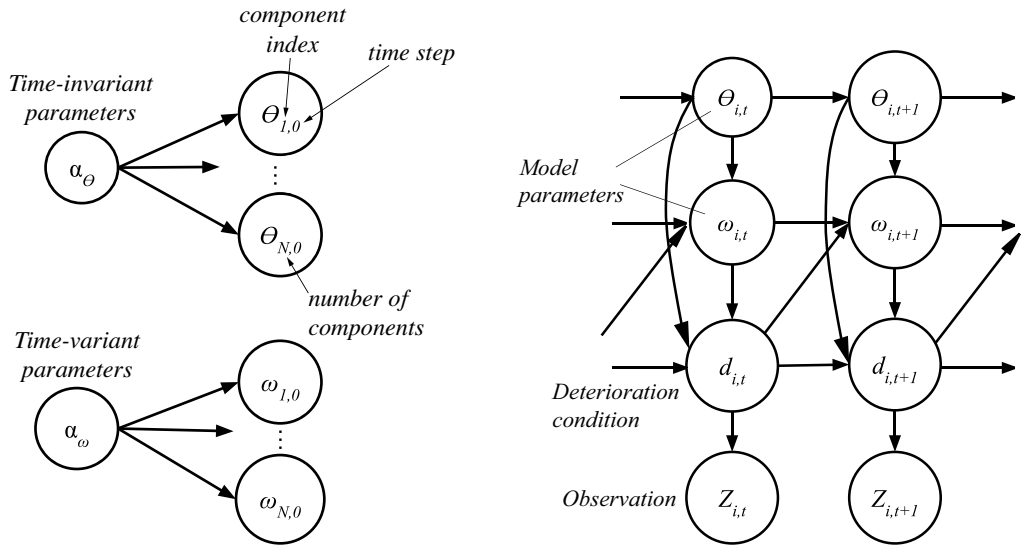
A more sophisticated parameter to quantify redundancy is the single element importance (SEI), which is defined, after Straub and Der Kiureghian (2011), as

$$\text{SEI}_i = \Pr(F_{sys} | \bar{F}_1 \cap \dots \cap \bar{F}_{i-1} \cap F_i \cap \bar{F}_{i+1} \cap \dots \cap \bar{F}_n) - \Phi(-\beta_{sys,0}), \quad (31)$$

where $\beta_{sys,0}$ is the annual reliability index of the intact system and $\Pr(F_{sys} | \bar{F}_1 \cap \dots \cap \bar{F}_{i-1} \cap F_i \cap \bar{F}_{i+1} \cap \dots \cap \bar{F}_n)$ is the annual probability of system failure conditional on failure of component i (F_i) and survival of the other $n - 1$ components ($\bar{F}_j, \forall j \neq i$). That is, the SEI measures the importance of a given component by how much the failure probability of the system increases if that component fails. In contrast with the RIF, the SEI accounts for the probabilistic model of the system.

Besides affecting the system reliability, the statistical dependence among deterioration processes influences the amount of information that one can get by inspecting or monitoring components of a structure. Based on the statistical dependence, the information that is obtained about the deterioration condition of one component can be used to update the predictions of the deterioration of other components. Therefore, implementing the deterioration dependencies into the structural reliability models can strongly affect the optimal design and inspection plan (Maljaars and Vrouwenvelder 2014).

Modelling structural systems and performing inference calculations is complex and computationally demanding. A promising approach are hierarchical BN models. Luque and Straub (2016) proposed a generic hierarchical BN to assess the time-dependent structural reliability of a system, see Figure 10. This BN is an extension of the model proposed in Straub (2009) that was illustrated in Figure 6. The spatial and temporal dependencies of the deterioration process are accounted for by the dependencies among time-variant ($\omega_{i,j}$) and time-invariant ($\theta_{i,j}$) parameters of the deterioration model, with i and j being the component and time indices, respectively. The dependencies of these parameters among the different components and time are captured through the hyper-parameters α_ω and α_θ , see Figure 10a. Let $d_{i,t}$ be an observable indicator of the deterioration condition of component i at time t . Initially, a prior model of $d_{i,t}$ is obtained using physics-based or empirical prediction models and the prior model of the parameters $\theta_{i,j}$ and $\omega_{i,j}$. If an imperfect measurement $z_{i,j}$ of $d_{i,t}$ is observed, the belief in $d_{i,t}$ can be updated. Furthermore, the observation evidence can be propagated through the BN to update the condition of all the components at all time steps. Efficient techniques for exact inference of the posterior distributions of the variables in the BN are available for discrete random variables (Straub 2009; Luque and Straub 2016).



(a) Dependence model of the deterioration parameters, based on Luque and Straub (2019).

(b) Deterioration process, adapted from Straub (2009).

Figure 10: Hierarchical Bayesian Network of multi-component systems subject to deterioration.

The BN is a visual representation of the causal interrelationships between the variables of the problem of interest. The visual aspect of BNs can be beneficial when discussing the model assumptions between the involved stakeholders. Computationally speaking, the performance of the exact inference algorithm presented in Luque and Straub (2016) are independent of the number of considered observation outcomes or the magnitude of the assessed probabilities of failure. On the negative side, the number of computations increases exponentially with the number of random variables in the deterioration model, which limits the modelling choices of deterioration and the system size. Furthermore, not all relevant dependence structures can be represented with the BN (Schneider 2020). Lastly, the efficiency of the BN is dramatically affected by the number of states used to discretize the continuous random variables. Although algorithms for efficient discretization have been developed in the literature, see e.g., Zhu and Collette (2015), their implementation requires additional efforts from the analyst.

Another existing approach to assess the time-variant reliability of a structural system is subset simulation (Au and Beck 2001). In contrast with the hierarchical BN, the subset simulation approach has the advantages of not being restricted by the number of considered random variables, requiring considerably less pre-processing efforts, and allowing for the implementation of more varied spatial and temporal dependence models (Schneider 2020). Limitations of the subset simulation approach are the errors incurred due to its sampling-based nature, and the reduced efficiency for increasing number of inference calculations and increasing reliability value to be estimated.

Chapter 2. Conclusions

In this chapter, the concluding remarks of the thesis are presented. First, the main findings and highlights of the appended scientific articles are summarised. After that, general conclusions are drawn and possibilities for further research are suggested.

1. Main findings and highlights

1.1. Paper I: Risk-based Fatigue Design Considering Inspections and Maintenance

State-of-the-art methods for fatigue design have largely neglected the joint optimisation of possible mitigation measures. Specifically, economical efforts dedicated to fatigue design and I&M could be balanced to more efficiently mitigate the fatigue failure risk. In this article, a common framework for the assessment of the performance of design and I&M fatigue mitigation measures is proposed. The performance of a life-cycle mitigation strategy is evaluated based on a risk-based objective function. A simplified cost model to coherently account for the costs associated with fatigue design and I&M is proposed for multimember structures such as truss systems and offshore jackets. The fatigue design of a structure can be efficiently specified by the fatigue design factor (FDF) of the fatigue hot spots, which is an indicator of the fatigue reliability. In this way, the structural design of a component is reduced to a single value.

A case study of a simple multimember offshore structure is used to exemplify the methodology. The hierarchical BN proposed in Luque and Straub (2019) is used to evaluate the time-variant system reliability and the expected life-cycle cost for various mitigation strategies. The results of the case study show the possibility of finding a balance between design and inspection and maintenance actions to efficiently mitigate fatigue failure risk in structural systems.

1.2. Paper II: Optimal life-cycle mitigation of fatigue failure risk for structural systems

Finding the optimal strategy to mitigate fatigue failure risk for a structural system is a highly demanding computational task. Currently, it cannot be expected that practi-

tioners conduct this type of optimisation for every structure. In this article, the patterns of the optimal fatigue mitigation strategy are studied as a function of key system features. The results of the study can be used to prescribe efficient mitigation strategies for structural systems.

The role played by a fatigue component within a system is captured by two parameters related to the redundancy and system size, after Straub and Der Kiureghian (2011). These two parameters determine a so-called equivalent Daniels system (EDS), which is a computationally advantageous system idealisation. A parametric study is performed over a reasonable range of the two parameters, covering common structural configurations. A cost model representative for offshore structures is used to study optimal reliability- and risk-based mitigation measures. The results show that it is often efficient to specify high fatigue reliabilities at design and less frequent inspections. Moreover, the results suggest that the higher fatigue design factors that are prescribed in design standards to avoid the need for inspections may not be sufficient. Lastly, we show that risk-based optimal mitigation strategies are often associated with lower reliabilities than the reliability-based optima. Therefore, it could be cost-efficient to lower the safety requirements for unmanned structures, such as OWT.

1.3. Paper III: Structural reliability analysis of offshore jackets for system-level fatigue design

The system-level fatigue design of offshore lattice structures is studied. System-level fatigue design consists of calibrating the fatigue reliabilities of the hot spots to achieve a given target system reliability. Offshore lattice structures contain a large number of fatigue hot spots, which makes the task of computing the system reliability unfeasible. Existing system-level fatigue design methods are based on approximations of the system reliability. Two existing methods are reviewed in the article: (a) The Health and Safety Executive (HSE) method (Moan 2002), and (b) The EDS method (Straub and Der Kiureghian 2011). Instead of using approximations, we propose a novel method named the *truncation algorithm* to compute upper and lower bounds of the system reliability. The truncation algorithm is used to assess the inherent safety level of HSE and the EDS design methods and to study system effects for several common bracing systems.

Observed evidence of low correlation among fatigue failures has been used as an argument to neglect the deterioration dependence in the analysis of the system reliability. We show numerically that these observations are nonetheless compatible with the observed evidence of high correlation among fatigue limit states, which is the relevant correlation to be considered for the assessment of the system reliability. Moreover, only first-member-failure deterioration states, i.e., deterioration states associated with one single member failed, are typically considered to assess the structural reliability of the deteriorated system. We demonstrate that complex deterioration states significantly contribute to the system probability of failure for redundant jacket systems. We show that the HSE method leads to highly unconservative designs for systems with medium to high redundancy, regardless of the correlation among fatigue processes. In contrast, the

EDS method leads to designs associated with close-to-target reliabilities while requiring computational demands comparable to the HSE method.

1.4. Paper IV: Analysis of fatigue test data of retrieved mooring chain links subject to pitting corrosion

Recent investigations have shown that the combined effect of pitting corrosion and fatigue is a safety hazard for mooring chains. There is a need to standardise the methods to assess this effect in order to inform design, reassessment and integrity management decisions of mooring systems. Fatigue resistance of mooring chains is typically assessed using S-N curves. In this article, we develop an extended S-N curve, from the analysis of fatigue test data of retrieved mooring chains, that explicitly takes into account the effect of pitting corrosion. Only limited and heterogeneous data is available, due to the high costs and difficulties of retrieving full-scale chain specimens. A hierarchical regression analysis is conducted to efficiently use available information and avoid possible biases in the quantification of the effects of interest. The analysis is based on a causal model of the deterioration process and a linear mixed-effects regression model. The inferred extended S-N model highlights that the effect of pitting corrosion is considerably higher than what can be explained by uniform corrosion alone. A case study is presented to illustrate the application of the model to the assessment of the structural reliability of a mooring chain segment.

1.5. Paper V: Value of information of in situ inspections of mooring lines

A framework based on VOI analysis is used to optimise discrete inspections of mooring systems. A discrete inspection comprises the evaluation of the corrosion level of a chain segment by an *in situ* technique. A mooring system is understood as hierarchically organised into four levels: (i) the chain segment, (ii) the mooring chain, (iii) the cluster of mooring chains, and (iv) the complete structural mooring system. It is economically unfeasible to inspect the complete mooring system, and therefore, discrete inspections should be optimised. The corrosion conditions of the various chain segments of a system are statistically dependent. Therefore, locally retrieved information can be used to update the predictions of the corrosion condition of the unobserved chain segments.

The state-of-the-art model proposed in Melchers (2004) is used to predict the time-evolution of pitting corrosion as a function of the seawater temperature. Thus, the corrosion conditions of the mooring segments are statistically dependent through their associated water temperature and the corrosion prediction model. A BN model is proposed to model the statistical dependence of the mooring system and to efficiently propagate locally retrieved information throughout the mooring system and thereby, update the estimation of the system reliability. The extended S-N model developed in Paper IV is employed to assess the fatigue resistance of a segment as a function of the fatigue load model and the corrosion condition. A VOI analysis is conducted to rank potential

inspection strategies at a given point in time. A case study is conducted to show the application of the method.

1.6. Paper VI: Risk-based Design of an Offshore Wind Turbine using VoI Analysis

A typical design objective for monopile support structures of offshore wind turbines is that the first natural frequency f_{n1} of the structural system lies within a given frequency band, called the soft-stiff region. The calculation of f_{n1} is typically based on finite element (FE) models considering soil-structure interaction, for which an estimate of the soil stiffness is needed. The soil stiffness can be estimated from *in situ* tests, which are costly and provide imperfect information. A VOI framework is proposed to support decisions on whether to conduct an additional soil test.

Failure is defined according to a fatigue limit state. A prior analysis is conducted to assess the optimal monopile diameter and thickness. A BN is proposed to conduct inference of potentially acquired information and conduct the preposterior decision analysis. This preliminary study provides the foundation for further research efforts to develop a rational framework to support decisions on *in situ* soil testing for the design of OWT. Furthermore, the results highlight one of the challenges of the VOI methodology, which is the definition of all possible limit states affecting the information retrieval decision.

2. General conclusions

Structural systems can be further optimised. The optimisation of structural design and integrity management is a major concern of structural engineering due to the large economical commitments dedicated to developing and maintaining the built environment and the magnitude of the environmental impact associated with building materials. The development and application of more sophisticated methods for the analysis and decision support of structures seem to be aligned with the societal preferences to address this concern. With this motivation in mind, the present thesis aims at improving the design and integrity management of deteriorating structures based on the integration of life-cycle decisions and the consideration of design at the system level.

2.1. Integrated life-cycle decisions

Decisions made sequentially can be coupled or integrated using Bayesian decision theory. In this thesis, the focus is primarily on the joint planning of design and I&M for deteriorating structures. In comparison to the separate planning of design and I&M mitigation measures, their joint planning, i.e., the planning of life-cycle mitigation strategies, allows to find more cost-efficient mitigation strategies. Generally, extending the design problem to consider I&M measures leads to more efficient life-cycle decisions. Furthermore, this approach is not detrimental for the achieved safety levels, as long as the I&M planning is reassessed throughout the service life of a structure.

The planning of life-cycle mitigation strategies is a sequential decision problem. That is, a design is to be specified first, followed by the assessment of an inspection plan conditional on the design specification. Provided that a sufficiently low number of candidate design specifications are considered, the optimal RBI plan can be assessed for each design and subsequently, the optimal life-cycle mitigation strategy can be computed, e.g., using the risk- or reliability-based objective functions proposed in this thesis. Thereby, the optimal assessment of life-cycle mitigation strategies scales linearly the computational demands of RBI planning with the number of considered design specifications.

RBI planning is a well explored, but computationally heavy decision problem. Methods exist in the literature to solve this problem, at least in a heuristic sense. Therefore, the optimisation of the integrated life-cycle mitigation strategy is also a feasible but computationally demanding task. Due to the demanding computations, the level of detail of the system model and the parametrization and scope of the design specifications should be carefully chosen. An appropriate design parametrization can be achieved through some indicator of the reliabilities of the deteriorating components, e.g., the FDF of the fatigue hot spots. This way, the design specifications consist of as many degrees of freedom as deteriorating components. Fatigue design standards prescribe a limited number of FDF values that lie within a narrow range. Thus, the extension of the scope of fatigue design standards to include life-cycle mitigation strategies seems feasible.

An attempt to balance the complexity and computational demands of the extended design problem is made in this thesis by generalising decision rules as a function of key system characteristics. The patterns of the optimal mitigation strategy were studied as a function of two parameters, which represent the redundancy of the system with respect to failure of a given component and the number of deteriorating components. This approach seems to be a promising solution to provide general recommendations on integrated life-cycle mitigation, and thereby extend their application to the general engineering practice.

In addition to the joint planning of design and I&M, other types of decisions can and should be combined into a common framework. For instance, decisions on information acquisition about site-specific parameters prior to construction can be coupled to design decisions. At the design point in time, the probabilistic model of the system can combine prior, generic information about the load and resistance parameters with site- and structure-specific information that can be obtained at a cost. VOI analysis can be employed to decide what information is worth obtaining, as it is illustrated in Paper VI.

2.2. System-level design

In contrast with component-level analysis, system-level analysis allows for a fairer assessment of the system reliability, resulting from the explicit assessment of the consequences of system and component failures, the consideration of system effects, and the propagation of information obtained at the component-level to update the system representation. Therefore, approximating a system by a number of independent (component-level) limit state functions is generally not justified.

System-level design is a consistent approach to design the deteriorating components

of structures to achieve a desired system reliability. Nonetheless, this design approach requires to compute the system reliability, which is a computationally demanding and often unfeasible task. The truncation algorithm proposed in this thesis can be employed to assess bounds of the structural reliability of systems subject to high-cycle fatigue and extreme environmental loads. These bounds are sufficiently narrow to conduct system-level design for most multimember offshore structures. Nevertheless, the computational costs of the truncation algorithm are too high to be iteratively applied to structural design. Instead, it is shown that the EDS algorithm proposed in Straub and Der Kiureghian (2011) is often a good and computationally efficient approximation. The truncation algorithm can then be used as a verification of the safety level associated with the obtained design solution.

Besides the larger computational costs of system-level design (compared to component-based design), another challenge is the ambiguity in the selection of the target system reliabilities. Design standards do not clearly state whether the prescribed target reliabilities apply to components or systems. Furthermore, it is not clear whether they apply to the intact or the deteriorated system. This challenge needs to be addressed, as discussed in the next section, to consistently apply system-level design.

The analysis of the reliability of fatigue deteriorating multimember offshore structures revealed that complex deterioration states, i.e., states characterised by several structural components failed due to fatigue, significantly contribute to the probability of system failure for redundant structures. Consequently, the criticality of a component cannot be simply characterised by what happens to the system should that component fail. Therefore, commonly used parameters to quantify structural redundancy, such as the residual influence factor or the single element importance, are not sufficient to generally characterise the redundancy of fatigue deteriorating systems.

3. Future outlook

3.1. Standardisation of integrated life-cycle mitigation

The following topics are suggested for further research:

- The statistical dependence of the deterioration processes among the components of a system has a strong impact on the system reliability, as shown in Section 5.2.3 and in Paper III. This statistical dependence is typically affected by several influencing factors, which are situation specific. Further studies should be carried out to assess the dependence among deterioration limit states for common design scenarios. Values of the correlation coefficients could be reported in design guidelines and standards so that practitioners can use them for system-level SRA, design and I&M planning. Furthermore, the statistical dependence among deterioration limit states should be considered when deriving semi-probabilistic formats for the design of the components of deteriorating systems.
- The investigation presented in paper II is a first attempt at generalising rules for the integrated design and I&M planning of deteriorating systems. Further

research should consider the comparison of the rules with the case-specific optimal mitigation strategies for a variety of structural systems and the implementation of other relevant deterioration models.

- Paper II contains a discussion on whether the target reliabilities prescribed by design standards refer to intact or deteriorated systems. This distinction is key for the optimal mitigation of deterioration in structural systems. Future studies should aim at optimising the two target reliabilities, i.e., a target reliability for the intact system and a target reliability for the deteriorated system.

3.2. Mitigation of human error effects

Although human errors in the design and execution of structures is identified as one of the main causes of structural failure, it is typically neglected in risk- and reliability-based design approaches (Melchers 1989). The mitigation of the failure risk due to human error is commonly left to be addressed by quality assurance and quality checks (El-Shahhat et al. 1995). Neglecting human error relies on the assumption that the optimal risk-based design or the optimal structural reliability is indifferent to it. This assumption is based on the fact that the risk-based objective function is not disturbed by human error in the vicinity of the optimum (Ditlevsen 1983). Whereas this assumption is reasonable for the optimisation of design parameters, it is not justified for the design or selection of structural configurations. Human errors may lead to significantly different consequences depending on the level of redundancy and robustness of the structural configuration. Therefore, the design of structural configurations can accommodate for the mitigation of human error consequences. As structural design moves its focus from the component to the system level, further studies should be conducted on the efficient mitigation of the consequences of human error.

3.3. Fatigue design of bottom-fixed offshore structures

Recommendations for further research applied to multimember offshore structures to support oil and gas and wind energy units and to monopiles for OWTs are derived based on the studies presented in papers III and VI.

3.3.1. Multimember offshore structures

- The truncation algorithm presented in paper III can be used to develop and test new approximate equations to assess the reliability of deteriorating systems. The plots in Figure 11 show, for systems with increasing redundancy, the exact (notional) system reliability index β_{sys} and the upper and lower bounds obtained with the truncation algorithm as a function of the pair-wise correlation coefficient among components' safety margins ρ_M . It can be seen that the exact value is closer to the lower bound for systems with low redundancy and becomes closer to the upper bound for increasing redundancy. Based on this pattern, approximate formulas to estimate the system reliability could be pursued.

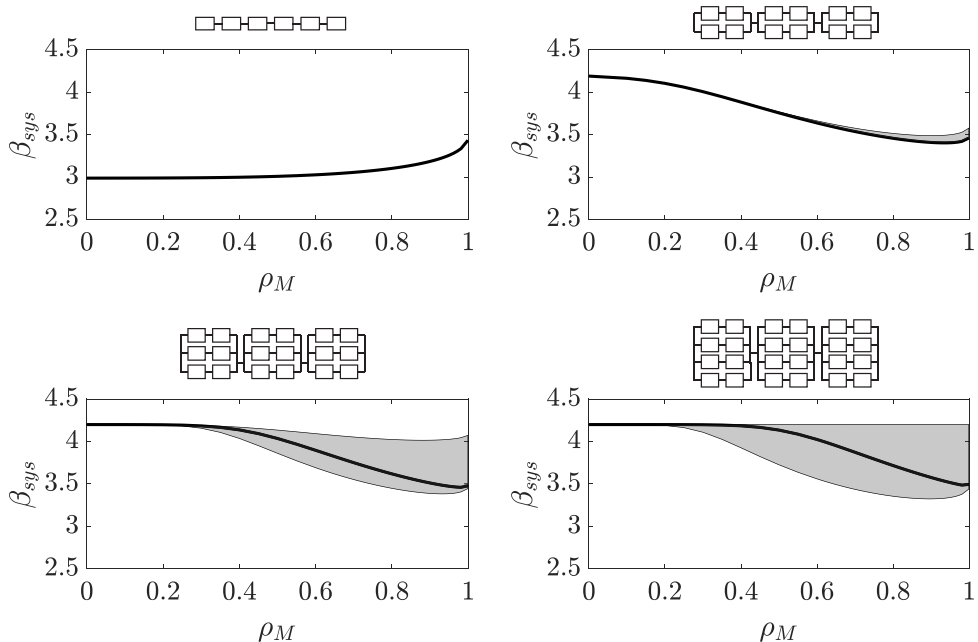


Figure 11: True system reliability index β_{sys} and upper and lower bounds obtained with the truncation algorithm (with truncation limit $n_{lim} = 3$) for mixed systems with increasing redundancy as a function of the pair-wise correlation coefficient among components' safety margins ρ_M . The intact reliability index is set to $\beta_{sys,0} = 4.2$ and the components' reliability indices to $\beta_C = 3.5$.

- The framework proposed in paper III can be used to estimate upper and lower bounds of the interval probability of system failure (see Eq. (15)) for multimember offshore structures subject to fatigue deterioration. The continuation of this work should consider the extension of the framework to assess the time-variant system reliability and to differentiate between design and I&M mitigation measures.
- Increasing redundancy for jacket-type systems is inevitably associated with increasing the number of welded connections and thereby, with increasing the probability of encountering fatigue hot-spot failures. Therefore, increasing redundancy while optimising the nominal design of the tubular members does not necessarily lead to safer structures. Further studies should be conducted on the efficiency of redundancy as a fatigue mitigation measure and on the joint optimisation of the fatigue design of the hot spots and the level of redundancy.

3.3.2. Monopiles for OWT

A study to quantify the value of *in situ* testing of the soil stiffness is presented in Paper VI. This is a preliminary study that should be continued before it is useful in practice. The following aspects should be further studied:

- A likelihood function that relates the soil test data with the soil-stiffness parameter

of interest was assumed in Paper VI. Further research should be devoted to developing this likelihood function from data. The following challenges are identified by taking as a reference the cone penetration test (CPT) (ISO 2012), which is one of the most common tests for the present purpose. The outcome of the CPT is the cone pressure at different depths, which is used to estimate a rather reliable soil stratigraphy and an average modulus of elasticity for each soil layer. These moduli of elasticity are estimated based on empirical models, which are associated with large uncertainties. It is noted that the estimated moduli of elasticity are not directly the parameters of interest, as the installation of the monopile, which is typically conducted by hammering, tends to compress the soil in the vicinity of the monopile. Therefore, the parameter of interest is the post-installation soil stiffness, which needs to be estimated using additional models. The uncertainties associated with the measured cone pressure and the models used to estimate the soil stiffness of interest need to be integrated to develop the likelihood function.

- The study in Paper VI considers the value of conducting one soil test and assumes a prior probabilistic model of the soil parameter of interest. In reality, a minimum number of CPTs are required (DNV-GL 2016). The results of these tests should be used to develop the prior probabilistic model of the soil parameter of interest. Ideally, this prior model should be developed based on all available test data, correlating the CPT results at different locations. The proposed VOI framework can then be used to decide among several potential *in situ* tests to be additionally conducted and the locations where they should be performed.

3.4. Design and integrity management of mooring systems subject to fatigue and pitting corrosion

Papers IV and V dealt with the design and integrity management of mooring systems subject to fatigue and pitting corrosion. The following topics are suggested to be further investigated:

- The mean stress effect and the corrosion effect could not be simultaneously inferred from the available data set. As a first attempt, existing models for mean stress correction were applied. This approach was successful at showing that the estimated corrosion effect is not significantly biased due to the various mean stresses applied at testing. Nevertheless, this approach cannot be used to account for the mean stress effect in the analysis of mooring systems, because the uncertainty associated with the application of the mean stress correction models to mooring chains is not known. Some of the available data could be used to develop mean stress correction models tailored to mooring chains and to assess the associated model uncertainties. To develop these models, stress-life diagrams could be developed to assess which model represents best the data. Furthermore, normalised amplitude-mean diagrams could be estimated to assess the model residuals, as described in Dowling (2013, p. 451–461). It is noted that this approach assumes that the mean stress and the corrosion effects are uncoupled, which should be verified.

- Provisionally, a subjective corrosion indicator was used to assess the severity of pitting corrosion for the chain specimens. An objective corrosion indicator should be developed to make the fatigue resistance model unambiguous and more useful in practice. The following approach is suggested to develop an objective corrosion indicator. It is assumed that three-dimensional (3D) scans of the chain-links that were tested for fatigue are available. Based on the 3D geometrical models, a number of presumably relevant features could be extracted, such as the pit depths and their location, the sharpness of the pits (first derivatives of the surface) and the number of pits. These features could be weighed depending on the location of the pits and combined into a single indicator. The weighting function can be developed based on failure frequency data (e.g., pits around the crown are often more critical than pits at the straight part) and FE analysis results of the stress field around a mooring link. Optimisation methods could be applied to find which indicator function of the surface condition predicts fatigue life the best.
- The effect of the number of chain links was neglected in the analysis of the fatigue test data. Haagenen and Köhler (2015) propose a method to estimate this effect based on order statistics and assuming full independence. More accurate estimations could be achieved by estimating the statistical dependence among the fatigue limit states at the different fatigue hot spots of a mooring chain. For this purpose, the correlation among common influencing factors should be measured. This is partially addressed with the BN model proposed in Paper V. Nevertheless, some factors that would affect the correlation were neglected to increase the computational efficiency of the model, e.g., the correlation due to common cyclic loading. Further empirical and analytical studies should be conducted to assess the effect of the number of chain links.
- The proposed VOI framework to rank *in situ* inspections of the corrosion condition of chain segments is a time-invariant approximation of the actual decision problem. A dynamic BN should be developed to assess the time-variant reliability of the mooring system and to assess the optimal sequential inspection plan. Although this extended BN would require significant additional computational demands and maybe render it unpractical, it could be used to test the validity of the approximate decision model proposed in Paper V.
- Corrosion pits act as stress raisers, accelerating the development of fatigue cracks and reducing the fatigue life of mooring chain links. Consequently, the efficiency of increasing the cross-sectional area of chain links as a fatigue mitigation measure is limited. The efficiency of inspection and maintenance measures is also questionable due to the elevated costs of offshore operations. The mooring system representation proposed in Paper V could be integrated into the framework proposed in Paper I to study optimal life-cycle mitigation strategies for mooring chains subject to combined pitting corrosion and fatigue.

References

- Almar-Naess, A., P. J. Haagenen, B. Lian, T. Moan, and T. Simonsen (Mar. 1984). “Investigation of the Alexander L. Kielland Failure—Metallurgical and Fracture Analysis”. In: *Journal of Energy Resources Technology* 106.1, pp. 24–31. ISSN: 0195-0738. DOI: 10.1115/1.3231014.
- ASCE (2021). *Infrastructure Report Card*. Tech. rep. American Society of Civil Engineers. URL: <https://infrastructurereportcard.org/wp-content/uploads/2020/12/Bridges-2021.pdf>.
- Athenosy, L., E. Omic, and J. Halb (2017). *Investing in Public Infrastructure in Europe*. Tech. rep. Council of Europe Development Bank. URL: https://coebank.org/media/documents/Investing_in_Public_Infrastructure_in_Europe.27dc1Pg.pdf.
- Au, S.-K. and J. L. Beck (2001). “Estimation of small failure probabilities in high dimensions by subset simulation”. In: *Probabilistic Engineering Mechanics* 16.4, pp. 263–277. ISSN: 0266-8920. DOI: 10.1016/S0266-8920(01)00019-4. URL: <https://www.sciencedirect.com/science/article/pii/S0266892001000194>.
- Bakens, W., G. Foliente, and M. Jasuja (2005). “Engaging stakeholders in performance-based building: lessons from the Performance-Based Building (PeBBu) Network”. In: *Building Research & Information* 33.2, pp. 149–158. DOI: 10/cqsp92.
- Baravalle, M. and J. Köhler (2019). “A risk-based approach for calibration of design codes”. In: *Structural Safety* 78, pp. 63–75. ISSN: 0167-4730. DOI: 10.1016/j.strusafe.2018.12.003. URL: <https://www.sciencedirect.com/science/article/pii/S0167473017303223>.
- Beck, A. T. (2003). “Reliability Analysis of Degrading Uncertain Structures-with Applications to Fatigue and Fracture under Random Loading”. PhD thesis. Newcastle, Australia: The University of Newcastle.
- Beck, A. T. and R. E. Melchers (2004). “Overload failure of structural components under random crack propagation and loading – a random process approach”. In: *Structural Safety* 26.4, pp. 471–488. ISSN: 0167-4730. DOI: j.strusafe.2004.02.001. URL: <https://www.sciencedirect.com/science/article/pii/S0167473004000165>.

- Beck, J. L. and S.-K. Au (2002). “Bayesian Updating of Structural Models and Reliability using Markov Chain Monte Carlo Simulation”. In: *Journal of Engineering Mechanics* 128.4, pp. 380–391. DOI: 10.1061/(ASCE)0733-9399(2002)128:4(380).
- Benjamin, J. R. and C. A. Cornell (2014). *Probability, statistics, and decision for civil engineers*. Mineola, New York: Dover publications, INC. ISBN: 978-0-486-78072-6.
- Bergström, M. (2017). “A simulation-based design method for arctic maritime transport systems”. PhD thesis. Trondheim, Norway: Norwegian University of Science and Technology.
- Bergström, M., S. O. Erikstad, and S. Ehlers (2016). “Assessment of the applicability of goal- and risk-based design on Arctic sea transport systems”. In: *Ocean Engineering* 128, pp. 183–198. ISSN: 0029-8018. DOI: 10.1016/j.oceaneng.2016.10.040. URL: <https://www.sciencedirect.com/science/article/pii/S0029801816304838>.
- Bismut, E., J. Luque, and D. Straub (2017). “Optimal prioritization of inspections in structural systems considering component interactions and interdependence”. In: *Proc. 12th International Conference on Structural Safety & Reliability ICOSSAR 2017, Vienna, Austria*.
- Bismut, E. and D. Straub (2021). “Optimal adaptive inspection and maintenance planning for deteriorating structural systems”. In: *Reliability Engineering & System Safety* 215, p. 107891. ISSN: 0951-8320. DOI: 10.1016/j.res.2021.107891. URL: <https://www.sciencedirect.com/science/article/pii/S0951832021004063>.
- Byers, W. G., M. J. Marley, J. Mohammadi, R. J. Nielsen, and S. Sarkani (1997). “Fatigue reliability reassessment applications: state-of-the-art paper”. In: *Journal of Structural Engineering* 123.3, pp. 277–285. DOI: [https://doi.org/10.1061/\(ASCE\)0733-9445\(1997\)123:3\(277\)](https://doi.org/10.1061/(ASCE)0733-9445(1997)123:3(277)).
- CEN (2002). *Eurocode 0: Basis of Structural Design*. Standard EN 1990:2002. Brussels, Belgium: European Committee for Standardization.
- Congresional Budget Office (2017). *Spending on Infrastructure and Investment*. Tech. rep. Accessed: 2018-05-31. URL: <https://www.cbo.gov/publication/52463>.
- Coyne, R. D., M. A. Rosenman, A. D. Radford, M. Balachandran, and J. S. Gero (1990). *Knowledge-Based Design Systems*. Ed. by R. D. Coyne. Addison-Wesley. ISBN: 978-0201103816.
- Daly, A. F. (2000). “Bridge management in Europe (BRIME): modelling of deteriorated structures”. In: *Bridge management 4*, pp. 552–559. DOI: 10.1680/bm4.28548.0066. URL: <https://www.icevirtuallibrary.com/doi/abs/10.1680/bm4.28548.0066>.
- Darwiche, A. (2009). *Modeling and reasoning with Bayesian networks*. Avenue of the Americas, New York: Cambridge university press. ISBN: 978-0-521-88438-9.
- Dasgupta, S., C. H. Papadimitriou, and U. V. Vazirani (2008). *Algorithms*. McGraw-Hill Higher Education New York.
- Ditlevsen, O. (1979). “Narrow Reliability Bounds for Structural Systems”. In: *Journal of Structural Mechanics* 7.4, pp. 453–472. DOI: 10.1080/03601217908905329.

- Ditlevsen, O. (1983). “Fundamental postulate in structural safety”. In: *Journal of Engineering Mechanics* 109.4, pp. 1096–1102. DOI: 10.1061/(ASCE)0733-9399(1983)109:4(1096).
- Ditlevsen, O. and H. O. Madsen (1996). *Structural reliability methods*. Copenhagen, Denmark: Wiley New York. ISBN: 0-471-96086-1.
- DNV-GL (2016). *Support structures for wind turbines*. Standard DNVGL-ST-0126.
- Dong, Y. and D. M. Frangopol (2015). “Risk-informed life-cycle optimum inspection and maintenance of ship structures considering corrosion and fatigue”. In: *Ocean Engineering* 101, pp. 161–171. ISSN: 0029-8018. DOI: 10.1016/j.oceaneng.2015.04.020. URL: <https://www.sciencedirect.com/science/article/pii/S0029801815000955>.
- Dowling, N. E. (2013). *Mechanical behavior of materials: engineering methods for deformation, fracture, and fatigue*. 4th ed. Boston, Mass: Pearson Education. ISBN: 9780131395060.
- Duijm, N. J. (2015). “Recommendations on the use and design of risk matrices”. In: *Safety Science* 76, pp. 21–31. ISSN: 0925-7535. DOI: 10.1016/j.ssci.2015.02.014. URL: <https://www.sciencedirect.com/science/article/pii/S0925753515000429>.
- Echard, B., N. Gayton, and M. Lemaire (2011). “AK-MCS: An active learning reliability method combining Kriging and Monte Carlo Simulation”. In: *Structural Safety* 33.2, pp. 145–154. ISSN: 0167-4730. DOI: 10.1016/j.strusafe.2011.01.002. URL: <https://www.sciencedirect.com/science/article/pii/S0167473011000038>.
- Eidsvik, J., G. Martinelli, and D. Bhattacharjya (2018). “Sequential information gathering schemes for spatial risk and decision analysis applications”. In: *Stochastic environmental research and risk assessment* 32.4, pp. 1163–1177. DOI: <https://doi.org/10.1007/s00477-017-1476-y>.
- Eidsvik, J., T. Mukerji, and D. Bhattacharjya (2015). *Value of information in the earth sciences: Integrating spatial modeling and decision analysis*. University Printing House, Cambridge, United Kingdom: Cambridge University Press. ISBN: 978-1-107-04026-7.
- Faber, M. H. (2015). “Codified risk informed decision making for structures”. In: *Proceedings of the symposium on reliability of engineering systems (SRES2015)*. Hangzhou, China.
- Faber, M., J. Qin, S. Miraglia, and S. Thöns (2017). “On the Probabilistic Characterization of Robustness and Resilience”. In: *Procedia Engineering* 198. Urban Transitions Conference, Shanghai, September 2016, pp. 1070–1083. ISSN: 1877-7058. DOI: 10.1016/j.proeng.2017.07.151. URL: <https://www.sciencedirect.com/science/article/pii/S1877705817329983>.
- Faber, M. and M. Stewart (2003). “Risk assessment for civil engineering facilities: critical overview and discussion”. In: *Reliability Engineering & System Safety* 80.2, pp. 173–184. ISSN: 0951-8320. DOI: 10.1016/S0951-8320(03)00027-9. URL: <https://www.sciencedirect.com/science/article/pii/S0951832003000279>.

- Farmer, F. R. (1967). “Siting Criteria-A New Approach”. In: *Proc. Symp. On the Containment and Siting of Nuclear Power Plants*, pp. 303–318.
- FHWA (2020). *National Bridge Inventory*. <https://www.fhwa.dot.gov/bridge/nbi/ascii.cfm> [Accessed: 2020-02-05].
- Fischer, K., E. Virguez, M. Sánchez-Silva, and M. H. Faber (2013). “On the assessment of marginal life saving costs for risk acceptance criteria”. In: *Structural Safety* 44, pp. 37–46. ISSN: 0167-4730. DOI: 10.1016/j.strusafe.2013.05.001. URL: <https://www.sciencedirect.com/science/article/pii/S0167473013000386>.
- Foliente, G. C. (2000). “Developments in performance-based building codes and standards”. In: *Forest Products Journal* 50.7/8, pp. 12–21.
- Fontaine, E., A. Kilner, C. Carra, D. Washington, K. Ma, A. Phadke, D. Laskowski, G. Kusinski, et al. (2014). “Industry survey of past failures, pre-emptive replacements and reported degradations for mooring systems of floating production units”. In: *Offshore Technology Conference*. OTC-25273-MS.
- Gordon, R. B., M. G. Brown, E. M. Allen, et al. (2014). “Mooring integrity management: a state-of-the-art review”. In: *Offshore Technology Conference*. OTC-25134-MS.
- Guedes, C., A. Jasionowski, J. Jensen, D. McGeorge, A. Papanikolaou, P. Esa, P. C. Sames, R. Skjong, J. Skovbakke, and D. Vassalos (2009). *Risk-based ship design: Methods, tools and applications*. Ed. by A. Papanikolaou. Springer Science & Business Media.
- Haagensen, P. J. and J. Köhler (Jan. 2015). *Fatigue testing of mooring chains - statistical analysis of data from test series with different number of chain links*. Memo. Department of Structural Engineering, NTNU.
- Hasofer, A. M. and N. C. Lind (1974). “Exact and invariant second-moment code format”. In: *Journal of the Engineering Mechanics division* 100.1, pp. 111–121.
- Hasofer, A. and N. C. Lind (1973). *An exact and invariant first-order reliability format*. Solid Mechanics Division, University of Waterloo.
- ISO (2012). *Geotechnical investigation and testing — Field testing — Part 1: Electrical cone and piezocone penetration test*. Standard ISO 22476-1:2012. Geneva, Switzerland: International Organization for Standardization.
- ISO (2015). *General principles on reliability for structures*. Standard ISO 2394:2015. Geneva, Switzerland: International Organization for Standardization.
- ISO (2020). *Petroleum and natural gas industries — Fixed steel offshore structures*. Standard ISO 19902:2020. Geneva, Switzerland: International Organization for Standardization.
- JCSS (2001). *Probabilistic Model Code. Part 1 - Basis of design*. Standard. Joint Committee on Structural Safety.
- Kalaitzidakis, P. and S. Kalyvitis (July 2005). ““New” public investment and/or maintenance in public capital for growth? The Canadian experience”. In: *Economic inquiry : journal of the Western Economic Association* 43.3, pp. 586–600. ISSN: 0095-2583.

- Kochenderfer, M. J. (2015). *Decision making under uncertainty: theory and application*. Cambridge, Massachusetts, USA: MIT press. ISBN: 978-0-262-02925-4.
- Kupolati, W. K. (2010). “Environmental Impact Assessment Of Civil Engineering Infrastructure Development Projects”. In: *OIDA International Journal of Sustainable Development* 2.4, pp. 57–66.
- Kurtz, N. and J. Song (2013). “Cross-entropy-based adaptive importance sampling using Gaussian mixture”. In: *Structural Safety* 42, pp. 35–44. ISSN: 0167-4730. DOI: 10.1016/j.strusafe.2013.01.006. URL: <https://www.sciencedirect.com/science/article/pii/S0167473013000131>.
- Lagerveld, S., C. Rockmann, M. Scholl, H. Bartelings, S. van den Burg, R. Jak, H. Jansen, J. Klijnstra, M. Leopold, M. Poelman, et al. (2014). *Combining offshore wind energy and large-scale mussel farming: background & technical, ecological and economic considerations*. Tech. rep. IMARES.
- Lotsberg, I., G. Sigurdsson, A. Fjeldstad, and T. Moan (2016). “Probabilistic methods for planning of inspection for fatigue cracks in offshore structures”. In: *Marine Structures* 46, pp. 167–192. ISSN: 0951-8339. DOI: 10.1016/j.marstruc.2016.02.002. URL: <https://www.sciencedirect.com/science/article/pii/S0951833916000071>.
- Luque, J. and D. Straub (2016). “Reliability analysis and updating of deteriorating systems with dynamic Bayesian networks”. In: *Structural Safety* 62, pp. 34–46. ISSN: 0167-4730. DOI: 10.1016/j.strusafe.2016.03.004. URL: <https://www.sciencedirect.com/science/article/pii/S0167473016300029>.
- Luque, J. and D. Straub (2019). “Risk-based optimal inspection strategies for structural systems using dynamic Bayesian networks”. In: *Structural Safety* 76, pp. 68–80. ISSN: 0167-4730. DOI: 10.1016/j.strusafe.2018.08.002. URL: <https://www.sciencedirect.com/science/article/pii/S0167473017302138>.
- Madsen, H. O. and J. D. Sørensen (July 1990). “Probability-based optimization of fatigue design, inspection and maintenance”. In: *Int. Symp. on Offshore Structures*.
- Madsen, H. O., S. Krenk, and N. C. Lind (2006). *Methods of structural safety*. Courier Corporation.
- Malioka, V. (2009). *Condition indicators for the assessment of local and spatial deterioration of concrete structures*. Vol. 321. VDF Hochschulverlag AG an der ETH Zürich.
- Maljaars, J. and A. Vrouwenvelder (2014). “Probabilistic fatigue life updating accounting for inspections of multiple critical locations”. In: *International Journal of Fatigue* 68, pp. 24–37. ISSN: 0142-1123. DOI: 10.1016/j.ijfatigue.2014.06.011. URL: <https://www.sciencedirect.com/science/article/pii/S0142112314001741>.
- Melchers, R. E. (2004). “Pitting corrosion of mild steel in marine immersion environment—Part I: Maximum pit depth”. In: *Corrosion* 60.9, pp. 824–836. ISSN: 0010-9312. eprint: <https://onepetro.org/corrosion/article-pdf/2186064/nace-04090824.pdf>.

- Melchers, R. and R. Jeffrey (2008). “Probabilistic models for steel corrosion loss and pitting of marine infrastructure”. In: *Reliability Engineering & System Safety* 93.3. Probabilistic Modelling of Structural Degradation, pp. 423–432. ISSN: 0951-8320. DOI: 10.1016/j.res.2006.12.006. URL: <https://www.sciencedirect.com/science/article/pii/S0951832007000051>.
- Melchers, R. (1989). “Human error in structural design tasks”. In: *Journal of structural engineering* 115.7, pp. 1795–1807. DOI: 10.1061/(ASCE)0733-9445(1989)115:7(1795).
- Melchers, R. E. and A. T. Beck (2018). *Structural reliability analysis and prediction*. West Sussex, UK: John Wiley & Sons Ltd. ISBN: 9781119265993.
- Memarzadeh, M., M. Pozzi, and J. Zico Kolter (2014). “Optimal planning and learning in uncertain environments for the management of wind farms”. In: *Journal of Computing in Civil Engineering* 29.5, p. 04014076. DOI: 10.1061/(ASCE)CP.1943-5487.0000390.
- Mendoza, J., E. Bismut, D. Straub, and J. Köhler (Mar. 2020). “Risk-based Fatigue Design Considering Inspections and Maintenance”. In: *ASCE ASME J Risk Uncertain Eng Syst A Civ Eng* 7.1, p. 04020055. DOI: 10.1061/AJRU6.0001104.
- Miedema, R. (2012). “Offshore Wind Energy Operations & Maintenance Analysis”. In: *Hoge school van Amsterdam*.
- Moan, T. (2002). “Target levels for reliability-based assessment of offshore structures during design and operation”. In: *Offshore Technology report 1990/060*. Vol. 60. HSE BOOKS. ISBN: 0-7176-2303-3.
- Moan, T. (2018). “Life cycle structural integrity management of offshore structures”. In: *Structure and Infrastructure Engineering* 14.7, pp. 911–927. DOI: 10.1080/15732479.2018.1438478. URL: <https://doi.org/10.1080/15732479.2018.1438478>.
- Moan, T. and R. Song (2000). “Implications of Inspection Updating on System Fatigue Reliability of Offshore Structures”. In: *Journal of Offshore Mechanics and Arctic Engineering* 122.3, pp. 173–180. ISSN: 0892-7219. DOI: 10.1115/1.1286601. eprint: https://asmedigitalcollection.asme.org/offshoremechanics/article-pdf/122/3/173/5930142/173_1.pdf.
- Nathwani, J. S., N. C. Lind, and M. D. Pandey (1997). “Affordable safety by choice: the life quality method”. In: *Institute for risk research* 245, p. 1997.
- Neumann, J. von and O. Morgenstern (1966). *Theory of games and economic behavior*. 3rd ed. Princeton university press.
- Nielsen, J. S. (2013). “Risk-based operation and maintenance of offshore wind turbines”. PhD thesis. Aalborg, Denmark: Aalborg University. ISBN: 978-87-93102-46-0.
- Nielsen, J. S., L. Miller-Branovacki, and R. Carriveau (2021). “Probabilistic and risk-informed life extension assessment of wind turbine structural components”. In: *Energies* 14.4. DOI: 10.3390/en14040821.

- Nielsen, J. S. and J. D. Sørensen (2012). “Maintenance optimization for offshore wind turbines using POMDP”. In: *Reliability and Optimization of Structural System: IFIP WG 7.5 working group conference*. American University of Armenia Press, Yerevan, Armenia, pp. 175–182.
- Nielsen, T. D. and F. V. Jensen (2009). *Bayesian networks and decision graphs*. New York, USA: Springer Science & Business Media.
- Papadimitriou, C. H. and J. N. Tsitsiklis (1987). “The complexity of Markov decision processes”. In: *Mathematics of operations research* 12.3, pp. 441–450. DOI: 10.1287/moor.12.3.441.
- Papaioannou, I., S. Geyer, and D. Straub (2019). “Improved cross entropy-based importance sampling with a flexible mixture model”. In: *Reliability Engineering & System Safety* 191, p. 106564. ISSN: 0951-8320. DOI: 10.1016/j.ress.2019.106564. URL: <https://www.sciencedirect.com/science/article/pii/S0951832019301528>.
- Papaioannou, I., C. Papadimitriou, and D. Straub (2016). “Sequential importance sampling for structural reliability analysis”. In: *Structural Safety* 62, pp. 66–75. ISSN: 0167-4730. DOI: 10.1016/j.strusafe.2016.06.002. URL: <https://www.sciencedirect.com/science/article/pii/S0167473016300169>.
- Papalambros, P. Y. and D. J. Wilde (2000). *Principles of Optimal Design. Modeling and Computation*. 2nd ed. Cambridge University Press.
- Pearl, J. (1988). *Probabilistic reasoning in intelligent systems: networks of plausible inference*. Ed. by M. B. Morgan. 2nd ed. San Francisco, CA 94104: Morgan Kaufmann publishers, INC. ISBN: 1-55860-479-0.
- Pozzi, M. and A. Der Kiureghian (2011). “Assessing the value of information for long-term structural health monitoring”. In: *Health monitoring of structural and biological systems 2011*. Vol. 7984. International Society for Optics and Photonics, 79842W. DOI: 10.1117/12.881918.
- Raiffa, H. and R. Schlaifer (1961). *Applied statistical decision theory*. Cambridge University Press.
- Rioja, F. (2013). “What is the value of Infrastructure Maintenance? A Survey”. In: *Infrastructure and Land Policies*. Vol. 13. Cambridge, Massachusetts: Lincoln Institute of Land Policy, pp. 347–365.
- Russell, S. and P. Norvig (2013). *Artificial Intelligence: A Modern Approach*. eng. Pearson custom library. Harlow: Pearson Education UK. ISBN: 9781292024202.
- Schneider, R. (2020). “Time-variant reliability of deteriorating structural systems conditional on inspection and monitoring data”. PhD thesis. Technische Universität München. DOI: 10.13140/RG.2.2.21487.87207.
- Schneider, R., S. Thöns, and D. Straub (2017). “Reliability analysis and updating of deteriorating systems with subset simulation”. In: *Structural Safety* 64, pp. 20–36. ISSN: 0167-4730. DOI: 10.1016/j.strusafe.2016.09.002. URL: <https://www.sciencedirect.com/science/article/pii/S0167473016300674>.

- El-Shahhat, A. M., D. V. Rosowsky, and W.-F. Chen (1995). “Accounting for human error during design and construction”. In: *Journal of Architectural Engineering* 1.2, pp. 84–92. DOI: 10.1061/(ASCE)1076-0431(1995)1:2(84).
- Soliman, M., D. M. Frangopol, and A. Mondoro (2016). “A probabilistic approach for optimizing inspection, monitoring, and maintenance actions against fatigue of critical ship details”. In: *Structural Safety* 60, pp. 91–101. ISSN: 0167-4730. DOI: 10.1016/j.strusafe.2015.12.004. URL: <https://www.sciencedirect.com/science/article/pii/S0167473016000047>.
- Solland, G., G. Sigurdsson, and A. Ghosal (2011). “Life Extension and Assessment of Existing Offshore Structures”. In: SPE Project and Facilities Challenges Conference at METS SPE 142858. Society of Petroleum Engineers. DOI: 10.2118/142858-MS. URL: <https://onepetro.org/spemets/proceedings-pdf/11METS/All-11METS/SPE-142858-MS/1696814/spe-142858-ms.pdf>.
- Straub, D. (2004). “Generic approaches to risk based inspection planning for steel structures”. PhD thesis. Zürich, Switzerland: Swiss Federal Institute of Technology Zürich.
- Straub, D. (2009). “Stochastic modeling of deterioration processes through dynamic Bayesian networks”. In: *Journal of Engineering Mechanics* 135.10, pp. 1089–1099. DOI: 10.1061/(ASCE)EM.1943-7889.0000024.
- Straub, D. (2011). “Reliability updating with equality information”. In: *Probabilistic Engineering Mechanics* 26.2, pp. 254–258. ISSN: 0266-8920. DOI: 10.1016/j.probenmech.2010.08.003. URL: <https://www.sciencedirect.com/science/article/pii/S026689201000069X>.
- Straub, D. (2014). “Value of information analysis with structural reliability methods”. In: *Structural Safety* 49. Special Issue In Honor of Professor Wilson H. Tang, pp. 75–85. ISSN: 0167-4730. DOI: 10.1016/j.strusafe.2013.08.006. URL: <https://www.sciencedirect.com/science/article/pii/S0167473013000611>.
- Straub, D. and A. Der Kiureghian (2011). “Reliability acceptance criteria for deteriorating elements of structural systems”. In: *Journal of Structural Engineering* 137.12, pp. 1573–1582. DOI: 10.1061/(ASCE)ST.1943-541X.0000425.
- Straub, D. and M. H. Faber (2005). “Risk based inspection planning for structural systems”. In: *Structural Safety* 27.4, pp. 335–355. ISSN: 0167-4730. DOI: 10.1016/j.strusafe.2005.04.001. URL: <https://www.sciencedirect.com/science/article/pii/S016747300500024X>.
- Straub, D. and I. Papaioannou (2014). “Bayesian updating with structural reliability methods”. In: *Journal of Engineering Mechanics* 141.3, p. 04014134. DOI: 10.1061/(ASCE)EM.1943-7889.0000839.
- Straub, D., R. Schneider, E. Bismut, and H.-J. Kim (2020). “Reliability analysis of deteriorating structural systems”. In: *Structural Safety* 82, p. 101877. ISSN: 0167-4730. DOI: 10.1016/j.strusafe.2019.101877. URL: <http://www.sciencedirect.com/science/article/pii/S0167473018303254>.

- Thoft-Cristensen, P. and M. J. Baker (2012). *Structural reliability theory and its applications*. Heidelberg, Germany: Springer Science & Business Media.
- Thöns, S. (2018). “On the Value of Monitoring Information for the Structural Integrity and Risk Management”. In: *Computer-Aided Civil and Infrastructure Engineering* 33.1, pp. 79–94. DOI: 10.1111/mice.12332.
- US NBS (1925). *Recommended Practice for Arrangement of Building Codes*. Standard. Washington DC, USA: US Department of Commerce.
- Vårdal, O., T. Moan, N.-C. Hellevig, et al. (1999). “Comparison between observed and predicted characteristics of fatigue cracks in North Sea jackets”. In: *Offshore Technology Conference*. OTC 10847.
- Verzobio, A., D. Bolognani, J. Quigley, and D. Zonta (2021). “Quantifying the benefit of structural health monitoring: can the value of information be negative?” In: *Structure and Infrastructure Engineering* 0.0, pp. 1–22. DOI: 10.1080/15732479.2021.1890139.
- Vrouwenvelder, A. C. W. M. (2004). “Spatial correlation aspects in deterioration models”. In: *Proceedings 2nd International Conference on Lifetime-Oriented Design Concepts*.
- Walker-Morison, A., T. Grant, and S. McAlister (2007). “The environmental impact of building materials”. In: *Environment Design Guide*, pp. 1–9.
- Yang, D. Y. and D. M. Frangopol (2021). “Risk-based inspection planning of deteriorating structures”. In: *Structure and Infrastructure Engineering* 0.0, pp. 1–20. DOI: 10.1080/15732479.2021.1907600.
- Zhang, K. and M. Collette (2021). “Experimental investigation of structural system capacity with multiple fatigue cracks”. In: *Marine Structures* 78, p. 102943. ISSN: 0951-8339. DOI: 10.1016/j.marstruc.2021.102943. URL: <https://www.sciencedirect.com/science/article/pii/S0951833921000095>.
- Zhu, J. and M. Collette (2015). “A dynamic discretization method for reliability inference in Dynamic Bayesian Networks”. In: *Reliability Engineering & System Safety* 138, pp. 242–252. ISSN: 0951-8320. DOI: 10.1016/j.ress.2015.01.017. URL: <http://www.sciencedirect.com/science/article/pii/S0951832015000277>.
- Ziegler, L. (2018). “Assessment of monopiles for lifetime extension of offshore wind turbines”. PhD thesis. Trondheim, Norway: Norwegian University of Science and Technology.

Appended papers

Paper I. Risk-based Fatigue Design Considering Inspections and Maintenance

Mendoza, J., E. Bismut, D. Straub, and J. Köhler (2020). “Risk-based Fatigue Design Considering Inspections and Maintenance”. In: *ASCE ASME J Risk Uncertain Eng Syst A Civ Eng* 7.1., pp. 04020055. DOI: 10.1061/AJRUA6.0001104.

The post-peer-review, copy-edited version of the article published in ASCE-ASME Journal of Risk and Uncertainty in Engineering Systems Part A: Civil Engineering is available at: <https://doi.org/10.1061/AJRUA6.0001104>.

The main idea of the paper was proposed by J. Mendoza. The computations were built on prior efforts by E. Bismut and D. Straub to assess inference using a hierarchical Bayesian Network. The case study was developed by J. Mendoza. The paper was structured and written by J. Mendoza, with editing by all co-authors.

This Paper is not included in NTNU Open due to copyright an archived version is available at <https://hdl.handle.net/11250/2680374> or publisher version at <https://doi.org/10.1061/AJRUA6.0001104>

Paper II. Optimal life-cycle mitigation of fatigue failure risk for structural systems

Mendoza, J., E. Bismut, D. Straub, and J. Köhler (2021). “Optimal life-cycle mitigation of fatigue failure risk for structural systems”. Submitted for publication to a peer-reviewed journal.

The main idea of the paper was proposed by J. Mendoza with contributions by D. Straub and J. Köhler. The code written by E. Bismut and D. Straub to assess inference using a hierarchical Bayesian Network was adapted and extended to the time-variant reliability of equivalent Daniels systems (EDS). D. Straub developed the code to estimate the equivalent Daniels system parameters. The computations were conducted by J. Mendoza. The paper was structured and written by J. Mendoza, with editing by all co-authors.

This Paper is awaiting publication and is not included in NTNU Open

Paper III. Structural reliability analysis of offshore jackets for system-level fatigue design

Mendoza, J., J.S. Nielsen, J.D. Sørensen, and J. Köhler (2021). “Structural reliability analysis of offshore jackets for system-level fatigue design”. Submitted for publication to a peer-reviewed journal.

The main idea of the paper was proposed by J. Mendoza with contributions by all co-authors. J.D. Sørensen contributed to attempting a fair representation of the ISO 19902:2007 and DNVGL-RP-C203 probabilistic models. J.S. Nielsen contributed to the modelling of structural members as subsystems of series hot spots, particularly to the estimation of the equivalent correlation coefficient among members’ safety margins. The calculations and coding were conducted by J. Mendoza. The paper was structured and written by J. Mendoza, with editing by all co-authors.

This Paper is awaiting publication and is not included in NTNU Open

Paper IV. Analysis of fatigue test data of retrieved mooring chain links subject to pitting corrosion

Mendoza, J., P. Haagenzen, and J. Köhler (2021). “Analysis of fatigue test data of retrieved mooring chain links subject to pitting corrosion”. Submitted for publication to a peer-reviewed journal.

The concept of the data analysis was developed by J. Mendoza and J. Köhler. The calculations were conducted by J. Mendoza. The procedures of the fatigue testing were controlled by P. Haagenzen, who also wrote, with editing by J. Mendoza, the corresponding section of the article describing the procedures. The remaining sections of the article were written by J. Mendoza, with editing by all co-authors.

© 2021 This manuscript version is made available under the CC-BY-NC-ND 4.0 license
<https://creativecommons.org/licenses/by-nc-nd/4.0/>

Analysis of fatigue test data of retrieved mooring chain links subject to pitting corrosion

Jorge Mendoza¹, Per J. Haagenen¹, Jochen Köhler¹

¹Norwegian University of Science and Technology

Abstract

Fatigue is one of the main failure mechanisms of catenary type mooring lines. Fatigue resistance is affected by a large number of factors. In this paper, the effect of pitting corrosion on the fatigue resistance of mooring lines is empirically estimated. Data from fatigue testing of both new and used chain links are considered. The used chain link samples were retrieved from several offshore floating units. A hierarchical statistical analysis is proposed to effectively use the available information. Mean stress effect is taken into account in the analysis of the data. Results show that the effect of pitting corrosion on the structural reliability of mooring lines is significant.

1. Introduction

Position keeping of offshore oil and gas floating facilities is secured by mooring systems. A mooring system is composed of several lines. Mooring lines typically include mooring chains, often in combination with polyester or wire ropes. An example of a common mooring line configuration with mooring chain and wire rope is shown in Figure 1. Mooring chains are non-redundant structures, meaning that failure of a link leads to failure of the mooring line. Subsequently, failure of a mooring line results in large replacement costs and, until detected, in an increased risk of failure of the mooring system due to progressive failure.

Fatigue and corrosion deterioration processes are among the most common causes of failure of chain links during operation [1, 2]. These two failure mechanisms are treated as weakly coupled phenomena in design standards, such as ISO 19901-7:2013 [3], API RP 2SK [4] and DNVGL-OS-E301 [5]. In these standards, the interaction between corrosion and fatigue is accounted for by considering a corrosion allowance in the fatigue limit state. This is considered to be a major simplification because the interaction between corrosion and fatigue is more complex in nature when pitting corrosion is present [6]. The fatigue-corrosion interaction has been observed to result in significantly lower fatigue lives than what is prescribed in design standards [7, 8, 9].

Mild and low-alloy steel components immersed in seawater tend to develop a type of local corrosion known as pitting corrosion. According to Melchers [10], pit growth fundamentally consists of an initial and relatively mild aerobic phase, and an aggressive

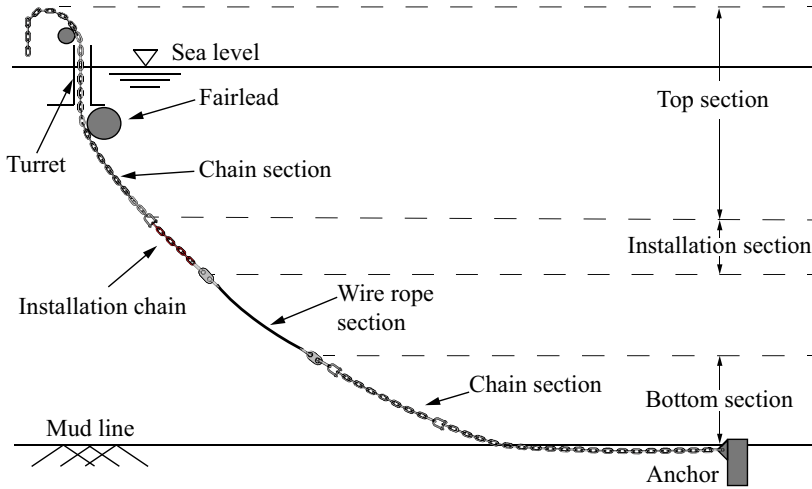


Figure 1: Example of a typical mooring line of oil and gas platforms in the North Sea and Norwegian Sea.

anaerobic phase. The anaerobic phase is mainly caused by microbial agents such as sulphate-reducing bacteria (SRB), whose growth and activity are highly influenced by the water temperature. This type of surface degradation is particularly present in two sections of the mooring line: (a) in the bottom part where the chain is buried under the sea bed; and (b) in the turret section in which conditions are favourable for marine growth and the subsequent microbial corrosion caused by SRB [7, 11]. Gabrielsen et al. [11, 12] report observations of mooring chain specimens suffering from significant pitting corrosion after 5 to 20 years in service. They identify the local geometry and the depth of the pits as important factors for fatigue resistance reduction. Furthermore, Kondo [13] shows that local stress concentrations at pits may lead to the development of fatigue cracks and the subsequent crack propagation under cyclic stresses.

In addition to the corrosion condition, recent studies have shown that the nominal mean stress that the mooring chains are subject to may have significant consequences on fatigue resistance [12, 14]. This effect is typically unaccounted for in design standards for mooring lines. It should nonetheless be noticed that the fatigue tests used to develop fatigue resistance models in API RP 2SK [4] and DNVGL-OS-E301 [5] were based on a constant high mean stress, which results in conservative practice. The mean stress effect should however be regarded for producing more accurate fatigue resistance models or when a variety of mean stresses are employed for fatigue testing.

Understanding and quantifying the effect of the corrosion condition on fatigue life reduction are relevant for the design and the reassessment of mooring systems, particularly, to inform integrity management decisions, such as inspection planning, repair, and replacement decisions. In the present article, we propose an engineering model to assess the fatigue resistance of mooring lines as a function of their corrosion condition. The proposed model builds on the current common practice, which is briefly outlined hereafter.

Typically, design standards prescribe the use of semiempirical S-N curves to assess the fatigue resistance of steel components, including mooring chains [4, 5, 15, 16, 17]. An S-N curve is a power law that represents the number of fatigue cycles N that a structural component with certain characteristics can survive as a function of the nominal stress range ΔS :

$$N = k \cdot \Delta S^{-m}, \quad (1)$$

where k and m are the model parameters.

Commonly, design standards specify the model parameters of the so-called design curves. The design curve is typically defined as the S-N curve associated with a non-exceedance probability of N given ΔS of 2.28% [18]. S-N models are fitted based on representative experimental data. Because fatigue life is affected by many variables that are not explicitly included in the S-N model, the validity of using a certain design curve in a given design scenario depends on the representativeness of the data employed to develop the curve. This limitation is partially addressed in design standards by providing several S-N curves that aim to cover most practical applications. For example, different design curves are found to be representative for different structural connections and types of welding. Consequently, the S-N model that is developed in the present study is valid for cases for which the analysed data is considered representative.

The proposed S-N curve is developed from the analysis of tension-tension fatigue test data of both new and retrieved full-scale chain segments. We refer to this S-N model as an extended S-N model because, in addition to the stress range, it includes a corrosion indicator as input variable. The obtained fatigue resistance model is used to estimate the effect of pitting corrosion on fatigue resistance. The characterisation of the retrieved specimens and the experimental methods used for fatigue testing are presented in Section 2. The fatigue data is presented in Section 3. The considered specimens are heterogeneous, meaning that they were retrieved from different platforms located in the North Sea and the Norwegian Sea and differ among each other according to several relevant features. In Section 4, we propose the use of a hierarchical method to abstract the causal effect of the corrosion condition on fatigue resistance from the data. The obtained extended S-N model is presented in Section 5. Furthermore, the sensitivity of the inferred model regarding the mean stress effect is studied in that section. The inferred fatigue resistance model is used in a case study in Section 6 to estimate the impact of the corrosion condition on the structural reliability of a mooring chain. The paper concludes with some general remarks and outlook for future research challenges.

2. Materials and experimental methods

Tension-tension fatigue tests of full-scale, studless chain links were conducted to produce the fatigue data. In total, the considered data set consists of 150 data points, see Table 1. The fatigue tests were part of three different test campaigns. Two of them dealt with retrieved chain segments and one with new, uncorroded specimens. The first subset, here called subset S1, comprises 19 results of tests on retrieved specimens that were conducted at the Norwegian University of Science and Technology (NTNU).

Table 1: Considered data set, including the platform from where specimens were retrieved. Values in square brackets correspond to $[min, max]$ of the property.

Subset	Platform	Type	Location	Service years	C	# tests
S1	P1	FPSO	bot./instal./top	[12, 20]	[4, 7]	15
	P2	FPSO	top	5	[1, 4]	4
S2	P1	FPSO	top	[10, 12]	[2, 6]	7
	P2	FPSO	bot.	18	[4, 7]	9
	P3	SEMI	top	12	1	9
	P4	SEMI	bot.	19	[2, 7]	11
	P5	SEMI	top	7	1	4
	P6	SEMI	top	15	1	4
	P7	SEMI	bot.	19	[2, 5]	9
	P8	FSO	bot.	19	[4, 5]	8
S3	ND	-	-	0	1	70

Notes: ND = Noble Denton; SEMI = Semi-submersible; FSO = floating storage and offloading vessel; FPSO = floating production, storage and offloading vessel; bot. = bottom; instal. = installation chain; C = Corrosion level.

Subset S2 consists of 61 tests of retrieved specimens conducted by Det Norske Veritas-Germanischer Lloyd (DNV-GL), which are partially reported in [7, 11, 12]. Subset S3 consists of 70 test results of new, uncorroded chains by Noble Denton [19, 20]. Note that subset S3 data were used to develop the design S-N curves in API RP 2SK [4] and DNVGL-OS-E301 [5].

2.1. Service life of the chains

The considered chain specimens were either new, i.e., subset S3, or retrieved after spending between 5 to 20 years in service, i.e., subsets S1 and S2. The distribution of the time in service of the tested specimens is shown in Figure 2 and the range of values per platform and subset is shown in Table 1. The data set contains data from 8 different platforms, which are located either in the North Sea or in the Norwegian Sea. Note that we use the term platform to refer to any floating offshore unit. In the considered data set, platforms are of three types, namely semi-submersibles (SEMI), floating storage and offloading vessels (FSO) or floating production, storage and offloading vessels (FPSO). Minimum 6 and maximum 19 independent tests have been conducted for chain segments belonging to the same platform. Specimens from the same platform may have been in service for a different number of years and sometimes differ in mechanical properties, such as diameter, grade, and minimum breaking load (MBL). Specimens were retrieved from several locations of the mooring systems, namely the top section, the installation section and the bottom section, see Figure 1. Note that the top section includes the splash zone and the turret, and the bottom section includes chain lengths below and above mudline.

The corrosion condition of the retrieved chain segments was visually assessed by a scientific researcher with 30 years of experience in material science and corrosion. The corrosion condition is measured by the corrosion level, which is an assigned integer

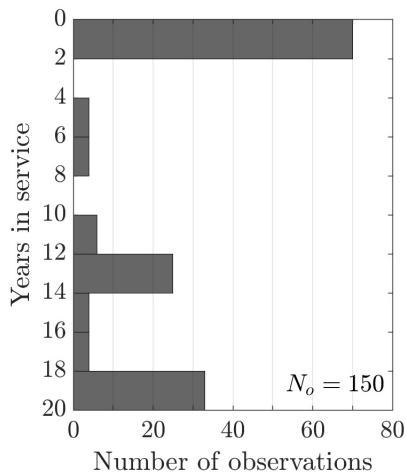


Figure 2: Distribution of the years in service of the chains in the data set, including all $N_o = 150$ tested specimens.

between 1 (no corrosion) and seven (severe corrosion). The corrosion level assignment is based on quantitative and qualitative information and is meant as a synthesis of aspects of the corrosion condition that are likely to have an impact on fatigue resistance. The reference used for describing the seven corrosion levels, see Table 2, was derived to be representative of the corrosion condition of the retrieved chains. All the assignments were conducted by a single person to avoid biases in judgement. The assignment was conducted after visual inspection and no detailed measurement of pit depth took place. Links with corrosion levels 2, 4 and 7 are shown in Figure 3. The ranges of corrosion levels of the specimens of the data set are shown in Table 1.

2.2. Mechanical properties

The considered specimens were produced following the required minimum mechanical properties in DNVGL-OS-E302 [21], which are given depending on grade. The actual

Table 2: Description of the seven corrosion levels used to characterise the corrosion condition of the specimens.

Level, C	Description
1	New chain; may be subject to mild uniform corrosion
2	Some scattered pitting, with pits less than 1 mm deep
3	Larger areas affected than level 2, with pit depths ca. 1 mm
4	Large area affected by pitting, with pit depths ca. 1-3 mm; crown area affected by pitting
5	Severe and widespread pitting, with pit depths up to 4 mm
6	Severe and widespread pitting, with pit depths up to 6 mm
7	Severe and widespread pitting, with heavily attacked crown; sharp pits, most being 3 to 6 mm deep, and some are even larger

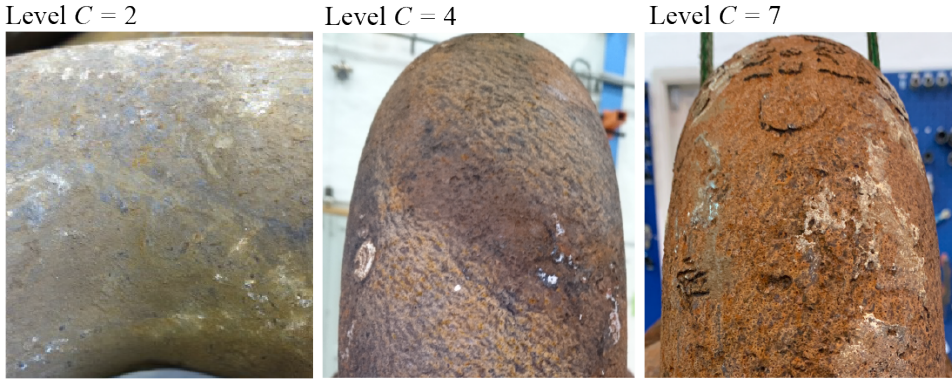


Figure 3: Examples of links with different corrosion levels.

mechanical properties of the specimens are typically well over the minimum requirements. The mechanical properties of the uncorroded steel of the links were provided by the manufacturers, see Table 3. The ratio between the measured average yield strength and tensile strength are also shown in Table 3. It can be seen that the measured yield strengths are quite above the minimum requirements in DNVGL-OS-E302, i.e., in the order of 50% over them in average. The measured tensile strengths differ less from the minimum requirements, being around 10% over them in average.

In addition, mechanical testing conducted at NTNU for the R4 material of subset S1, see Table 4. The cyclic material properties are not investigated in the current study. The reader can refer to [22] for the cyclic properties of corroded links that are similar to the considered ones.

Table 3: Mechanical properties of the chain specimens in the data set. Values in square brackets correspond to $[min, max]$ of the property.

	Subset S1	Subset S2	Subset S3
Nominal diameter [mm]	114	[114, 145]	76
Grade	R4	R3 & R4	R3 & R4
Yield strength* [MPa]	870	R3: 620; R4: 827	R3: 620; R4: 890
Yield strength*/ R_e	1.47	R3: 1.51; R4: 1.43	R3: 1.51; R4: 1.53
Tensile strength* [MPa]	954	R3: 741; R4: 931	R3: 740; R4: 980
Tensile strength*/ R_m	1.08	R3: 1.07; R4: 1.08	R3: 1.07; R4: 1.14

Notes: *mean value from mechanical testing of few specimens;

R_e = minimum yield strength [21]; R_m = minimum tensile strength [21].

Table 4: Mechanical properties of the R4 material of subset S1 tested at NTNU, compared to the minimum requirements in DNVGL-OS-E302 [21].

	Elongation A_6	Reduction of of area Z	Charpy V-notch energy at -20°C	
			Average of 3	Minimum
Test data	19%	71%	179 J	177 J
Required	12%	50%	50 J	38 J

2.3. Test setup

The main settings of the experimental setups are summarised in Table 5. The test rig used for subset S1 is shown in Figure 4. It consists of a load frame with a 280 t servo hydraulic actuator placed at the top, and a load cell at the bottom. An Instron 8800 console was used to control and monitor the actuator load. The corrosion system consists of a stainless-steel cylindrical chamber, which can be sealed with a steel front plate. The inside of the chamber is painted to avoid rust contamination. The tests of subset S2 employed two different test rigs with capacities of 450 t and 750 t. The setups of these two rigs are similar to the one just described. Tests of subset S3 were conducted several decades ago, and the capacity of the rig is unknown to the authors. The rig

Table 5: Characteristics of the fatigue test setup. Values in square brackets correspond to $[min, max]$ of the property.

	Subset S1	Subset S2 [7]	Subset S3 [19, 20]
Test rig capacity	280 t	450 t and 750 t	Unknown
Number of links	3 and 5	5 and 6	5*
Temperature	$[20, 23]^{\circ}\text{C}$	$[19, 27]^{\circ}\text{C}$	$[6, 9]^{\circ}\text{C}$
Frequency	0.5 Hz	$[0.3, 0.5]$ Hz	$[0.2, 0.7]$ Hz
pH	7	$[6.5, 8.1]$	$[8, 8.2]$

Note: *tests were conducted up to third-link failure.

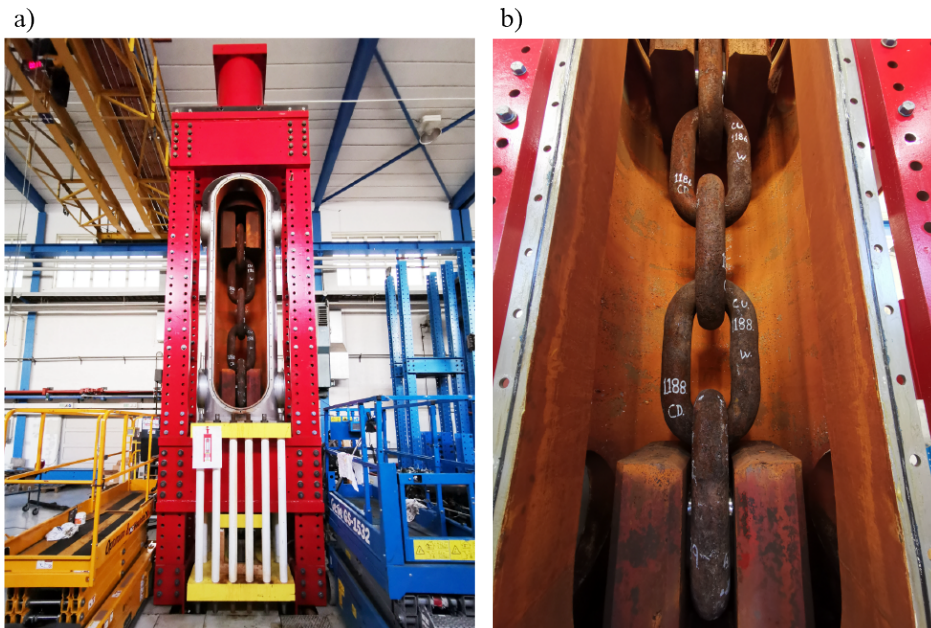


Figure 4: a) Test rig with 280 t load capacity used for subset S1, with a five-link specimen in position. During testing, a front panel is attached to seal the test chamber, which is subsequently filled with salt water. b) Close-up of the five-link specimen in position inside the test chamber.

employed for these tests had a horizontal layout in contrast to the vertical layout of the rigs of subsets S1 and S2. Nevertheless, this detail is not expected to have any significant effect on the results since these tests were conducted with high mean tension.

During testing, the segments were submerged in synthetic seawater containing 3.5% w/w of sodium chloride (NaCl), which was circulated by means of a pump. Even though corrosion degradation is not expected to significantly worsen during testing, the experiments are conducted in salted water since the medium may potentially affect crack growth development [23]. The salt content was monitored, and it remained stable throughout testing. Additionally, the pH and water temperature were monitored to follow the values in Table 5.

The frequency of the tests was set to be higher than the typical wave frequency in the North Sea, which is in the order of 0.17 Hz, see Table 5. Similar frequencies were employed for subsets S1 and S2, while subset S3 employed slightly higher frequencies. This frequency was chosen to reduce testing time, since it takes around 23 days to test one million cycles at 0.5 Hz. The effect of frequency on corrosion-fatigue crack growth of mooring chain steel in seawater was investigated by Zhang et al. [24] for grades R3, R4 and R5. The results from this study indicate a negligible difference in fatigue crack growth between 0.17 Hz and 0.5 Hz. A similar study by Hudak et al. [25] performed on high strength riser steels arrived at a similar conclusion. Based on these investigations, it is assumed that frequency effects can be neglected for the current data set.

Tests were conducted for specimens with different number of links, see Table 5. The more links are contained in one specimen, the sooner it is expected to fail for fatigue, due to the serial nature of the specimens. Therefore, the number of links is a statistically relevant parameter of the tests. Nevertheless, the effect of the number of links is not considered in the current study. The implications of this assumption are discussed in Section 7. It should be noticed that the S3 tests were conducted up to third-link failure, as opposed to the tests of subsets S1 and S2. Third-link failure implies that after failure of a link, the link was replaced by a Kenter link (as specified in [26]) and the test was continued, repeating this approach twice [20]. Testing a five-link chain up to third-link failure is somewhat similar to testing a three-link chain. Thus, this particularity is associated with similar limitations as those associated with neglecting the effect of number of links.

The contact area of each bolt was fitted to the curvature of each link to maximise the contact area. This was done to reduce stresses in the contact area between the link and the test rig, thereby reducing the probability of failure at these locations. Termination of the test was based on the actuator stroke monitoring. The test was set to stop after a pre-set target elongation of the test segment was reached. The target elongation, which is associated with through-thickness fracture, was based on the position of the actuator piston and was set to 10 mm, in addition to the elongation caused by the maximum load of the test.

2.4. Fatigue test inputs

The tests were conducted for various stress range values and for one or more mean stress levels. The experimental design of these two variables is shown in Figure 5 and their scope is summarised in Table 6. Note that the majority (76%) of tests of retrieved specimens were conducted with a mean stress in the range 10% to 18% of MBL. In addition, the stress ratio R is shown in the table for direct comparison with the literature. The stress ratio is defined as

$$R = \frac{\sigma_{min}}{\sigma_{max}} = 1 - \frac{\Delta S}{\sigma_m + \Delta S/2} \quad (2)$$

with σ_{min} and σ_{max} being the minimum and maximum nominal stresses during testing and σ_m being the mean nominal stress.

3. Experimental results

The main outcome of the fatigue tests is the number of cycles to failure. The relation between the obtained cycles to failure and the applied stress ranges is plotted in log-log scale in Figure 6. Furthermore, the locations of the observed fatigue failures are reported hereafter.

Fatigue failure of chain links tends to occur at one of the four fatigue hot spots: crown, K_t point, weld or straight areas. The K_t point is the intersection between the straight

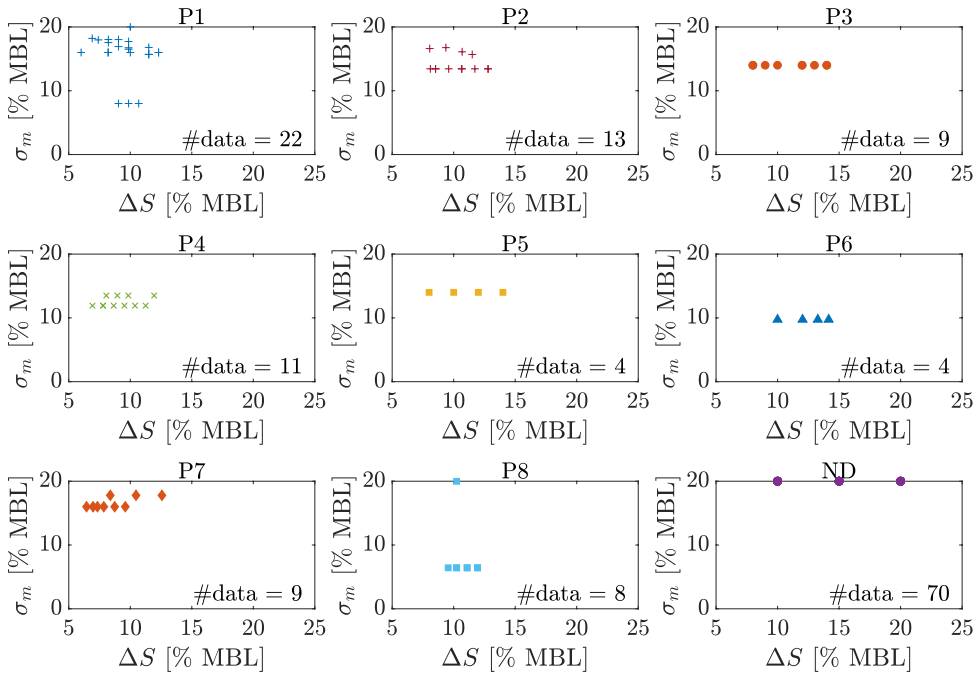


Figure 5: Nominal mean stress and stress range input of the fatigue tests expressed.

Table 6: Range of values of the nominal mean stress and stress range input of the fatigue tests. Values in square brackets correspond to $[min, max]$ of the variable.

Subset	Platform	Mean stress σ_m		Stress range ΔS		R [-]
		[MPa]	[% MBL]	[MPa]	[% MBL]	
S1	P1	[96, 110]	[15.7, 18.2]	[42, 70]	[6.9, 11.5]	[0.2, 0.7]
	P2	[97, 101]	[15.7, 16.7]	[49, 85]	[8.0, 14.0]	[0.4, 0.6]
S2	P1	[96, 122]	[15.7, 20]	[37, 75]	[6.0, 12.3]	[0.4, 0.7]
	P2	63	13.4	[38, 60]	[8.1, 12.8]	[0.4, 0.5]
	P3	80	14.0	[46, 80]	[8.0, 14.0]	[0.3, 0.6]
	P4	[69, 80]	[11.9, 13.5]	[40, 71]	[6.9, 11.9]	[0.4, 0.5]
	P5	[80, 81]	14.0	[46, 81]	[8.0, 14.0]	[0.3, 0.6]
	P6	55	9.7	[57, 80]	[10.0, 14.2]	[0.2, 0.3]
	P7	[92, 100]	[16.0, 17.8]	[37, 70]	[6.4, 12.6]	[0.5, 0.7]
	P8	[38, 117]	[6.4, 20.0]	[56, 70]	[9.6, 11.9]	[0.1, 0.6]
S3	ND	[108, 132]	20.0	[54, 132]	[10.0, 20.0]	[0.3, 0.6]

Notes: ND = Noble Denton; R = stress ratio.

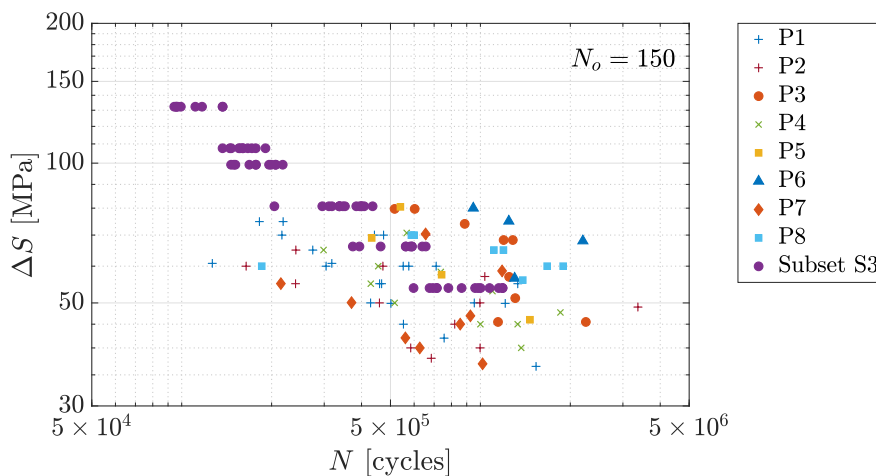


Figure 6: Raw S - N data plotted in log-log scale, differentiating according to platform (P1-P8) and including new, uncorroded chain links. All $N_o = 150$ data points are included.

and bent parts of a link [27]. The different fatigue failure hot spots are illustrated in Figure 7. The frequency of observed fractures at the hot spots are reported in Figure 8 for the tested retrieved chain specimens (subsets S1 and S2). The great majority of failures occurred at the crown location, with the remaining failures happening at the K_t point and straight/weld parts. The frequency of the fracture locations is also presented in Table 7, which distinguishes between the three subsets. Observed frequencies of subsets S1 and S2 are comparable, although a higher frequency of failures at the straight part is reported for subset S1. Nevertheless, this difference may be accounted for by the fact that subset S1 comprises only 19 observations. What is more noticeable is that the observed frequencies for corroded specimens significantly differ from those observed for new, uncorroded chains (subset S3). Fracture of these specimens is characterised by a

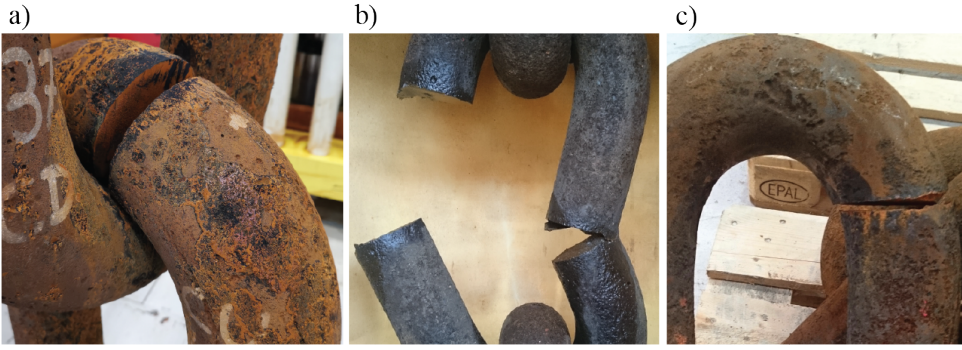


Figure 7: Example of fracture locations after tension-tension fatigue testing: a) crown failure; b) Straight/weld failure; c) K_t point failure.

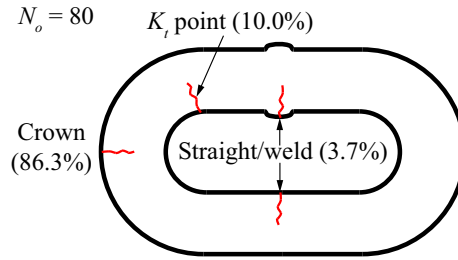


Figure 8: Obtained frequency of fracture locations from the $N_o = 80$ fatigue testing results of retrieved corroded chains.

Table 7: Comparison of the frequency of the fracture locations between the three subsets S1, S2 and S3.

Location	Subset S1	Subset S2	Subset S3
Crown	84.2%	86.9%	34.0%
K_t point	5.3%	11.5%	52.0%
Straight/weld	10.5%	1.6%	14.0%

much larger proportion of failures in the K_t point and the straight and weld areas, and a significantly lower proportion at the crown area. The fact that a horizontal test machine was employed for subset S3 is not likely to be the explanation for the difference in the frequencies of the failure locations. This assertion is supported by evidence from other horizontal testing campaigns of corroded specimens by Ma et al. [28], where five out of five link failures were observed at the crown. The large difference between the results of new and corroded specimens may be explained by two factors. First, used links present a larger wear at the crown, which leads to a reduced cross section. Second, finite element investigations by Zarandi et al. [27] indicate that pits at the crown are the most critical pits for fatigue crack initiation.

4. Data analysis methodology

4.1. Hierarchical structure of the data

Full-scale fatigue test data are typically scarce and different subpopulations are often combined in the development of S-N curves. This is the for the considered data set. As described in Section 2, the links were retrieved from several offshore platforms and differ from each other according to relevant features. Furthermore, the data set has been obtained from fatigue testing of chain links at several laboratories. Hierarchical models can be employed to address data belonging to different subpopulations in a consistent manner. The theoretical background of hierarchical models in the context of regression analysis is well documented in [29]. Based on the above considerations, it is clear that the data do not come from one homogeneous population. If the hierarchical character of the data is ignored, two extreme alternatives of analysis are:

- a) **No-pooling.** That is, to estimate separate models for each group or subpopulation. This means that different S-N curves can be fitted for each subpopulation by only considering the data belonging to them. Considering that the number of tests per subpopulation is very limited, this alternative leads to models with high statistical uncertainty. The excess of statistical uncertainty leads to over-fitting the data within each subpopulation. In other words, differences among subpopulations would be overstated and the inferred models would likely appear more different among each other than they would be if more data were available. This is due to the fact that the data shares important features across the different subpopulations. Therefore, isolating them in distinct subpopulations and analysing them separately results in a non-efficient use of available information.
- b) **Complete-pooling.** That is, to combine all data from different subpopulations and fit a single model. This analysis excludes categorical predictors from the model, which will lead to biases in the obtained model. This means that specific knowledge that could be learnt from the different subpopulations is averaged out and thereby partially lost.

The use of hierarchical models takes advantage of the complete data set while using subpopulation-specific information. In this study, we use a linear mixed-effects model to address the hierarchical structure of the data. A brief overview of the theory of linear mixed-effects models and its application to the modelling of the considered data set are presented hereafter.

4.2. Linear mixed-effects regression analysis

Random-effects models were proposed by Laird and Ware [30]. Linear mixed-effects models (LMEM) are a sub-type of the random-effects models. The principles of linear mixed-effects regression analysis are briefly presented in the following. A data set with

N_o observations is considered. The data set is understood as composed of J disjoint subpopulations. Each subpopulation contains $n_{o,j}$ observations, so that

$$\sum_{j=1}^J n_{o,j} = N_o. \quad (3)$$

Generally speaking, an LMEM of the data is composed of the superposition of a fixed-effects model and a random-effects model, and is mathematically represented by the following equation:

$$\mathbf{y} = \mathbf{X}\boldsymbol{\beta} + \mathbf{Z}\boldsymbol{\gamma} + \boldsymbol{\varepsilon}, \quad (4)$$

where \mathbf{y} is the $N_o \times 1$ vector of uncontrolled response variables; $\boldsymbol{\beta}$ is the $p \times 1$ vector of fixed-effects coefficients, with p being the number of predictors, including the intercept; \mathbf{X} is the $N_o \times p$ design matrix of the p predictor controlled variables, with the first column being a column of ones; \mathbf{Z} is the $N_o \times q \cdot J$ design matrix of the q random-effects, which maps the random-effects with the subpopulation with which they are associated; $\boldsymbol{\gamma}$ is the $q \cdot J \times 1$ vector of random-effect coefficients; and $\boldsymbol{\varepsilon}$ is the $N_o \times 1$ vector of residuals.

The fixed-effects coefficients $\boldsymbol{\beta}$ are common to all subpopulations and are computed using the complete data set, while the random-effects coefficients $\boldsymbol{\gamma}_j$ only use observations in subpopulation j . The part of the LMEM associated with subpopulation j is

$$\mathbf{y}_j = \mathbf{X}_j\boldsymbol{\beta} + \mathbf{Z}_j\boldsymbol{\gamma}_j + \boldsymbol{\varepsilon}_j. \quad (5)$$

Let $N(\boldsymbol{\mu}, \boldsymbol{\Sigma})$ denote, generally, the multi-variate normal distribution with mean vector $\boldsymbol{\mu}$ and covariance matrix $\boldsymbol{\Sigma}$. According to the central limit theorem, the distribution of the vector of random-effects coefficients of a given subpopulation is assumed to be $\boldsymbol{\gamma}_j \sim N(0, \mathbf{D})$. Similarly, and assuming statistical independence among responses \mathbf{y}_j conditional on the model parameters, the distribution of the residuals is $\boldsymbol{\varepsilon}_j \sim N(0, \sigma^2\mathbf{I})$, where \mathbf{I} is the $N_o \times N_o$ identity matrix. It then follows that the marginal distribution of the response is $\mathbf{y}_j \sim N(\mathbf{X}_j\boldsymbol{\beta}, \mathbf{Z}_j\mathbf{D}\mathbf{Z}_j^T + \sigma^2\mathbf{I})$ [30]. Note that the term $\mathbf{Z}_j\mathbf{D}\mathbf{Z}_j^T$ introduces statistical dependence among observations from the same subpopulation.

For the particular case of having $p = 1$ predictor variables, with fixed slope β_1 and fitted intercept β_0 , and $q = 1$ random-effects, i.e., only random intercepts, the model simplifies to

$$\mathbf{y} = \beta_0 + \beta_1\mathbf{x} + \boldsymbol{\gamma}_0 + \boldsymbol{\varepsilon}, \quad (6)$$

where $\boldsymbol{\gamma}_0$ is the $J \times 1$ random intercept vector, with distribution $\boldsymbol{\gamma}_{0,j} \sim N(0, \tau_0^2)$.

In this case, the correlation among two observations i and l of the same subpopulation j is

$$\text{Corr}[y_{j,i}; y_{j,l}] = \frac{\text{Cov}[y_{j,i}; y_{j,l}]}{\sqrt{\text{Var}[y_{j,i}]\text{Var}[y_{j,l}]}} = \frac{\tau_0^2}{\tau_0^2 + \sigma^2} \quad \text{with } i \neq l, \quad (7)$$

with $\text{Corr}[\cdot; \cdot]$, $\text{Cov}[\cdot; \cdot]$ and $\text{Var}[\cdot]$ being the correlation, covariance and variance operators, respectively. When using the best estimates of τ_0 and σ , here denoted τ_0^* and σ^* respectively, the value that results from this equation is typically known as the intra-class correlation (ICC). Thus, the LMEM interprets the hierarchy in the data as a linear

correlation among data from the same subpopulation.

4.3. Process behind the data

The observed fatigue life from the experiments is the result of complex stochastic phenomena that are influenced by many variables. Figure 9 shows a simplified representation of the causal relation between influencing variables and fatigue life. This type of representation is a so-called causal network [31], which allows to clearly state the underlying assumptions of the data analysis. In a causal network, the circular nodes represent variables, and the arcs represent causal relationships, with the arrows pointing from cause to effect.

In the proposed causal model, the obtained number of cycles to failure N of a chain segment is directly affected by several non-controlled and controlled variables. The non-controlled variables are the number of years in service T_S , the corrosion condition C , and a set of (unobserved) additional variables M_1 . The controlled variables are the applied stresses during fatigue testing, which include the nominal mean stress σ_m and the nominal stress range ΔS . Because these variables are controlled during testing, they are independent of the platform. Following the same logic, the non-controlled variables T_S , C and M_1 do depend on the platform P from where the chain segments have been sampled. Note that P affects C through a set of mediator variables M_2 . M_1 and M_2 are two disjoint sets. The set M_1 includes all variables that affect fatigue life and do not affect the corrosion condition, such as initial defects, the residual stresses, and the experienced stresses during time in service. The set M_2 includes all variables that affect the corrosion condition but do not directly affect fatigue life, such as temperature, dissolved oxygen and pH [10, 32].

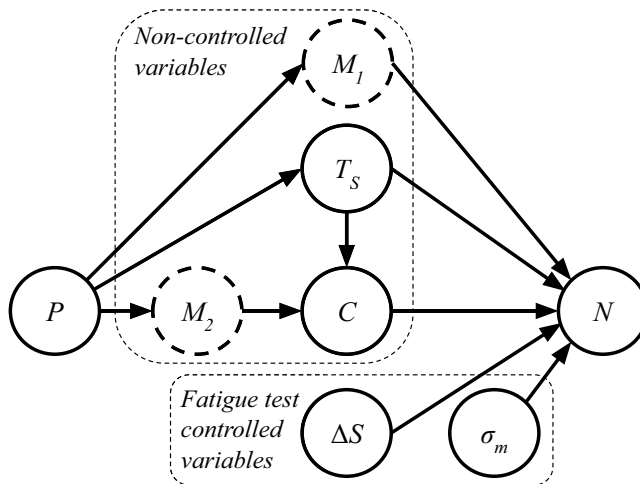


Figure 9: Causal diagram to study the effect of corrosion on fatigue life. The following nomenclature is used: P = platform; N = fatigue life; C = corrosion condition; T_S = time in service; ΔS = nominal stress range; σ_m = nominal mean stress; M_1 = unobserved set 1 of mediators; and M_2 = unobserved set 2 of mediators.

A variable that simultaneously affects the corrosion condition and the fatigue life may result in a confounding bias, meaning that if this variable is not properly controlled for, the statistical analysis may result in a larger estimation of the statistical dependence among corrosion and fatigue life than can be accounted for by the actual causal effect. Thus, these variables are to be explicitly represented in the causal diagram. In the model, N and C are both dependent on the time in service T_S , because this variable simultaneously increases the corrosion condition and the expected accumulated fatigue damage. Nevertheless, time in service affects corrosion condition and fatigue life in fundamentally different ways. The development of pitting corrosion in time is a concave functional relationship [10], implying that its development decelerates with time, whereas crack growth is a convex function [24]. The latter implies that mooring chains are not expected to accumulate significant fatigue damage during most of their service life, particularly considering that they are typically designed with large fatigue safety margins [12]. Furthermore, the tested specimens did not present any visible initial fatigue cracks. The same observation was reported in Gabrielsen et al. [11], which reports that fracture of the specimens considered in that investigation took place in the base material, with no prior identification of cracks. In addition, corrosion condition leads to a change in the fatigue failure location, as shown in Table 7. Thus, most of the fatigue damage accumulated during the initial years of service is not occurring at the most likely failure location of a corroded link, which is the crown. Due to these considerations, the confounding effect caused by the time in service is expected to be low and therefore, it is neglected for simplicity.

Furthermore, the following additional assumptions are implicit in the model. For a given stress range, the effect of diameter on fatigue life is not significant [33]. Similarly, the effect of grade has little influence on fatigue life, see [34, 33], and is consequently neglected in the model for simplicity.

According to these considerations, we conclude that dividing the data set into sub-populations based on platform allows us to deconfound the effect of corrosion condition on fatigue life. Lastly, the controlled variables of the fatigue test are regarded. The scope of the applied nominal mean stresses and stress ranges is shown in Table 6 and Figure 5. For any given platform, the scope of applied nominal stress ranges is sufficiently representative to assess the effect of this variable. Specially, considering that it is common practice to assume that this effect is known and represented by a value of $m = 3$ in Eq. (1). However, the same cannot be argued for the scope of applied nominal mean stresses. On the contrary, the variability of the applied mean stresses is rather low or even non-existent within most platforms. This is the case for the data of platforms P3 to P8 and the Noble Denton data. Thus, mainly the data from platforms P1 and P2 are valuable to empirically assess the mean stress effect. Since the focus of the current study is on the assessment of the corrosion effect, all considered data should be regarded to have a representative set of specimens showing a wide range of corrosion levels. Thus, it is concluded that the considered data set is not suitable for simultaneously assessing the corrosion and mean stress effects. Even though the mean stress effect cannot be properly assessed empirically using the considered data set, alternative methods exist

in the literature to take it into account. In the following subsection, the application of some of the available mean stress correction methods are discussed in the context of the current study.

4.4. Consideration of mean stress effect with correction models

The effect of the applied mean stresses during testing should be considered in the analysis to abstract the effect of the corrosion condition from the data. Unfortunately, the experimental designs of the three considered data sets is not suitable to assess the mean stress effect. Alternatively, one can use available mean stress correction models to deterministically take this effect into account. As an example, Fernandez et al. [14] use three well known mean stress correction models, namely Goodman, Gerber and Smith-Watson-Topper (SWT), to assess the effect of mean stress on the intercept of the S-N curves. In the current study, we consider the same three correction models, which are presented in Table 8 as per the formulation in [35].

According to these correction models, an equivalent stress range can be computed as a function of the applied mean stress and stress range, and in the case of the Goodman and Gerber models, also the ultimate tensile strength of the steel. The equivalent stress range is the completely reversed stress range that leads to the same damage as the pair of stress range and mean stress. The completely reversed stress range is associated with a stress ratio $R = -1$, or equivalently, $\sigma_m = 0$.

By applying the different correction models to the data, one can estimate how sensitive is the estimated corrosion effect with respect to the consideration of the mean stress effect for the current data set. Thus, these models are used in Section 5 to assess the influence of the mean stress effect on the inferred fatigue resistance models.

4.5. Linear mixed-effects model of the fatigue data

According to the considerations in section 4.3, the data set is divided into $J = 9$ subpopulations, see Table 9. The generic LMEM in Eq. (4) is then adapted to the

Table 8: Considered mean stress correction models. ΔS_{eq} is the equivalent fully reversed stress range.

Name	Model
Goodman	$\Delta S_{eq} = \frac{\Delta S}{1 - \frac{\sigma_m}{\sigma_u}}$
Gerber	$\Delta S_{eq} = \frac{\Delta S \frac{\sigma_u}{\sigma_m}}{1 - (\frac{\sigma_m}{\sigma_u})^2}$
SWT	$\Delta S_{eq} = \sqrt{\Delta S(2\sigma_m + \Delta S)}$
Note: σ_u = ultimate tensile strength of the steel.	

current case:

$$\log_{10}(N_{i,j}) = -m \cdot \log_{10}(\Delta S_{i,j}) + \beta_2 \cdot \log_{10}(C_{i,j}) + \log_{10}(k) + \gamma_{0,i,j} + \varepsilon_{i,j}, \quad (8)$$

where $i = 1, 2, \dots, N_{o,j}$ refers to a data point of subpopulation $j = 1, 2, \dots, J$. The following substitutions are made:

- $y_{i,j} = \log_{10}(N_{i,j})$;
- $\mathbf{x}_{i,j} = [\log_{10}(\Delta S_{i,j}), \log_{10}(C_{i,j})]$;
- $\boldsymbol{\beta} = [\beta_0 = \log_{10}(k), \beta_1 = -m, \beta_2]$.

The stress range effect is assumed to be fixed to $m = 3$, according to industry convention [5, 16]. Consequently, the model has the following degrees of freedom: three regression parameters for the fixed-effects model $(k, \beta_2, \varepsilon)$ and $J = 9$ random intercepts $\boldsymbol{\gamma} = \{\gamma_1, \gamma_2, \dots, \gamma_J\}$. Note that the mean stress correction models in Table 8 can be easily implemented by substituting $\Delta S_{i,j}$ with the corresponding equivalent stress range $\Delta S_{eq,i,j}$.

5. Results of data analysis

In this section, the data set is used to infer a fatigue resistance model of the form of Eq. (8). First, the regression analysis is conducted by neglecting the mean stress effect. The obtained model is referred to as the “reference model” in the following. The model parameters are computed using the Statistics and Machine Learning Toolbox of Matlab[®] [36], which employs a two-step integration using restricted maximum likelihood and maximum likelihood methods.

The inferred parameters of the reference model are shown in Table 10. The standard deviation of the model residuals results in $\sqrt{\tau_0^2 + \sigma_\varepsilon^2} = 0.268$. The obtained ICC indicates that the data belonging to a given platform are moderately correlated to each other. The mean S-N curves of the different subpopulations are estimated using their associated

Table 9: Hierarchically structured data set. Values in square brackets correspond to [min, max] of the property.

Subpopulation	Platform	$N_{o,j}$	Corrosion level	Years in service
G1	P1	19	[2, 6]	[10, 20]
G2	P2	15	[1, 7]	[5, 18]
G3	P3	9	1	12
G4	P4	11	[2, 7]	[12, 19]
G5	P5	4	1	7
G6	P6	4	1	15
G7	P7	9	[2, 5]	[16, 19]
G8	P8	8	[5, 7]	[19, 20]
G9	Noble Denton [20]	70	1	0

Table 10: Maximum likelihood estimation of the linear mixed-effects model parameters of the reference model, i.e., without accounting for mean stress effect. Units are in accordance with stresses in MPa.

Parameter	Type	Mean	Std. deviation
m	Deterministic	3	-
$\log_{10} k$	Normal	11.478	0.099
β_2	Normal	-0.802	0.125
σ_ε	Normal	0.165	0.0251
τ_0	Normal	0.211	0.0392
ICC	Deterministic	0.621	-

Notes: σ_ε = std. deviation of the model residuals;
 τ_0 = std. deviation of the random effects; ICC =
 Intra-class correlation.

random-effects terms and the average corrosion level of their specimens. These curves are plotted in Figure 10, including the mean fixed-effects curve for reference.

According to the extended S-N model, the relation between the number of cycles to failure (N_1 and N_2) associated with two different corrosion levels (C_1 and C_2) is given by

$$\frac{N_1}{N_2} = \left(\frac{C_1}{C_2} \right)^{\beta_2}. \quad (9)$$

If we regard the typical S-N relation in Eq. (1), differences in the number of cycles to failure are solely caused by differences in the stress range. Let A_1 and A_2 be the

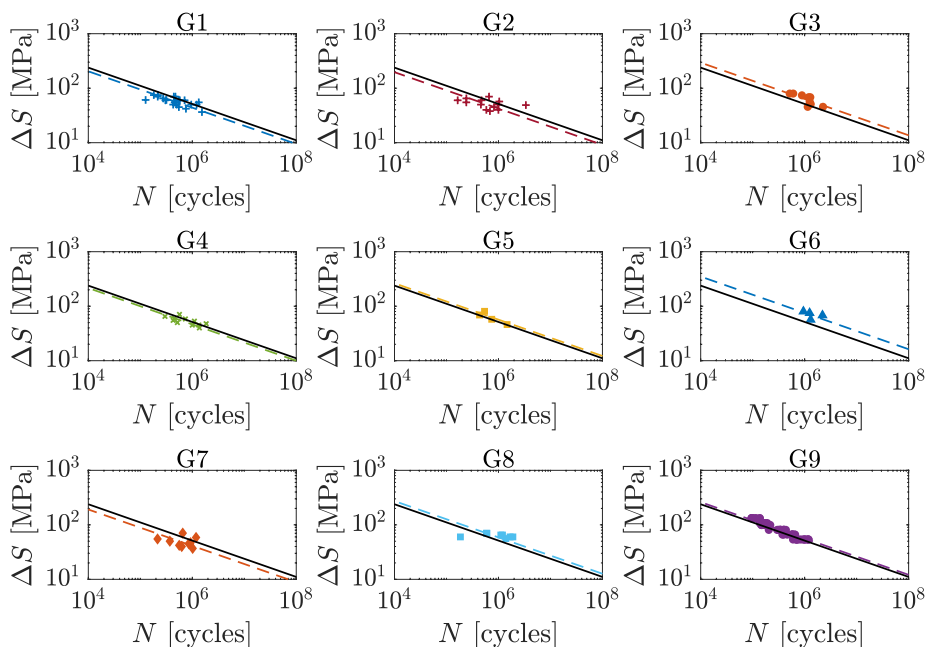


Figure 10: Mean S-N curve for the different subpopulations. Additionally, the mean fixed-effects curve is plotted for reference in continuous black.

nominal cross-section areas associated with the stress ranges ΔS_1 and ΔS_2 , respectively. The nominal stress range of a chain link is inversely proportional to the cross-section area. Thus, from Eq. (1), we get that the ratio between N_1 and N_2 for constant nominal tension is

$$\frac{N_1}{N_2} = \left(\frac{A_1}{A_2} \right)^m. \quad (10)$$

Combining Eqs. (9) and (10) leads to:

$$\frac{A_1 - A_2}{A_1} = 1 - \left(\frac{C_2}{C_1} \right)^{\beta_2/m}, \quad (11)$$

which represents the reduction in cross section (from A_1 to A_2) that should be observed if the corrosion-effect would be simply attributed to uniform corrosion. Based on Eq. (11), it is deduced that an increase of the corrosion level from $C_1 = 1$ to $C_2 = 7$ would need to be explained by a reduction in cross-section area of approximately $1 - 7^{-0.802/3} \approx 40\%$. This estimate corresponds to a reduction of ca. 23% of the chain diameter. Since the observed reduction of the diameters for the tested specimens with $C = 7$ is significantly lower than that, it is concluded that the fatigue-corrosion effect is more complex in nature and leads to significantly lower fatigue lives than what can be accounted for by uniform corrosion. Thus, the corrosion condition should be implicitly included as an input of the S-N curve to consider this effect.

To address the effect of mean stress on the inferred fatigue resistance models, the mean value estimates of the parameters of the reference model and of the three considered mean stress corrected models are shown in Table 11. The inferred parameters are independent of the stress ratio R , with the exception of the intercept $\log_{10} k$. The corrosion-effect parameter β_2 is not significantly affected by the consideration of the mean stress effect for the current data set. In particular, the Gerber corrected model leads to the lowest difference in the estimation of this parameter. In general, applying a mean stress correction model leads to a reduced uncertainty of the inferred model. The largest reduction is achieved with the SWT correction, which leads to a standard deviation of the model residuals of $\sqrt{\tau_0^2 + \sigma_\varepsilon^2} = 0.214$, which is 20% lower than for the reference model. This result is in line with the conclusions in Fernandez et al. [14], which indicate that the SWT provides the best representation of the effect among the three correction models.

The main implications of the mean stress effect are the reduction of fatigue resistance for increasing mean stress. The intercept of the typical two-dimensional S-N curve is plotted in Figure 11 as a function of the stress ratio. This intercept can be easily computed by adding the corrosion effect to $\log_{10} k$, i.e., $\log_{10} k + \beta_2 \cdot C$. The SWT model is employed for these plots for illustration purposes and because it provides the largest reduction of model uncertainty among the considered mean stress correction models, see Table 11. Furthermore, the SWT model has the advantage of being independent from any material property. It can be observed that for values of R within the range of the data set, i.e., between 0.1 to 0.7 (see Table 6), the corrosion effect has a larger potential for reducing fatigue life than the mean stress effect.

Table 11: Comparison of the mean value of the inferred model parameters between the reference model and the mean stress corrected models. Units are in accordance with stresses in MPa.

Parameter	Reference model	Goodman	Gerber	SWT
$\log_{10} k$	11.478	11.614	11.492	12.342
β_2	-0.802	-0.837	-0.808	-0.882
σ_ε	0.165	0.158	0.164	0.139
τ_0	0.211	0.192	0.208	0.163
ICC	0.621	0.595	0.617	0.579

Notes: σ_ε = std. deviation of the model residuals; τ_0 = std. deviation of the random effects; ICC = Intra-class correlation.

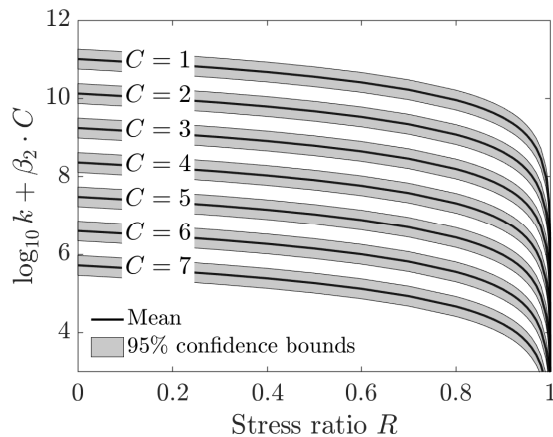


Figure 11: Sum of the intercept $\log_{10} k$ and the corrosion effect $\beta_2 \cdot C$ of the SWT-corrected model as a function of the stress ratio R and for the different corrosion levels.

6. Case study

In this section, the inferred extended S-N model is applied to computing the structural reliability of a mooring line segment. The cumulative probability of fatigue failure of a mooring line segment with a remaining service life of T years is denoted $P_{f,T}$. A mooring line segment is assumed to consist of a similar number of links to those of the specimens of the employed data set, i.e., between 3 and 5. A function g that limits the fatigue failure domain by $g \leq 0$ is introduced. $P_{f,T}$ results then from integrating the joint distribution of the involved random variables \mathbf{X} over the failure domain, i.e.,

$$P_{f,T} = \Pr[g(\mathbf{x}; T) \leq 0]. \quad (12)$$

The Palmgren-Miner failure criterion is used to elaborate the limit state function g of the S-N fatigue resistance model:

$$g(\mathbf{x}; T) = \Delta - D(\mathbf{x}; T). \quad (13)$$

In this equation, $D(\mathbf{x}; T)$ is the damage accumulated during the period T and Δ is the uncertain Palmgren-Miner failure threshold, which is represented as a log-normal distributed random variable with mean 1 and coefficient of variation 0.3, according to JCSS [37].

Given that the average number of stress cycles in a year ν is known, $D(\mathbf{x}; T)$ can be approximated from the expected damage per cycle as

$$D(\mathbf{x}; T) = 1 = \sum_{i=1}^{\nu \cdot T} \Delta D_i \approx \nu \cdot T \cdot \mathbb{E}_T [\Delta D_i(\mathbf{x})], \quad (14)$$

where ΔD_i is the increase in damage due to cycle i and $\mathbb{E}[\cdot]$ represents the expectation operator. The variable ν is assumed to be $5 \cdot 10^6$ cycles/year, which is typical for North Sea conditions [38].

The expected damage per fatigue cycle conditional on the corrosion level C follows from the model in Eq. (8):

$$\mathbb{E}_T [\Delta D_i | C] = \mathbb{E} \left[\frac{1}{N} \right] = \frac{1}{k \cdot 10^\varepsilon} \cdot \mathbb{E}_T [\Delta S(t)^m] \cdot C^{-\beta_2}, \quad (15)$$

where $\Delta S(t)$ is the fatigue stress range process. Assuming that the cyclic stresses are dominated by the wave-induced loading, $\Delta S(t)$ is typically well represented by a Weibull distribution, with scale parameter k_w and shape parameter λ [39]. This process can then be reduced to an equivalent fatigue stress range ΔS_e that leads to the same expected fatigue life as the process, and which is given by

$$\Delta S_e = \mathbb{E}_T [\Delta S(t)^m]^{1/m} = k_w \cdot \Gamma \left(1 + \frac{m}{\lambda} \right)^{1/m}, \quad (16)$$

where $\Gamma(\cdot)$ is the complete gamma function. This equivalent fatigue stress ΔS_e is not to be confused with ΔS_{eq} in Table 8.

The expected damage per fatigue cycle can then be explicitly computed by substituting Eq. (16) into Eq. (15). The conditional limit state function is then given by substitution of Eqs. (14) and (15) into Eq. (13):

$$g(\mathbf{x}; T | C) = \Delta - \nu \cdot T \cdot \frac{1}{k \cdot 10^\varepsilon} \cdot k_w \cdot \Gamma \left(1 + \frac{m}{\lambda} \right) \cdot C^{-\beta_2}. \quad (17)$$

Inserting Eq. (17) into Eq. (12) provides an expression for the probability of failure conditional on the corrosion level $P_{f,T|C}$. This expression can be solved by using e.g., the first order reliability method (FORM). The parameters of the fitted fatigue resistance model that are used in Eq. (17) are the ones of the reference model shown in Table 10. The rest of the involved random variables are summarised in Table 12. The parameter k_w of the Weibull distribution representing the fatigue stresses is calibrated so that the probability of failure of the uncorroded mooring line is 10^{-5} for a total design service life of 30 years. The coefficient of variation of k_w is taken as 0.22 after Moan and Song [40].

The conditional probability of failure $P_{f,T|C}$ is plotted as a function of the corrosion level and for different values of the remaining service life T in Figure 12. The results are

Table 12: Probabilistic distribution of the involved variables.

Random variable	Type	Mean	Std. deviation
k_w [N/mm ²]	Log-normal	1.25	0.28
λ [-]	Deterministic	0.8	-
ν [cycles/year]	Deterministic	10^5	-

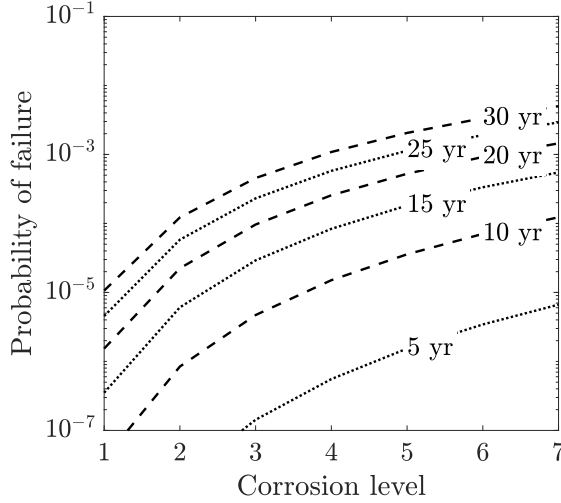


Figure 12: Conditional probability of fatigue failure $P_{f,T|C}$ of a mooring line segment with a design service life of 30 years, as a function of the corrosion level C and for different values of the remaining service life T .

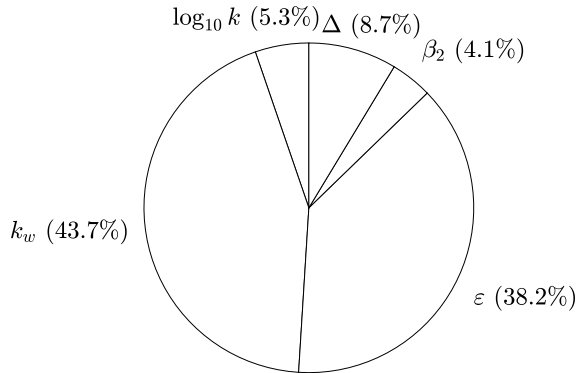


Figure 13: FORM sensitivity factors for corrosion level 5 expressed as a percentage.

indicative for the estimation of the increase of the conditional probability of failure for increasing corrosion level. For instance, it can be seen that should the corrosion level stay constant in time, the 10-year cumulative probability of failure for $C = 4$ is more than 100 times higher than for $C = 2$.

The square of the FORM-sensitivity factors are plotted in Figure 13. An intermediate

but relatively severe corrosion level ($C = 5$) is chosen for the plot to show the sensitivity of the corrosion-effect parameter β_2 . Choosing a lower or higher corrosion level results in, respectively, a higher or lower share of the sensitivity of the other parameters. Note that the differences in the sensitivity factors for other corrosion levels are not significant and are not shown for clarity. It is seen that the probability of failure is largely dominated by the model uncertainty ε and the parameter k_w of the fatigue stress distribution. Although the model uncertainty can be partially reduced by conducting additional experiments, this uncertainty is largely associated with the level of simplification implicit in the S-N representation of fatigue resistance. Therefore, significant savings can be achieved by conditioning the model on situation-specific data. Most of the uncertainty associated with k_w is aleatoric in nature and thus cannot be reduced. Nevertheless, the large sensitivity associated with this parameter indicates that efforts dedicated to improving the accuracy of the load modelling will have a significant impact in the estimation of the structural reliability.

7. Discussion

Fatigue test data were analysed to study the effect of the corrosion condition of mooring chains on their fatigue resistance. The results of the data analysis rely on the assumptions used to describe the relationship among the involved variables. A causal diagram has been proposed to explicitly display the assumptions employed to hierarchically organise the data. This can be used to study the validity of the proposed causal model in future studies. A linear mixed-effects model is implemented to efficiently use available information. The random-effects part of the model consists of the random-intercepts of the different subpopulations. No random slopes are considered, mainly because little variation of the corrosion level exists within a given subpopulation. Larger data sets that include larger variations of the corrosion condition could be used in future studies to validate the presented results and to improve their statistical significance.

The study shows that the effect of the corrosion condition on fatigue resistance is significant. Nevertheless, limited knowledge exists about which features of corrosion are more relevant to the prediction of fatigue resistance. In this article, the corrosion level C is used as an indicator of the corrosion condition. The corrosion level is a subjectively assigned number used to quantify the general severity of pitting corrosion, wear, and uniform corrosion. Thus, it is a synthesis of many factors that are hypothesised to be of relevance. Further studies should be conducted to investigate which features of corrosion have a higher impact on fatigue resistance. An objective indicator function could then be learned from these factors. The present results could be used as a reference for the development of the objective corrosion indicator. The objective indicator function could be used to assess the corrosion condition from collected in-situ information using, for instance, surface scanning technology.

The results of the reliability case study in Section 6 show that the corrosion effect has a significant impact on the reliability of a mooring segment conditional on the corrosion level. The level of detail of the analysis is guided by the level of detail of the represen-

tation of fatigue and corrosion, i.e., by the proposed extended S-N curve. It should be noted that corrosion deterioration is a time-dependent process. Hence, a time-evolution model of corrosion needs to be used to compute the unconditional reliability. Available models in the literature, see e.g. [10], suggest that the anaerobic growth of pit depths is very aggressive initially and slows down with time. According to this type of growth, chain segments that belong to nearby locations of a mooring line but that initially present different corrosion levels would tend to have more similar corrosion levels with time and likely spend most of their remaining lives with similar corrosion levels. Thus, we argue that the difference between the unconditional probabilities of failure of two segments of a line with different corrosion levels is lower than the difference between the conditional probabilities in Figure 12.

Failure of a mooring chain occurs when any of its links fails. Thus, the number of links is statistically relevant to assess the structural reliability of mooring lines. In the present study, the effect of the number of links is not taken into account. This corresponds to assuming the different failure mechanisms of the tested specimens to be fully dependent, which is in line with the methods used in DNVGL-OS-E301 [5]. Some methods have been proposed to treat this effect based on order statistics and assuming full independence of the failure mechanisms [41]. In reality, the true effect will be in between the assumptions of dependence and independence. It is worth noticing that the dependence of the failure mechanisms is given by the dependence among material properties and load effects that affect fatigue resistance. Thus, dependence is expected to be significantly higher for chains subject to pitting corrosion than for new chains because this type of corrosion is shown to influence the location of fatigue failure and to reduce fatigue resistance. It is noted that the dependence assumption implicit in the current study and in DNVGL-OS-E301 [5] is however in contradiction with continuing the tests after the first failure is encountered, which is the case for the Noble Denton data of subset S3. It is recommended to conduct further studies to assess the true effect of the number of links. Nevertheless, it should be kept in mind that the uncertainty associated with not considering this effect is significantly lower than the inherent uncertainty of the fatigue phenomenon.

The effect of the number of links is of special relevance for applying the derived models for the assessment of long mooring lines, since the tested specimens contain a low number of links. The authors argue that this effect decays for increasing number of links. That is, for sufficiently long mooring lines, adding an additional link does not significantly increase their probability of failure. This is due to the fact that the probability of failure of the chain is dominated by few failure mechanisms. Further studies should be performed to validate this assumption.

Design standards for the design of mooring lines often neglect the mean stress effect [4, 5]. This assumption is based on the presumption that failure occurs at welded connections, where there are large residual stresses [16]. As shown in the current experimental study, corroded links fail at the crown in most cases. Thus, the hypothesis used to neglect mean stress effects does not hold and further studies should be conducted to understand and quantify this phenomenon. In the present study, we use well known mean

stress correction models, namely the Goodman, Gerber and SWT models, to account for the mean stress effect. We show that, for the regarded data set, the estimated corrosion effect is not very sensitive to which correction model is used or even if a correction model is used at all. This is of course not in contradiction with the fact that mean stress may have a significant impact on the fatigue resistance of corroded chains. Future research studies should aim at empirically assessing the mean stress effect for mooring chains, developing, and identifying the most appropriate models to assess this phenomenon and quantifying the uncertainty associated with the models.

8. Conclusions

Tension-tension fatigue test results of new and retrieved mooring chain segments were analysed to study the effect of the corrosion condition on fatigue resistance. The considered data set contains new as well as previously published data. The fatigue test setup and employed procedures were described. A hierarchical approach is proposed to analyse the data to maximise the use of available information. An extended S-N curve that includes a corrosion level indicator is developed using a linear mixed-effects model. The assessed effect of corrosion condition on fatigue resistance is significant. Well known mean stress correction models were used to assess how accounting for the mean stress effect affects the estimated corrosion effect. It was shown that the estimated corrosion effect is not significantly affected by mean stress correction. A numerical example is presented to illustrate the implications of the assessed fatigue-corrosion damage effect on the structural reliability of mooring lines. The results of the analysis can be used to inform integrity management and life-extension decisions of existing mooring systems and to enhance the design of new mooring chains.

Acknowledgements

The authors would like to acknowledge the KPN Lifemoor project (RCN contract No: 280705) for providing the fatigue test data used in this article. In particular, the authors would like to acknowledge the insights provided by Øystein Gabrielsen and the assistance of Christian Frugone. Furthermore, the comments by Cody Owen are much appreciated.

References

- [1] E. Fontaine, A. Kilner, C. Carra, D. Washington, K. Ma, A. Phadke, D. Laskowski, G. Kusinski, et al. "Industry survey of past failures, pre-emptive replacements and reported degradations for mooring systems of floating production units". In: *Offshore Technology Conference*. OTC-25273-MS. Offshore Technology Conference. 2014.

- [2] R. B. Gordon, M. G. Brown, E. M. Allen, et al. “Mooring integrity management: a state-of-the-art review”. In: *Offshore Technology Conference*. OTC-25134-MS. Offshore Technology Conference. 2014.
- [3] ISO. *Petroleum and natural gas industries - Specific requirements for offshore structures — Part 7: Stationkeeping systems for floating offshore structures and mobile offshore units*. Standard ISO 19901-7:2013. Geneva, Switzerland: International Organization for Standardization, 2013.
- [4] API. *Design and Analysis of Stationkeeping Systems for Floating Structures, Third Edition*. Recommended Guide API RP 2SK. Washington, D.C, USA, 2015.
- [5] DNV-GL. *Position mooring*. Offshore Standard DNVGL-OS-E301. 2015.
- [6] R. Pérez-Mora, T. Palin-Luc, C. Bathias, and P. [Paris]. “Very high cycle fatigue of a high strength steel under sea water corrosion: A strong corrosion and mechanical damage coupling”. In: *International Journal of Fatigue* 74 (2015), pp. 156–165. ISSN: 0142-1123. DOI: <https://doi.org/10.1016/j.ijfatigue.2015.01.004>. URL: <http://www.sciencedirect.com/science/article/pii/S0142112315000067>.
- [7] S. Fredheim, S. Reinholdtsen, L. Håskoll, and H. Lie. “Corrosion fatigue testing of used, studless, offshore mooring chain”. In: *International Conference on Ocean, Offshore and Arctic Engineering*. OMAE2013-10609. American Society of Mechanical Engineers Digital Collection. 2013.
- [8] A. Arredondo, J. Fernández, E. Silveira, and J. L. Arana. “Corrosion fatigue behavior of mooring chain steel in seawater”. In: *International Conference on Ocean, Offshore and Arctic Engineering*. OMAE2016-54426. American Society of Mechanical Engineers Digital Collection. 2016.
- [9] M. Morgantini, D. MacKenzie, Y. Gorash, and R. van Rijswick. “The effect of corrosive environment on fatigue life and on mean stress sensitivity factor”. In: *MATEC Web of Conferences*. Vol. 165. EDP Sciences. 2018. DOI: <https://doi.org/10.1051/mateconf/201816503001>.
- [10] R. E. Melchers. “Pitting corrosion of mild steel in marine immersion environment—Part 1: Maximum pit depth”. In: *Corrosion* 60.9 (2004), pp. 824–836.
- [11] Ø. Gabrielsen, K. Larsen, and S.-A. Reinholdtsen. “Fatigue testing of used mooring chain”. In: *International Conference on Ocean, Offshore and Arctic Engineering*. OMAE2017-61382. American Society of Mechanical Engineers Digital Collection. 2017.
- [12] Ø. Gabrielsen, K. Larsen, O. Dalane, H. B. Lie, and S.-A. Reinholdtsen. “Mean Load Impact on Mooring Chain Fatigue Capacity: Lessons Learned From Full Scale Fatigue Testing of Used Chains”. In: *International Conference on Ocean, Offshore and Arctic Engineering*. OMAE2019-95083. American Society of Mechanical Engineers Digital Collection. 2019.
- [13] Y. Kondo. “Prediction of fatigue crack initiation life based on pit growth”. In: *Corrosion* 45.1 (1989), pp. 7–11.

- [14] J. Fernández, A. Arredondo, W. Storesund, J. J. González, et al. “Influence of the Mean Load on the Fatigue Performance of Mooring Chains”. In: *Offshore Technology Conference*. OTC-29621-MS. Offshore Technology Conference. 2019.
- [15] A. F. Hobbacher. *Recommendations for Fatigue Design of Welded Joints and Components*. Recommended Guide IIW-2259-15. International Institute of Welding, 2016.
- [16] DNV-GL. *Fatigue Design of Offshore Steel Structures*. Recommended Practice DNVGL-RP-C203. DNV-GL, 2016.
- [17] BSI. *Guide to fatigue design and assessment of steel products*. Recommended Guide BS 7608:2014. The British Standards Institution, 2014.
- [18] G. Edwards and L. Pacheco. “A Bayesian method for establishing fatigue design curves”. In: *Structural Safety* 2.1 (1984), pp. 27–38. ISSN: 0167-4730. DOI: [https://doi.org/10.1016/0167-4730\(84\)90005-5](https://doi.org/10.1016/0167-4730(84)90005-5). URL: <https://www.sciencedirect.com/science/article/pii/0167473084900055>.
- [19] J. Mathisen, T. Hørte, V. Moe, and W. Liean. *Calibration of a Fatigue Limit State – Joint Industry Project DeepMoor Design Methods for Deep Water Mooring Systems*. DNV Report 98-3110. DNV, Dec. 1998.
- [20] M. J. White. *Corrosion Fatigue Testing of 76mm Grade R3 & R4 Studless Mooring Chain, H5787/NDAI/MJW, Rev 0*. Tech. rep. Joint Industry Report. Noble Denton Associates, Inc., May 2002.
- [21] DNV-GL. *Offshore mooring chain*. Offshore Standard DNVGL-OS-E302. 2018.
- [22] E. P. Zarandi and B. H. Skallerud. “Experimental and numerical study of mooring chain residual stresses and implications for fatigue life”. In: *International Journal of Fatigue* 135 (2020), p. 105530.
- [23] A. Vasudevan and K. Sadananda. “Classification of environmentally assisted fatigue crack growth behavior”. In: *International Journal of Fatigue* 31.11 (2009). Fatigue Damage of Structural Materials VII, pp. 1696–1708. ISSN: 0142-1123. DOI: <https://doi.org/10.1016/j.ijfatigue.2009.03.019>. URL: <http://www.sciencedirect.com/science/article/pii/S0142112309001236>.
- [24] Y. Zhang, N. Zettlemoyer, and P. Tubby. “Fatigue crack growth rates of mooring chain steels”. In: *International Conference on Ocean, Offshore and Arctic Engineering*. OMAE2012-84223. American Society of Mechanical Engineers Digital Collection. 2012.
- [25] S. J. Hudak Jr, J. H. Feiger, and J. A. Patton. “The effect of cyclic loading frequency on corrosion-fatigue crack growth in high-strength riser materials”. In: *International Conference on Ocean, Offshore and Arctic Engineering*. OMAE2010-20705. 2010.
- [26] API. *6th Edition, Specification for Mooring Chain*. Standard API SPEC 2F. API, June 1997.

- [27] E. P. Zarandi and B. H. Skallerud. “Cyclic behavior and strain energy-based fatigue damage analysis of mooring chains high strength steel”. In: *Marine Structures* 70 (2020), p. 102703.
- [28] K.-t. Ma, Ø. Gabrielsen, Z. Li, D. Baker, A. Yao, P. Vargas, M. Luo, A. Izadparast, A. Arredondo, L. Zhu, et al. “Fatigue Tests on Corroded Mooring Chains Retrieved From Various Fields in Offshore West Africa and the North Sea”. In: *International Conference on Ocean, Offshore and Arctic Engineering*. OMAE2019-95618. American Society of Mechanical Engineers Digital Collection. 2019.
- [29] A. Gelman and J. Hill. *Data analysis using regression and multilevel/hierarchical models*. Cambridge university press, 2006. ISBN: 978-0521686891.
- [30] N. M. Laird and J. H. Ware. “Random-effects models for longitudinal data”. In: *Biometrics* (1982), pp. 963–974.
- [31] J. Pearl. *Causality*. Cambridge university press, 2009.
- [32] R. E. Melchers, T. Moan, and Z. Gao. “Corrosion of working chains continuously immersed in seawater”. In: *Journal of marine science and technology* 12.2 (2007), pp. 102–110.
- [33] Y.-H. Zhang and P. Smedley. “Fatigue Performance of High Strength and Large Diameter Mooring Chain in Seawater”. In: *International Conference on Ocean, Offshore and Arctic Engineering*. OMAE2019-95984. American Society of Mechanical Engineers Digital Collection. 2019.
- [34] J. Fernández, W. Storesund, and J. Navas. “Fatigue performance of grade R4 and R5 mooring chains in seawater”. In: *International Conference on Ocean, Offshore and Arctic Engineering*. OMAE2014-23491. American Society of Mechanical Engineers Digital Collection. 2014.
- [35] N. E. Dowling. *Mechanical behavior of materials: engineering methods for deformation, fracture, and fatigue*. eng. Fourth. Boston, Mass: Pearson Education, 2013. ISBN: 9780131395060.
- [36] *Mathworks: Linear Mixed-Effects Models*. <https://www.mathworks.com/help/stats/linear-mixed-effects-models.html>. Accessed: 2021-07-08.
- [37] JCSS. *Probabilistic Model Code. Part 3: Resistance Models*. Standard. Joint Committee of Structural Safety, 2001.
- [38] J. D. Sørensen. “Reliability-based calibration of fatigue safety factors for offshore wind turbines”. In: *The Twenty-first International Offshore and Polar Engineering Conference*. International Society of Offshore and Polar Engineers. 2011.
- [39] H. O. Madsen. “Stochastic modeling of fatigue crack growth and inspection”. In: *Probabilistic methods for structural design*. Springer, 1997, pp. 59–83.
- [40] T. Moan and R. Song. “Implications of inspection updating on system fatigue reliability of offshore structures”. In: *Journal of Offshore Mechanics and Arctic Engineering* 122.3 (2000), pp. 173–180.

- [41] P. J. Haagenzen and J. Köhler. *Fatigue testing of mooring chains - statistical analysis of data from test series with different number of chain links*. Memo. Dept. of Structural Engineering, NTNU, Jan. 2015.

Paper V. Value of information of in situ inspections of mooring lines

Mendoza, J., J. Paglia, J. Eidsvik, and J. Köhler (2021). “Value of information of in situ inspections of mooring lines”. In: *Proceedings of the Institution of Mechanical Engineers, Part O: Journal of Risk and Reliability* 235.4, pp. 556–567. DOI: 10.1177/1748006X20987404.

The post-peer-review, copy-edited version of the article published in the Journal of Risk and Reliability is available at: <https://doi.org/10.1177/1748006X20987404>.

The concept of the article was developed by J. Mendoza and J. Köhler. The formulation of the Bayesian Network received input from all co-authors. The implementation of the Bayesian Network was conducted by J. Paglia and J. Mendoza. The Value of Information analysis was implemented by J. Paglia. The evaluation of the system reliability was implemented by J. Mendoza. The article was mainly written by J. Mendoza. The section *Value of information of discrete inspections* was largely written by J. Paglia and J. Eidsvik. The case study was jointly written by J. Mendoza and J. Paglia. The remaining sections were mainly written by J. Mendoza, with editing by all co-authors.

Value of information of in situ inspections of mooring lines

Jorge Mendoza , Jacopo Paglia, Jo Eidsvik and Jochen Köhler

Proc IMechE Part O:
J Risk and Reliability
2021, Vol. 235(4) 556–567
© IMechE 2021
Article reuse guidelines:
sagepub.com/journals-permissions
DOI: 10.1177/1748006X20987404
journals.sagepub.com/home/pio



Abstract

Mooring systems that are used to secure position keeping of floating offshore oil and gas facilities are subject to deterioration processes, such as pitting corrosion and fatigue crack growth. Past investigations show that pitting corrosion has a significant effect on reducing the fatigue resistance of mooring chain links. In situ inspections are essential to monitor the development of the corrosion condition of the components of mooring systems and ensure sufficient structural safety. Unfortunately, offshore inspection campaigns require large financial commitments. As a consequence, inspecting all structural components is unfeasible. This article proposes to use value of information analysis to rank identified inspection alternatives. A Bayesian Network is proposed to model the statistical dependence of the corrosion deterioration among chain links at different locations of the mooring system. This is used to efficiently update the estimation of the corrosion condition of the complete mooring system given evidence from local observations and to reassess the structural reliability of the system. A case study is presented to illustrate the application of the framework.

Keywords

Bayesian network, value of information, pitting corrosion, fatigue, mooring line, structural system

Date received: 7 May 2020; accepted: 16 November 2020

Introduction

Mooring systems secure the position keeping of floating offshore platforms and consist of several mooring lines that connect the platform to an anchor on the seabed. The main structural part of mooring lines is usually constituted by steel chains, although alternative configurations and materials exist, such as synthetic fiber rope, steel wire rope or a combination of all of them.¹ In this article, we focus on mooring lines constituted by studless steel chains. The integrity of mooring chains can be treated as a serial system, since failure of a single link leads to structural failure of the complete mooring line. A mooring line failure increases the load level on the adjacent lines and thereby increases the probability of progressive collapse of the mooring system. This is associated with large environmental and economical consequences, such as oil spill, loss of production, and loss of reputation of the involved companies. Consequently, the detection of failures in a mooring line system is usually followed by operation shutdown, which is associated with large economical loss. Manufacturing of chain links is costly and it demands large amounts of steel. Furthermore, integrity management measures of mooring systems require large financial investments, making it unfeasible to

inspect all components or to apply mitigation measures when any deterioration is observed. Therefore, resources invested in risk mitigation need to be carefully allocated to ensure a cost-efficient and safe operation.

Mooring lines are subject to large environmental cyclic loading while being exposed to a highly corrosive environment, leading to fatigue and corrosion deterioration. Fontaine et al.¹ report that these deterioration processes account for the majority of observed mooring line failures. Recommended practice guidelines, such as API RP 2SK,² and industry standards, such as ISO 19901-7:2013³ and DNVGL-OS-E301,⁴ consider that these deterioration processes can be addressed independently from each other for the design and integrity management of mooring lines. Corrosion deterioration is typically assessed by estimating the lifetime chain diameter reduction, assuming uniform corrosion and wear per year. Fatigue design is commonly

Norwegian University of Science and Technology, Trondheim, Norway

Corresponding author:

Jorge Mendoza, Norwegian University of Science and Technology, Høgskoleringen 1, 7491 Trondheim, Trøndelag, Norway.
Email: jorge.m.espinosa@ntnu.no

conducted using S-N curves, which are curves that assess the number of cycles to fatigue failure for a given cyclic stress range.

Several investigations emphasize the significant effect of corrosion on the fatigue life of mooring chains.⁵⁻⁷ Structural failure is in general not a linear superposition of the effects of corrosion and fatigue, but a complex combination of phenomena. Among the several ways in which the two deterioration phenomena interact, it is identified that localized corrosion, commonly known as corrosion pits, act as stress raisers on the chain link surface, fostering fatigue crack initiation.^{8,9} Gabrielsen et al.¹⁰ report results of visual surface inspection of retrieved mooring chains, which reveal significant local wear at the contact region of links close to the winch on the installations and severe spatially distributed pitting corrosion. Fatigue testing in laboratory conditions of these retrieved links suggests that surface roughness and pitting depth are the main indicators of the reduction of fatigue resistance, which is aligned with the findings in other research studies.¹¹ The unaccounted interaction between these phenomena in design standards may explain why observed failure rates of mooring lines are larger than expected and admissible.^{1,12}

The deterioration conditions of the different chain links constituting the mooring system are statistically dependent. Dependence among different locations is mainly due to common influencing factors related to the environment and to the manufacturing process of the links. Examples of such factors are material parameters, load history, pH, temperature, and the amount of dissolved oxygen. It is important to take this dependence into account because (i) it affects the structural reliability of the system¹³ and consequently, integrity management decisions; (ii) it has a large impact on the amount of information to be learned from local inspections at discrete points in time, since information gathered at one location can be used to update the belief on the deterioration condition at other parts of the structural system.¹⁴ Hence, the statistical modeling affects optimal planning of inspection campaigns.

This study pursues to inform and support integrity management decisions regarding the allocation of discrete inspections in mooring line systems. For that purpose, we propose a Bayesian Network (BN) to model the dependence in the surface condition within the components of the mooring system and its effect on the fatigue life of the mooring lines and the structural integrity of the mooring system. Value of information (VOI) analysis is then used to assess the most valuable data to collect.^{15,16} The use of BNs for modeling the problem helps with the integration of observations (evidence) about variables of interest and to efficiently perform statistical inference. BNs have been used for decision making support and VOI analysis in various contexts.^{17,18} Arzaghi et al.¹⁹ use a dynamical BN to study pitting corrosion and fatigue degradation over time for submerged pipelines. Li et al.²⁰ apply BNs for

modeling corrosion of pipelines and to study an optimal maintenance plan with a particular focus on risk-based maintenance. Rather than providing a maintenance plan, the present study focuses on using VOI analysis to assess the most valuable data to gather in order to inform integrity management decisions for mooring systems.

Problem setting

The structural integrity of the mooring system of a floating oil and gas production unit is regarded. The decision maker is the operator of the production unit. At a given point in time of the service life of the mooring system, the decision maker is to efficiently plan an inspection campaign. An inspection campaign provides information on the corrosion condition of one or several chain segments. Possible decisions that the decision maker can choose from are to inspect any given number of segments, or not to conduct any inspection. The gathered evidence is used to inform actions on the structural system, such as to repair or replace any line segment, or to do nothing. It is assumed that both replacement and repair of segments set their corrosion condition back to completely uncorroded.

The structural system is subdivided into four hierarchical levels, as illustrated in Figure 1. The first level corresponds to the complete system of mooring chains,

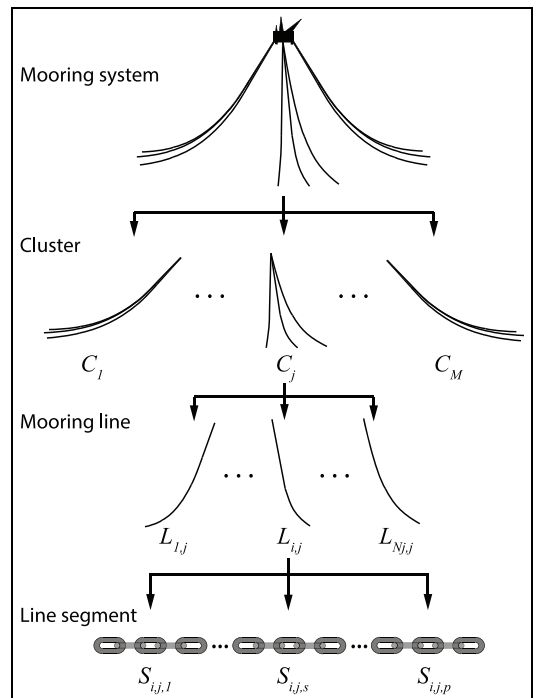


Figure 1. Hierarchical organization of the components of the mooring system.

which is constituted by a set of $M \in \mathbb{N}$ clusters of mooring lines $\mathcal{C} = \{C_1, \dots, C_M\}$. At the second level, a cluster C_j is comprised of $N_j \in \mathbb{N}$ mooring lines $\mathcal{L}_j = \{L_{1,j}, \dots, L_{N_j,j}\}$. The third level is the mooring line level, where line $L_{i,j}$ is subdivided into $p \in \mathbb{N}$ mooring line segments $\mathcal{S}_{i,j} = \{S_{i,j,1}, \dots, S_{i,j,p}\}$, with each segment containing a number of chain links with approximately the same expected deterioration condition. Finally, the fourth level is constituted by the line segment.

Information about the corrosion condition of mooring links can be gathered using in situ techniques, for instance by surface scanning using a remotely operated vehicle (ROV). The subdivision of a mooring line into segments should be performed so that one local observation, say of the surface of one link, can be used to characterize the condition of the entire segment with sufficient accuracy. By embedding the presented hierarchical structure in a probabilistic model, information retrieved from a particular segment can be used to update the belief on the corrosion condition of the entire mooring system. Prior knowledge is required to train the model for the corrosion conditions. This is done using state of the art physics-based models, as described below. Given a model that relates corrosion condition and fatigue resistance, the structural reliability of the mooring system can be subsequently reassessed when more information is available.

Decisions regarding which segment to inspect are ranked based on VOI analysis. The theoretical background of VOI analysis is briefly presented in the next section. An estimate of the structural reliability of the system is needed in order to conduct the VOI analysis. A BN is developed and used to relate the corrosion condition of the chain segments, including all available information at the decision point in time, with the structural reliability of the mooring system one year ahead. We use this estimate of the system reliability for the VOI analysis. This is a simplification, since inspection planning optimization is in general a sequential decision problem, that is, inspection ranking at a given year depends on the subsequent inspection planning. Assessing the sequential decision problem is computationally demanding, since it would require to evaluate a dynamic BN in order to compute the evolution of the structural reliability in time and to explore a set of possible inspection alternatives which grows exponentially with the remaining service time of the structure. Due to computational limitations, the authors approach this issue by treating it as a static problem in this article.

Value of information of discrete inspections

Decisions on when and where inspections of the surface condition of mooring chain links are to be conducted are made with the intention to balance the large costs associated with these inspections and the value that

they bring. Among the several approaches that one can regard to inform these decisions, VOI analysis is identified as a rational tool to make more conscious decisions by minimizing the expected costs. The value of conducting an inspection is a measure of the potential that retrieving new evidence has on triggering different actions upon the structural components of the system. At its roots, the VOI is the maximum monetary value that a decision maker should be willing to pay for a new observation.¹⁶ In practice, the VOI associated with a variety of possible inspection schemes can be used to rank these schemes and to provide a useful basis for decision support.

Let $a \in \mathcal{A}$ denote actions or alternatives that the decision maker can choose among. In the current application, these actions relate to repair, replace or do nothing for different combinations of segments, lines, and clusters. The value function $v(\mathbf{x}, a)$ describes the monetary value as a function of the alternative a and the uncertain variables of interest \mathbf{x} . Boldface notation is used to indicate that \mathbf{x} is a vector consisting of the indicators for the corrosion condition at the various segments, lines, and clusters, and also the temperatures at different sea depths and other variables that contribute to a useful statistical representation of the system. Before any inspection is done, the decision maker will select the alternative that maximizes the expected value of $v(\mathbf{x}, a)$. This is called the prior value (PV), and it is defined as

$$PV = \max_{a \in \mathcal{A}} \{\mathbb{E}[v(\mathbf{x}, a)]\}. \quad (1)$$

Decisions on inspection planning are conducted prior to obtaining the information. The evaluation of inspection alternatives is based upon conditional values, given the observation outcomes. The preposterior value (PPV) integrates over all the possible observation outcomes

$$PPV_\kappa = \int_{\mathbf{y}_\kappa} \max_{a \in \mathcal{A}} \{\mathbb{E}[v(\mathbf{x}, a) | \mathbf{y}_\kappa]\} \Pr(\mathbf{y}_\kappa) d\mathbf{y}_\kappa, \quad (2)$$

where the (possibly multivariate) retrieved data \mathbf{y}_κ denotes the outcome of inspection scheme κ . Note that there are many possible combinations of inspections schemes κ , such as inspecting a given segment or a combination of them. One wants to choose these wisely so that inspection results \mathbf{y}_κ are likely to improve the actions related to repair or replacement.

The VOI associated with a potential inspection alternative κ is obtained by subtracting the PV to the PPV

$$VOI_\kappa = PPV_\kappa - PV. \quad (3)$$

Given the fact that inspections come with a cost, the decision maker can compare the VOI with the inspection cost (c_κ), and acquire data only if $VOI(\mathbf{y}_\kappa) - c_\kappa > 0$. Moreover, one can rank inspection

alternatives according to their information gain. The optimal inspection alternative is then

$$\kappa_{opt} = \underset{\kappa}{\operatorname{argmax}} \operatorname{PPV}_{\kappa} \quad (4)$$

Pit depth growth model

The division of the mooring line in smaller segments allows the modeling of statistical dependencies between segments of the same line at different depths and between segments of different lines. The physical variable of interest is the maximum pit depth d . When modeling d , it is necessary to consider the possible factors that can affect pit growth. Melchers²¹ shows that the development of pitting in steel components immersed in seawater can be divided in two major phases: aerobic and anaerobic. Initially, during a period that can comprise some months to few years, pit depth growth is driven by anaerobic action and is, in general, significantly lower than the one caused by the subsequent phase. During this first phase, biological activity, water velocity, and the amount of dissolved oxygen have relevant effects on the pit growth. For the remaining service life of the chain, the growth of corrosion pits is part of the anaerobic phase. Growth during this phase is largely caused by biological agents, such as sulfate-reducing bacteria (SRB). The water temperature is found to play a central role for the growth of SRB. Pits can reach extreme depths during this phase, which may lead to failure of the mooring line in combination with fatigue deterioration. Here, we focus on the second, anaerobic phase when modeling pit growth.

It is assumed, in accordance with the model by Melchers,²¹ that the anaerobic phase starts right after the aerobic phase at a time t_a . This time is found to mainly depend on temperature T and its best estimate is represented by $t_a^* = 6.61 \exp(-0.088T)$. For a typical range of temperatures in the North Sea (between 6.9°C and 19.0°C), t_a^* varies between 3.6 and 1.2 years. At time t_a , the expected maximum pit depth, denoted \bar{d} is found as a function of temperature

$$\bar{d}(t_a, T) = 0.99 \exp(-0.052T). \quad (5)$$

A piece-wise function is proposed by Melchers²¹ to model the time evolution of the mean maximum pit depth, which is constituted by an initial non-linear growth curve followed by a linear one. At time $t = t_a$, the maximum pit depth grows fast with an initial slope r_{ap} , which depends on temperature T according to the following functional relationship

$$\left. \frac{\partial \bar{d}(t, T)}{\partial t} \right|_{t=t_a} = r_{ap} = 0.596 \exp(0.0526T). \quad (6)$$

Afterwards, the growth rate decreases until it reaches a constant value, which is modeled by a line with slope r_{sp} and intercept c_{sp} . In this study, the piece-wise function is simplified to a single power-law of the form

Table 1. Best estimates of the parameters of the maximum pit depth time propagation model.

Temperature (°C)	f_{aT}	t_a^* (years)	a_T	b_T
6.9	0.862	3.60	1.064	0.616
9.8	0.880	2.79	1.100	0.562
12.0	0.889	2.30	1.108	0.539
14.4	0.896	1.86	1.110	0.526
16.6	0.901	1.53	1.111	0.519
19.0	0.905	1.24	1.116	0.518

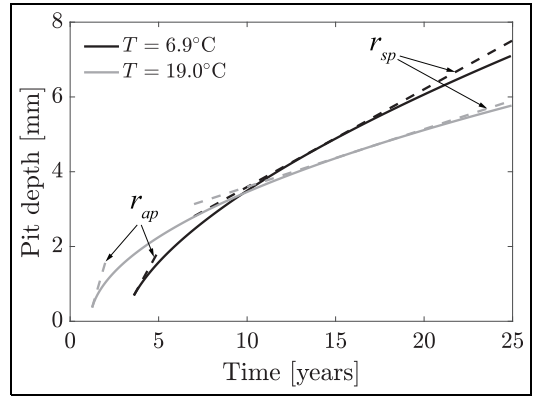


Figure 2. Time evolution model for the anaerobic phase of the expected maximum pit depth d for typical temperatures T in the North Sea.

$$\bar{d}(t) = a_T \cdot (t - t_a^* f_{aT})^{b_T} \quad t \geq t_a, \quad (7)$$

where the parameters a_T and b_T are estimated by applying the constraints in equations (5) and (6) using a relaxation parameter f_{aT} .

The model parameters are provided in Table 1 for a range of typical temperatures in the North Sea. Note that this simplified model is justified for short term predictions. For longer term predictions, say more than 15 years, the power law model may underestimate the growth in comparison with the piece-wise function, as shown in Figure 2. Nevertheless, such predictions are not needed for the purpose of inspection planning, since evidence is provided in shorter intervals. Figure 2 shows the time evolution model for the expected maximum pit for two temperatures.

The uncertainty associated with the prediction of the pit depth at a given time is taken into account with a multiplicative Log-normal error δ_2

$$d(t) = \delta_2 \bar{d}(t) \quad t \geq t_a, \quad (8)$$

where $\bar{d}(t)$ is the expected maximum pit depth in equation (7) and δ_2 has mean value $\mu_{\delta_2} = 1$ and standard deviation σ_{δ_2} , which is varied to study its sensitivity later in the paper.

Corrosion levels

It is assumed that the decision maker uses seven levels to characterize the corrosion condition, with $\gamma_c = 1$ being the uncorroded state and $\gamma_c = 7$ being associated with heavy corrosion and large pits. A corrosion level is assigned to a chain link by visual assessment conducted by trained personnel. The assignment synthesizes several aspects of the corrosion condition, such as the average cross-section reduction due to uniform corrosion, the number of pits and the distribution of pit depths and their shape. There is uncertainty associated with the assignment of corrosion levels due to the nature of the visual inspection. In the current case, the assignment of a corrosion level is assumed to be largely correlated with the maximum pit depth d present in the inspected specimen. This is consistent with the dependence among pit depths in a given chain link. The decision maker provides a probabilistic model of the distribution of the largest pit depth conditional on the corrosion level, see Table 2 and Figure 3.

In the BN, the corrosion levels are defined conditional on the maximum pit depths. Hence, for each segment, the probability of the corrosion level conditional on the maximum pit depth needs to be specified. This conditional probability is computed using the Bayes' formula

Table 2. Mean μ and coefficient of variation (CoV) of the probability density function $f_{D|\Gamma_c}(d|\gamma_c)$ of pit depth d conditional on the corrosion level.

Corrosion level	Distribution	μ (mm)	CoV
1	Exponential	0.05	1.0
2	Normal	0.30	0.2
3	Normal	0.70	0.2
4	Normal	1.10	0.2
5	Normal	1.40	0.2
6	Normal	2.00	0.2
7	Normal	3.00	0.2

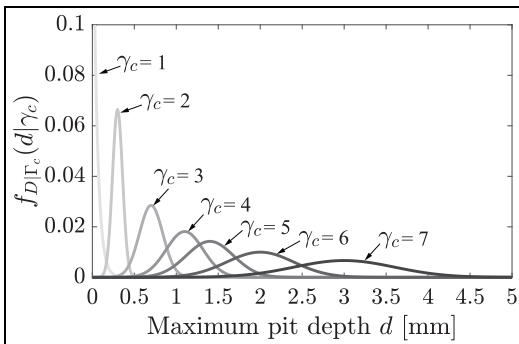


Figure 3. Probability density function $f_{D|\Gamma_c}(d|\gamma_c)$ of pit depth d conditional on the corrosion level $\Gamma_c = [1, 2, \dots, 7]$.

$$\Pr(\gamma_c|d) = \frac{\Pr(d|\gamma_c)\Pr(\gamma_c)}{\sum_{\gamma_c} \Pr(d|\gamma_c)\Pr(\gamma_c)}, \tag{9}$$

where $f_{D|\Gamma_c}(d|\gamma_c)$ is the conditional probability density function of the maximum pit depth given the corrosion level and $\Pr(\gamma_c)$ is the uniform distribution over the seven corrosion levels. In order to evaluate this equation, the continuous space of possible maximum pit depths ($D \in \mathbb{R}^+$) is discretized.

Effect of pitting corrosion on fatigue resistance

The following model is used to assess the combined effect of cyclic stresses and pitting corrosion on fatigue life

$$N_F(\Delta S, \gamma_c) = \delta_1 \cdot k \cdot \Delta S^{-m} \cdot \gamma_c^{\beta_2}, \tag{10}$$

where N_F is the number of cycles to failure, ΔS are the fatigue stress ranges, δ_1 is the model uncertainty, and k , m , and β_2 are regression parameters that mainly depend on the material characteristics and geometry of the structural component of interest. Here, $\delta_1 = 10^\varepsilon$, with ε being Normal distributed with zero mean and standard deviation σ_ε . The model parameters are summarized in Table 3.

Fatigue damage is a cumulative process. As the result of a time dependent deterioration process, the probability of fatigue failure is typically represented by the cumulative probability of failure given a reference period T_{ref} . The accumulated fatigue damage at year t is denoted $D(t)$. For a given stress range ΔS_i and corrosion level γ_c , a fatigue cycle i contributes to fatigue damage as

$$\Delta D_i(\Delta S_i, \gamma_c) = \frac{1}{N_F(\Delta S_i, \gamma_c)}. \tag{11}$$

Note that the stress range ΔS_i is a realization of the process $\Delta S(t)$. The expected damage per cycle conditional on the corrosion level $\mathbb{E}[D_i|\gamma_c]$ is used in the following to simplify the computation of the cumulative damage as

$$D(t, L) = 1 = \sum_{i=1}^{v \cdot t} \Delta D_i \approx v \cdot t \cdot \mathbb{E}[\Delta D_i|\gamma_c], \tag{12}$$

Table 3. Mean μ and standard deviation σ of the parameters of the model in equation (10) for fatigue failure of a mooring line segment with studless chain links.

Parameter	Distribution	μ	σ
m	Deterministic	3.0	0
$\log_{10} k$	Normal	11.200	0.100
β_2	Normal	-0.800	0.150
σ_ε	Normal	0.170	0.030

Table 4. Calibration of the expected shape parameter of the Weibull distributed fatigue stresses $\mathbb{E}[k_w]$ as a function of the service life of the mooring line T_{SL} for a target probability of failure of 10^{-5} .

T_{SL} (years)	20	25	30	35	40
$\mathbb{E}[k_w]$ (N/mm ²)	5.1	4.7	4.4	4.2	4.0

where ν is the average number of stress cycles in a year, which is assumed to be 10^5 cycles/year.

The expected damage per fatigue cycle can be elaborated using the model in equation (10):

$$\begin{aligned} \mathbb{E}[\Delta D_i | \gamma_c] &= \mathbb{E} \left[\frac{1}{N_F(\Delta S_e, \gamma_c)} \right] \\ &= \frac{1}{k \cdot \delta_1} \cdot \Delta S_e^m \cdot \gamma_c^{-\beta_2}, \end{aligned} \quad (13)$$

where ΔS_e is the equivalent stress range of the wave-induced stress process $\Delta S(t)$, which is defined as the constant stress that leads to the same accumulated damage as the time-dependent process. ΔS_e is assumed to be Weibull distributed with parameters k_w and λ_w . Then ΔS_e is given by

$$\Delta S_e = \mathbb{E}_{\Delta S}[\Delta S(t)^m]^{1/m} = k_w \cdot \Gamma \left(1 + \frac{m}{\lambda_w} \right)^{1/m}, \quad (14)$$

where $\Gamma(\cdot)$ is the complete gamma function. This expression is substituted in equation (13) to compute the expected damage per cycle.

The equivalent stress range ΔS_e is calibrated so that the uncorroded mooring line segment is associated with a target cumulative probability of fatigue failure of 10^{-5} at the end of service life when no inspections nor repairs are conducted. Note that this target probability of failure is somewhat larger than the requirements in some offshore standards, such as DNVGL-OS-E301,⁴ which is typically prescribed to be 10^{-3} . The reason for this is that these standards do not consider the effect of pitting corrosion in the fatigue limit state. We assume that the mooring lines were provided at design with some additional safety to accommodate for the additional contribution of corrosion to fatigue failure. The mean value of k_w is calibrated to match the target probability of failure, where k_w is assumed to be Log-normal distributed with coefficient of variation (CoV) equal to 0.22, and λ_w is deterministic and equal to 0.8. Some values of the calibrated parameter are given in Table 4 for service lives T_{SL} between 20 and 40 years.

The probability of failure of a mooring line segment with a remaining service life of t years and subject to a corrosion level γ_c is denoted $P_{f|\Gamma_c}$ and assessed using the limit state function (LSF) g

$$P_{f|\Gamma_c}(t) = \Pr[g(\mathbf{x}; t|\gamma_c) \leq 0], \quad (15)$$

where $g \leq 0$ defines the failure domain and \mathbf{X} is a vector collecting the involved random variables, which have a

Table 5. Layers of the Bayesian network, with a description of the nodes.

Layers	Description	Node
Layer 1	Hyperparameter	α_T
Layer 2	Temperature	T_s
Layer 3	Max pit depth	$d_{i,j,s}$
Layer 4	Corrosion level	$\gamma_{c,i,j,s}$
Layer 5	Segment integrity	$E_{S,i,j,s}$
Layer 6	Line integrity	$E_{L,i,j}$
Layer 7	Cluster integrity	$E_{C,j}$
Layer 8	System integrity	E_{sys}

joint probability distribution $f_{\mathbf{X}}(\mathbf{x}; t)$ defined via the BN model.

The limit state function g can then be written according to the Palmgren-Miner failure criterion²²

$$g(\mathbf{x}; t|\gamma_c) = \Delta - D(\mathbf{x}; t|\gamma_c), \quad (16)$$

where $D(\mathbf{x}; t|\gamma_c)$ is given by equation (12) and Δ is a random variable representing the uncertainty associated with the fatigue failure criterion. JCSS²³ recommends to model Δ by a Log-normal distribution with mean 1 and CoV 0.3.

The probability of failure of a mooring line segment is defined conditional on its corrosion level by equation (15). This equation can be evaluated with standard structural reliability methods, such as the first order reliability method (FORM). Note that the LSF depends on the fatigue damage accumulated during a period t . During this time, an equivalent fatigue stress is introduced to represent the effect of the wave-induced stress range distribution. However, an equivalent corrosion level is not available in the literature. Corrosion is a complex deterioration process that evolves with time. We assume as a simplification that the corrosion condition can be regarded as constant within a reference period of about a year.

The Bayesian network

A BN is a directed acyclic graph consisting of nodes and arcs. The nodes represent the variables of interest, with discretized sample space in our case, and the arcs between the nodes represent the dependencies. A BN is a convenient representation of the problem where explicit use of causal relations is incorporated via the arrangement of the network. Moreover, the BN model allows efficient inference of the conditional distributions when data become available at a subset of nodes. The BN is formally represented on the computer by a list of nodes and its neighbors along with conditional probability tables (CPTs) for each variable. The Bayes Net Toolbox²⁴ is used for computing the models in MATLAB[®].

We propose a BN with 8 layers to represent the dependence structure of the decision problem. A summary of the layers is shown in Table 5 and a brief description is provided hereafter.

- Layer 1: at the highest layer of the network we have the hyperparameter α_T , which is used to introduce statistical dependence among the temperature at the different water depths.
- Layer 2: this layer is constituted by the nodes of the influencing parameters of pitting corrosion, which in our model is only the temperature nodes T_s . Note that T_s refers to the yearly average temperature of the segments $S_{i,j,s}$. The temperature nodes are represented by a discrete distribution.
- Layer 3: here we have the maximum pit depth nodes $d_{i,j,s}$, which are specified conditional on the corresponding temperature T_s .
- Layer 4: this layer is constituted by the corrosion level nodes $\gamma_{c,i,j,s}$. Each of them is specified conditional on the corresponding maximum pit depth node $d_{i,j,s}$.
- Layer 5: In order to assess the integrity of a segment $E_{S,i,j,s}$, the accumulated probability of fatigue failure of the segment is computed conditional on its corrosion level $\gamma_{c,i,j,s}$.
- Layer 6: the integrity of a mooring line $E_{L,i,j}$ is specified conditional on the integrity of its segments $E_{S,i,j,s}$, with $s = 1, 2, \dots, p$.
- Layer 7: a simplified ultimate limit state is introduced to specify the integrity of a cluster $E_{C,j}$ conditional on the state of its lines $E_{L,i,j}$, with $i = 1, 2, \dots, N_j$.
- Layer 8: the integrity of the mooring system E_{sys} is calculated conditional on the state of the clusters $E_{C,j}$, with $j = 1, 2, \dots, M$.

The modeling of the dependence structure in the BN (Layers 1–3) and the implementation of the structural integrity model (Layers 4–8) are elaborated in more detail hereafter.

Statistical dependence model

The statistical dependence of the corrosion condition among line segments is captured in the BN in two ways, see Figure 4. First, the dependence of the corrosion condition among segments belonging to the same partition s of the mooring lines is modeled by conditioning the maximum pit depth nodes $d_{i,j,s}$ on the corresponding temperature node T_s . Second, the dependence among the condition of segments from different partitions is modeled through the statistical dependence of the seawater temperature at different water depths. This correlation is introduced by conditioning the seawater temperature nodes on a hyperparameter α_T . A Gaussian copula with given correlation coefficient is used to represent the joint distribution of the temperature nodes, according to the approach proposed by Luque and Straub.²⁵

Other parameters of the employed deterioration model may be correlated among different chain segments. The consideration of additional parameter correlations would require to explicitly represent those

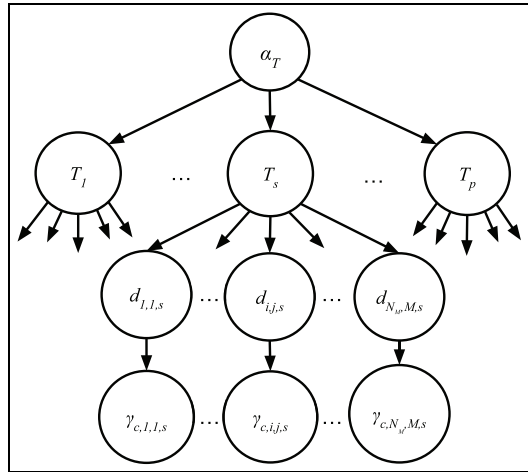


Figure 4. Hierarchical structure of the upper layers of the Bayesian network. The corrosion level nodes $\gamma_{c,i,j,s}$ are specified conditional on the maximum expected pit depth nodes $d_{i,j,s}$, which in turn are specified conditional on the temperature node of the corresponding water depth T_s . The temperature nodes are correlated through the hyperparameter α_T .

parameters in the BN. This would largely increase the complexity of the BN. Since the aim of the decision framework is to rank the efficiency of inspecting chain segments, the authors have prioritized to limit the computational demand of the BN and not to include these additional correlations. However, this would not be justified if an accurate estimation of the reliability of the mooring system would be needed to, for example, include target reliability constraints.

Mooring line integrity

The structural integrity of the p segments is denoted $E_{S,i,j,1}, \dots, E_{S,i,j,p}$, respectively. The fatigue integrity of a line $L_{i,j}$, denoted $E_{L,i,j}$, is defined conditional on the integrity of its segments, as illustrated in Figure 5. Note that the integrity of the segments is conditional on their corrosion level. Both the integrity of a segment and of the whole line have a binary representation (0: *Safe* or 1: *Fail*). Therefore, the CPT of $E_{L,i,j}$ needs to be defined for 2^p combinations of the segments states. The CPT mainly consists of zeros and ones, since the mooring line survives only when all its segments take the *Safe* state and fails in all other situations.

Integrity of a cluster of mooring lines

The modeling of the integrity of a cluster of mooring lines $E_{c,j}$ is shown in Figure 6. $E_{c,j}$ has a binary representation (0: *Safe* or 1: *Fail*). It is assumed that the undamaged cluster is associated with an annual probability of failure of 10^{-5} , as prescribed in DNVGL-OS-E301.⁴ The probability of failure of a cluster

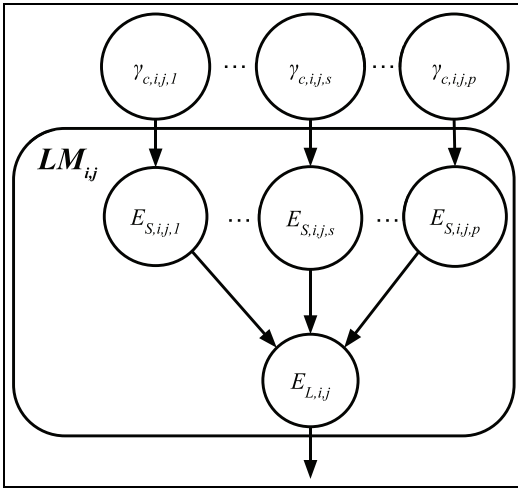


Figure 5. Module LM_{ij} modeling the structural integrity a mooring line $E_{L,ij}$ as a serial system of the line segments $E_{S,ij,1}, \dots, E_{S,ij,p}$.

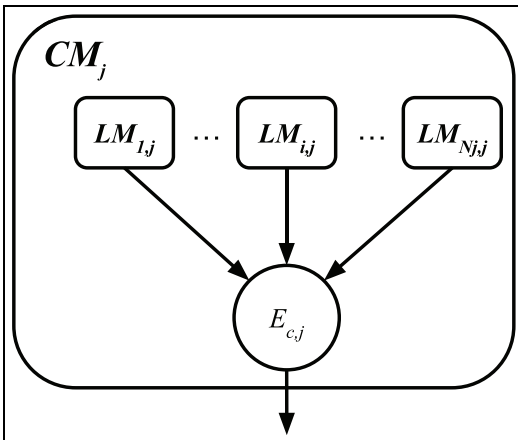


Figure 6. Module CM_{ij} modeling the structural integrity of a cluster $E_{c,j}$ which constituted by N_j parallelly connected mooring lines.

conditional on the number of failed lines $\Pr(E_{c,j} = Fail|N_F = \ell)$ is computed assuming brittle failure due to ultimate load, that is, a failed line does not contribute to load bearing. The probability of cluster failure conditional on the number of failed lines is then given by

$$\Pr(E_{c,j} = Fail|N_F = \ell) = \int_Q \Pr[E_{c,j} = Fail|q, (N_j - \ell)]f_Q(q) dq, \quad (17)$$

where f_Q is the probability density function of the annual extreme load Q and $\Pr[E_{c,j} = Fail|q, (N_j - \ell)]$ is

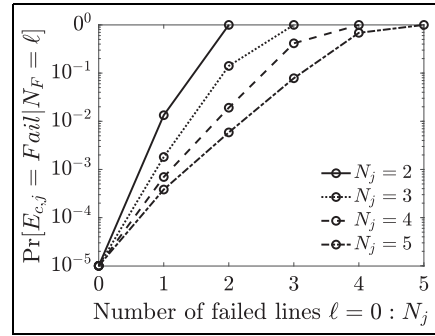


Figure 7. Conditional probability of failure of a cluster with N_j mooring lines for increasing number of failed lines ℓ .

the probability of failure of the cluster conditional on the load and the number of survived lines, which is computed according to the solution by Daniels.²⁶

It is assumed that the lines of a cluster have independent and identically distributed ultimate load capacity R_i , which is Log-normal distributed with CoV 0.15. The ratio between the mean capacity of the undamaged cluster, that is, $N_j \cdot \mu_{R_i}$, and the mean annual maximum load μ_Q is calibrated so that the cluster has the appropriate probability of failure in the undamaged state. Q is assumed to be Gumbel distributed with CoV 0.3. The conditional probability of failure of a cluster is plotted in Figure 7 for clusters containing different number of mooring lines N_j .

Structural integrity of the mooring system

The structural integrity of the mooring system E_{sys} is represented in the BN by a node with two states: 0: *Safe* or 1: *Fail*. The integrity of the system depends on the integrity of the different clusters conforming it. This dependence is case dependent and it is influenced by the configuration of the anchoring system of the offshore floating unit. It is often the case that the failure of a cluster of mooring lines leads to loss of sufficient anchorage and consequently to disproportionate consequences, such as oil spill and associated loss of reputation. The BN model of the integrity of the mooring system is illustrated in Figure 8. Note that E_{sys} is conditional on the integrity of the clusters $E_{c,j}$, with $j = 1, \dots, M$, which are defined by the module CM_j in Figure 6.

Case study

The potential benefits of the presented framework are demonstrated alongside a case study on optimal inspection planning for the mooring system of an oil and gas platform in the North Sea. The case study contains several simplifications to keep the complexity in comprehensible limits.

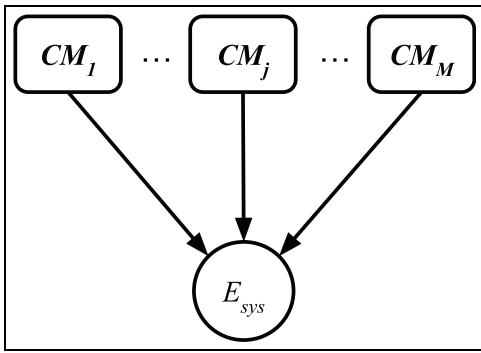


Figure 8. Structural integrity E_{sys} of the mooring line system constituted of M mooring clusters.

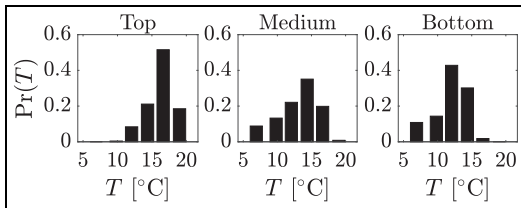


Figure 9. Probability mass function $\Pr(T)$ of the average seawater temperature at top, medium, and bottom locations.

The considered mooring system consists of four clusters, each of them with four mooring lines. The mooring system fails if any of the clusters fail. It is assumed that all the mooring lines have been placed at the same time, and no repairing or replacement have been conducted prior to the assessment. The platform is located in an area where the average water depth is ca. 100 m. The focus is on the submerged parts of the mooring lines, which are divided in three segments; the top segment ranging in the water depth 0–20 m, the medium segment ranging in the water depth 20–50 m and the bottom segment ranging deeper than 50 m. In this case study, the VOI of inspecting the corrosion condition of the different segments is assessed. The simultaneous observation of several segments during one inspection campaign is not considered for simplicity.

The assumptions for distribution and correlation of water temperature are based on observations collected at the UK shelf.²⁷ The yearly average temperature in each depth segment is modeled with the probability mass functions in Figure 9, which has a discretization of intervals of ca. 3°C from the minimum to the maximum temperature, which are 5.5°C and 20.7°C, respectively. The temperature is averaged over observations at each interval, which corresponds to the values shown in Table 1. The linear correlation coefficient among the average temperature of the segments is found to be around 0.8.

The structure was designed with a service life of 30 years. Hence, the expected shape parameter of the fatigue stress range is taken as $\mathbb{E}[k_w] = 4.4 \text{ N/mm}^2$, according to Table 4. The current analysis considers potential inspections at year 5 and the projections of the structural integrity are assessed for an additional year, that is, potential failure between years 5 and 6. It is assumed that the corrosion condition can be considered constant during 1 year.

A series of actions or decision alternatives that the decision maker can choose from are to be specified to define the value function in equations (1) and (2). It is noted that the VOI of an inspection scheme depends largely on the consideration of these actions. We provide a variety of decision alternatives in order to mimic the multiple options that would be explored in a more realistic sequential decision analysis, where not only repair options but also additional sequential inspection alternatives would be assessed. The representation of the latter would be by far too complex for this case study. Here, the decision maker can choose to not take any action ($a = 0$), to repair the top, medium, or bottom segment of a given line (denoted $a = 1$, $a = 2$, and $a = 3$, respectively) or to repair the top, medium, or bottom segment of one line per cluster ($a = 4$, $a = 5$, and $a = 6$). Furthermore, the decision maker can replace a complete line in a cluster ($a = 7$) or a complete line in each cluster ($a = 8$). It is also possible to repair all the top, medium and bottom segments of a cluster ($a = 9$, $a = 10$, and $a = 11$) or of the entire system ($a = 12$, $a = 13$, and $a = 14$).

Assuming that inspection results \mathbf{y}_κ can be available, the PPV calculation requires the expected values for all possible observation outcomes. For the PV, the inspection just denotes the empty set. First, for the alternative of no repair or replacement ($a = 0$), the expected value is then defined as

$$\begin{aligned} \mathbb{E}[v(\mathbf{x}, 0)|\mathbf{y}_\kappa] = & \\ & - c_l \max_{i,j} \{ \Pr(E_{L_{i,j}} = 1 | \mathbf{y}_\kappa) \} - c_s \Pr(E_{sys} = 1 | \mathbf{y}_\kappa), \end{aligned} \tag{18}$$

where c_l is the cost of failure of a mooring line and c_s is the cost of system failure. Here, c_l is taken as €20 mln and it is mainly associated with the cost of replacing the failed line, including the production loss from the detection of the failure until the line is replaced. The consequences of system failure is taken as $c_s = €180 \text{ mln}$.

For the other alternatives $a > 0$, we let $\gamma_c(\mathbf{x}_a)$ denote the corrosion level of the segments that have been repaired or replaced and consequently returned to the uncorroded state, that is, $\gamma_c(\mathbf{x}_a) = 1$. The expected values are then

$$\begin{aligned} \mathbb{E}[v(\mathbf{x}, a)|\mathbf{y}_\kappa] = & \\ & - c_l \max_{h,l} \{ \Pr(E_{L_{h,l}} = 1 | \gamma_c(\mathbf{x}_a) = 1, \mathbf{y}_\kappa) \} \\ & - c_s \Pr(E_{sys} = 1 | \gamma_c(\mathbf{x}_a) = 1, \mathbf{y}_\kappa) - c_a n_a, \end{aligned} \tag{19}$$

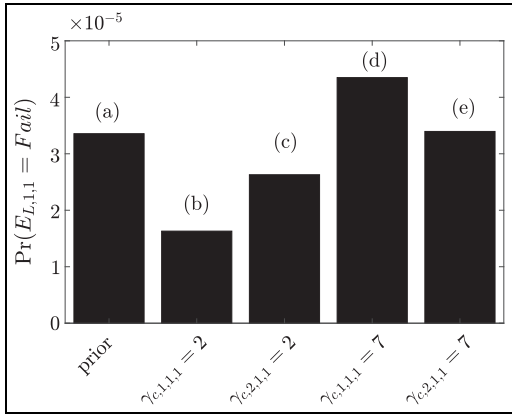


Figure 10. Effect of belief propagation on the probability of failure of a line $\Pr(E_{L,1,1} = Fail)$. Evidence of low corrosion in the top segments of the assessed line and a nearby one is shown in (b) and (c), respectively. (d) and (e) present the effect of observing high corrosion in the same segments.

where $c_a = \{c_r, c_{rl}\}$ is the cost of repairing ($c_r = \text{€}0.7$ mln) or replacing ($c_{rl} = \text{€}0.9$ mln) a segment depending on the decision taken, and n_a is the number of segments that are repaired or replaced; The costs c_a are assumed to be the same for all segments.

Given the structure of the value function, and that we deal with discretizations of the continuous distributions, it is possible to explicitly compute the PV and PPV. VOI analysis, as formally introduced above, is used in the following to select which segments to inspect.

Results

VOI analysis is first performed with the assumed standard deviation of the pitting corrosion model uncertainty set to $\sigma_{\delta_2} = 0.5$. Afterwards, the effect of increasing or reducing the model accuracy is investigated.

The effect of observing the corrosion condition of different segments on the assessment of the probability of failure of a line is illustrated in Figure 10. The effect of observing the corrosion condition of a segment of the line of interest can be seen in cases (b) and (d). Observing a low corrosion level ($\gamma_c = 2$) decreases the probability of failure by approximately half with respect to the prior case, and an observation of a high corrosion level ($\gamma_c = 7$) increases it by 30%. Inference from observations of a segment of a different line are shown in (c) and (e) and show as well a considerable effect, although weaker than for (b) and (d).

The computation of the VOI is conducted for a given line of the system, where single observations of the corrosion level are possible. Note that these results are

Table 6. Results of VOI analysis for observations of the corrosion level of the top, medium, and bottom segment of a given line, when the decision alternatives are the ones described in the case study section.

	Top	Medium	Bottom
VOI	€285	€278	€283

Table 7. Results of VOI analysis for the observation of the corrosion level of the top, medium, and bottom segment of a given line for different values of the standard deviation of the multiplicative model error σ_{δ_2} .

	Top	Medium	Bottom
VOI at $\sigma_{\delta_2} = 0.1$	€294	€298	€304
VOI at $\sigma_{\delta_2} = 0.3$	€292	€289	€295
VOI at $\sigma_{\delta_2} = 0.7$	€272	€264	€269
VOI at $\sigma_{\delta_2} = 0.9$	€260	€250	€254

valid for any line of the system due its symmetry in terms of number of segments and of number of lines in a cluster. Table 6 summarizes the results of the VOI analysis for the three segments (top, medium, and bottom). The obtained VOI can be used to assess the most valuable location for inspection. The results show that observing the corrosion level of the top segments is the most valuable inspection.

The sensitivity of the results with respect to the modeling error as parametrized by the standard deviation σ_{δ_2} is studied. Table 7 shows a decrease of the VOI as the standard deviation increases. On the one hand, a large uncertainty in the estimation of the maximum pit depth results in a less informative prior assessment. This suggests that newly obtained information has the potential to drastically change the expectation of the system condition. On the other hand, a large model uncertainty also yields a broad likelihood function of the inspection outcomes, which reduces the efficiency of the inspections. We argue that due the large costs associated with the mitigation actions and the consequences of failure, the latter has a larger impact on the results. The fact that new observations become more valuable when the model accuracy increases emphasizes the importance of uncertainty quantification and the development of an accurate model for pitting corrosion degradation. It is observed that the most valuable inspection switches from being the bottom segment inspection to be the top segment inspection for a value of σ_{δ_2} somewhere in between 0.3 and 0.5.

Finally, VOI is studied for a situation similar to the one of Table 6, where the only difference is that now the study is done after 10 years of service life of the system. The larger VOI in Table 8 shows how gathering information on a more deteriorated system will be of greater value for the decision maker. This is due to the

Table 8. Results of VOI analysis for observations of the corrosion level of the top, medium, and bottom segment of a given line after 10 years of service life of the system.

	Top	Medium	Bottom
VOI	6225	6223	6239

larger variation that the probability of failure of a line presents depending on the corrosion condition and due to the overall larger probability of system failure.

The computational complexity of the framework developed is mostly associated with the evaluation of the VOI, assuming a BN is already set with all the CPT computed. For the preposterior value (PPV), a sum must be computed over the possible outcomes of the observation (y_k), and for each outcome, the CPT are updated to get the conditional expressions. For each outcome, this takes only about 1 s, and overall the BN fitting and VOI calculation only take about 3 min on a commercial laptop with a 3.1 GHz Dual-Core Intel Core i7 processor. A benefit of BN models is that they represent the important variables in a compact manner and large size computer intensive evaluations are often avoided.

Discussion

The proposed framework aims at supporting inspection planning decisions for mooring systems based on VOI analysis. Relevant features that affect the decisions at hand and their interactions are explicitly represented in a BN model. The framework is ultimately a simplification of a highly complex decision problem. The actual sequential decision problem is simplified by neglecting the effect of future inspections in the planning of inspections at a given year. Furthermore, the assessment of the structural reliability is conducted with projections of an additional year from the decision point in time. This leads to low estimates of the probability of failure, which in turn leads to low estimates of the VOI. As a consequence, the results of the analysis cannot be used to determine whether inspections should be conducted, but only to rank which inspections should be conducted first. It is nonetheless common practice that the decision maker first chooses if it is needed to conduct inspections, and then decides what to inspect. The proposed framework can be used in the second step to guide that type of decision.

Currently available models for pitting corrosion are associated with large uncertainties. Despite these uncertainties, integrity management decisions need to be made. This stresses the importance of uncertainty quantification and of integrating these uncertainties into a formal framework in order to support decisions according to the best available knowledge. More accurate modeling of the deterioration processes could be added when available to improve the quality of the outcomes.

Results from the case study show the value of improving the model accuracy, see Table 7.

A simplified model is used to assess the fatigue integrity of a mooring segment conditional on its corrosion condition. Since the corrosion condition evolves with time, the unconditional probability of failure should be dynamically assessed. The obtained estimation of the probability of failure at a given year t is thus a conservative approximation in which the corrosion at that year is used to represent the condition at all the previous years. This is justified at the early stages of the deterioration due to the power-law growth of corrosion, in which pits rapidly reach significant depths followed by a steadier growth. If the lifetime cumulative probability of failure of a mooring line segment was to be more accurately computed, the unconditional limit state function $g(x; t; T_{SL}) \leq 0$ should be considered instead of equation (16), where $g(x; t)$ is defined as

$$g(x; t) = \Delta - \sum_{\tau=1}^t \sum_{\Gamma_c} D(x; \tau | \gamma_c) \Pr(\gamma_c; \tau). \quad (20)$$

A dynamic BN should be developed to evaluate this equation. This BN would drastically increase the computational demand as compared to the one proposed in this article. Nonetheless, it is unclear whether this would lead to significantly better decisions.

Conclusion

A method based on value of information analysis is presented in this paper with the aim of supporting efficient planning of in situ inspections of the corrosion condition of structural elements of a mooring systems. We focus on the particular case of mooring systems constituted by steel chain mooring lines. Chain links in marine conditions are subject to pitting corrosion, which leads to an increased probability of fatigue failure of the chain links under cyclic loading. An ultimate load limit state is used in order to assess the integrity of the deteriorating system, which is subject to a combination of pitting corrosion and fatigue. A state-of-the-art model is used to model the growth of corrosion pits in time. The model assumes that pit growth is mainly caused by the action of sulfate reducing bacteria under anaerobic conditions, which is driven by the average seawater temperature at a given location.

The mooring system is regarded as hierarchically structured with four levels: (i) the mooring system, (ii) the cluster of mooring lines, (iii) the mooring line, and (iv) the line segment, which is constituted by a number of chain links. We propose a Bayesian network to model statistical dependence of the corrosion among line segments and to estimate the structural integrity of the mooring system. The network allows for efficient updating of the corrosion condition of the mooring segments and reassessment of the integrity of the system when new observations become available. This allows to efficiently conduct value of information

analysis, which is used to rank inspection alternatives. The application of the framework is illustrated with a case study. Results emphasize the importance of the accuracy of the corrosion model to increase the value of the inspections.

Acknowledgement

The authors would like to acknowledge the members of the KPN Lifemoor project for the discussions and useful insight.


Declaration of conflicting interests

The author(s) declared no potential conflicts of interest with respect to the research, authorship, and/or publication of this article.

Funding

The author(s) received no financial support for the research, authorship, and/or publication of this article.

ORCID iD

Jorge Mendoza  <https://orcid.org/0000-0002-1190-5919>

References

- Fontaine E, Kilner A, Carra C, et al. Industry survey of past failures, pre-emptive replacements and reported degradations for mooring systems of floating production units. In: *Offshore technology conference*, Houston, TX, 5–8 May 2014. Offshore Technology Conference.
- API. Design and analysis of stationkeeping systems for floating structures. 3rd ed. In: *API RP 2SK*. Washington, DC: API Publishing Services, 2015.
- ISO. ISO 19901-7:2013. Petroleum and natural gas industries – specific requirements for offshore structures – part 7: stationkeeping systems for floating offshore structures and mobile offshore units. Techreport, International Organization for Standardization, Geneva, Switzerland, 2013.
- DNV-GL. *DNVGL-OS-E301 position mooring*. DNV-GL, 2015.
- Pérez-Mora R, Palin-Luc T, Bathias C, et al. Very high cycle fatigue of a high strength steel under sea water corrosion: a strong corrosion and mechanical damage coupling. *Int J Fatigue* 2015; 74: 156–165.
- Arredondo A, Fernández J, Silveira E, et al. Corrosion fatigue behavior of mooring chain steel in seawater. In: *Proceedings of the ASME 2016 35th international conference on ocean, offshore and arctic engineering*, Busan, South Korea, 19–24 June 2016. American Society of Mechanical Engineers Digital Collection.
- Morgantini M, MacKenzie D, Gorash Y, et al. The effect of corrosive environment on fatigue life and on mean stress sensitivity factor. *MATEC Web Conf* 2018; 165: 03001.
- Kondo Y. Prediction of fatigue crack initiation life based on pit growth. *Corrosion* 1989; 45(1): 7–11.
- Cerit M, Genel K and Eksi S. Numerical investigation on stress concentration of corrosion pit. *Eng Fail Anal* 2009; 16(7): 2467–2472.
- Gabrielsen Ø, Larsen K and Reinholdtsen SA. Fatigue testing of used mooring chain. In: *Proceedings of the ASME 2017 36th international conference on ocean, offshore and arctic engineering*, Trondheim, Norway, 25–30 June 2017. American Society of Mechanical Engineers Digital Collection.
- Lindley T, McIntyre P and Trant P. Fatigue-crack initiation at corrosion pits. *Met Technol* 1982; 9(1): 135–142.
- Gordon RB, Brown MG, Allen EM, et al. Mooring integrity management: a state-of-the-art review. In: *Offshore technology conference*, Houston, TX, 5–8 May 2014. *Offshore Technology Conference*.
- Straub D and Der Kiureghian A. Reliability acceptance criteria for deteriorating elements of structural systems. *J Struct Eng* 2011; 137(12): 1573–1582.
- Luque J, Hamann R and Straub D. Spatial probabilistic modeling of corrosion in ship structures. *ASCE ASME J Risk Uncertain Eng Syst B Mech Eng* 2017; 3(3): 031001.
- Raiffa H and Schlaifer R. *Applied statistical decision theory*. Boston, MA: Harvard University Press, 1961.
- Eidsvik J, Mukerji T and Bhattacharjya D. *Value of information in the earth sciences: integrating spatial modeling and decision analysis*. Cambridge: Cambridge University Press, 2015.
- Chan TU, Hart BT, Kennard MJ, et al. Bayesian network models for environmental flow decision making in the Daly river, Northern territory, Australia. *River Res Appl* 2012; 28(3): 283–301.
- Martinelli G, Eidsvik J, Sinding-Larsen R, et al. Building Bayesian networks from basin-modelling scenarios for improved geological decision making. *Pet Geosci* 2013; 19(3): 289–304.
- Arzaghi E, Abbassi R, Garaniya V, et al. Developing a dynamic model for pitting and corrosion-fatigue damage of subsea pipelines. *Ocean Eng* 2018; 150: 391–396.
- Li X, Zhu H, Chen G, et al. Optimal maintenance strategy for corroded subsea pipelines. *J Loss Prev Process Ind* 2017; 49: 145–154.
- Melchers RE. Pitting corrosion of mild steel in marine immersion environment – part 1: maximum pit depth. *Corrosion* 2004; 60(9): 824–836.
- Miner MA. Cumulative damage in fatigue. *J Appl Mech* 1945; 12(3): 159–164.
- JCSS Probabilistic Model Code. *Part 3: Resistance models*. Standard, Joint Committee of Structural Safety, 2001.
- Murphy K. The bayes net toolbox for matlab. *Comput Sci Stat* 2001; 33(2): 1024–1034.
- Luque J and Straub D. Reliability analysis and updating of deteriorating systems with dynamic Bayesian networks. *Struct Saf* 2016; 62: 34–46.
- Daniels HE. The statistical theory of the strength of bundles of threads. *I. Proc R Soc Lond A Math Phys Sci* 1945; 183(995): 405–435.
- Morris D, Andres O, Ayers R, et al. ScanFish – North and Celtic Seas, 2016. DOI: 10.14466/CefasDataHub.20.

Paper VI. Risk-based Design of an Offshore Wind Turbine using VoI Analysis

Mendoza, J., and J. Köhler (2019). “Risk-based Design of an Offshore Wind Turbine using VoI Analysis”. In: *13th International Conference on Applications of Statistics and Probability in Civil Engineering, ICASP13*.

This is the post-peer-review version of the paper published in the proceedings of the 13th International Conference on Applications of Statistics and Probability in Civil Engineering, ICASP13; which was presented at the conference in Seoul, 2019. A digital version can be found at: <http://s-space.snu.ac.kr/bitstream/10371/153456/1/300.pdf>.

The main idea of the paper was proposed by J. Mendoza with contributions by J. Köhler. The calculations were conducted by J. Mendoza, with acknowledgement to M. Muskulus to the implementation of the wind spectra. The paper was structured and written by J. Mendoza, with editing by J. Köhler.

Risk-based Design of an Offshore Wind Turbine using VoI Analysis

Jorge Mendoza

PhD student, Department of Structural Engineering, Norwegian University of Science and Technology, Trondheim, Norway

Jochen Köhler

Professor, Department of Structural Engineering, Norwegian University of Science and Technology, Trondheim, Norway

ABSTRACT: Monopiles are the most common solution for supporting wind turbines in offshore conditions. At the design phase of a monopile, a frequency check is to be performed to avoid the resonance hazard with the 1P and 3P excitation, i.e. the frequency domains at which the rotor provokes excitations. However, the estimation of the first natural frequency of the structure is associated with large uncertainties, especially due to lack of knowledge about the soil-structure interaction. Resonance with the dynamic excitations results in a reduced fatigue life. In this paper, the frequency check is addressed following a probabilistic formulation. A rational decision framework is proposed to find an optimum design, based on the evaluation of the expected consequences of failure using risk metrics. Furthermore, the value of acquiring further site-specific information on the soil characteristics is addressed by means of a value of information analysis. A Bayesian network is developed to represent the system and facilitate the analysis. The results provide insight on (1) the relation between design parameters and the risk associated with dynamic amplifications; and (2) how to efficiently distribute the resources at the design point in time.

1. INTRODUCTION

Monopiles are the preferred offshore wind turbine (OWT) support structure (Remy and Mbistrova, 2018). Optimization of the support structure design is essential for the purpose of reducing the levelized cost of wind energy and thus, keeping the growing trend of the technology (McAuliffe et al., 2017).

OWTs are complex structural systems subject to several sources of dynamic loading, which may induce dynamic amplification of the structural response. According to guidelines, such as DNV-GL (2016b), the structural design of an OWT is to verify that resonance with the rotor (1P) and blade-passing (3P) excitations is avoided. This is addressed with a frequency check, in which a deterministic minimum acceptable margin between the estimated natural frequencies of the OWT and the excitation regions is imposed. However, evidence exists of this type of resonance happening in oper-

ational conditions (Hu et al., 2014). Mitigating this issue in operational conditions instead of during the design phase is associated with higher costs and risk. Therefore, the deterministic frequency check is not sufficient. A more thorough study of the limitations of this approach can be found in Mendoza and Köhler (2019). This motivates the development of alternative methodologies, in which the risk associated with a certain design is assessed explicitly.

For a three-bladed pitch-controlled wind turbine, the frequency domain can be divided into five regions, which are synthesized in the form of a Campbell diagram in Figure 1. Note that Ω_0 and Ω_r are the cut-in and rated rotor speeds, respectively. The regions are, from smaller to larger frequencies, (1) the soft-soft region; (2) the 1P region; (3) the soft-stiff region; (4) the 3P region; and (5) the stiff-stiff region. Designs whose first natural frequency f_{n1} lies in the soft-soft region do not provide enough

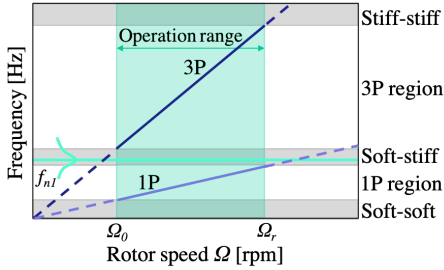


Figure 1: Campbell diagram illustrating the rotor and blade-passing excitation regions.

stiffness, meaning that the flexibility of the compliant structure is detrimental for stable energy production and for the fatigue life of the mechanical components in the rotor-nacelle assembly. Designs in the stiff-stiff region are not cost-efficient. Therefore, the design space is restricted to the soft-stiff region in general. The prediction of the natural frequencies of the OWT at the design phase is associated with large uncertainties. The uncertainty can be understood as composed from an epistemic and a stochastic part. The epistemic part is associated, among others, to the uncertainty in the estimation of soil parameters, the depths of soil stratification, and the soil-structure interaction modeling. The stochastic uncertainty becomes larger the further in time from the estimation point in time and cannot be fully reduced by acquiring further information. Examples are the scour development, or the soil softening or stiffening (Schafhirt et al., 2016).

At the design stage, there are several ways of dealing with the uncertainties mentioned above. On the one hand, the design can be over-engineered in order to compensate the state of imperfect information. This strategy is commonly used in practice. However, as the extension of the soft-stiff region becomes narrower for larger wind turbine rotors, an over-engineered design may yield a first natural frequency close to or in the 3P region. On the other hand, it is possible to partially reduce the uncertainties by acquiring information. In general, a compromise between the two mentioned possibilities should be pursued in order to manage the risk at minimum cost and maximum revenue.

In this paper, a risk-based decision framework is

developed with the following two objectives: (1) to determine a cost-effective design based on available prior information and (2) to quantify the value of additional information procured by testing the site-specific soil condition. In the following section, the methodology used to address the objectives is described. The characteristics of the numerical model employed to implement the methodology is documented in Section 3. The results are presented in Section 4. The main conclusions and the future outlook are reported in Section 5.

2. METHODS

A risk-based decision framework is proposed to assess the expected consequences of the resonance hazard with the 1P and 3P regions. The optimum design is evaluated using utility theory (von Neumann and Morgenstern, 1966). The decision variables are the design parameters. Two design parameters are considered: the monopile diameter and thickness at a reference height. A parametric definition of the structure is developed based on the two design parameters, so that a combination of the two defines a monopile design. This is further explained in the following section. A discrete set of designs $\mathbf{d}_s = \{d_1, d_2, \dots, d_n\}$ is generated, constituting the design decision vector. The optimum design d_{opt} is found according to Eq. (1), i.e. by minimizing the expected total cost $E[C_T|\mathbf{d}_s]$.

$$d_{opt} = \arg \min_{d_{opt} \in \mathbf{d}_s} \{E[C_T|\mathbf{d}_s]\} \quad (1)$$

The expected total cost is computed using Eq. (2). The costs of manufacturing a cylindrical and a conical section are set to 2€/kg and 3€/kg, respectively, according to the cost model in De Vries et al. (2011). The failure costs are set to $C_f = 2C_c$ in this example.

$$E[C_T] = C_c + E[C_f] = C_c + C_f P_f \quad (2)$$

In general, structural resonance with the wave loading and the 1P and 3P excitations do not cause structural failure due to the high aerodynamic damping. Nevertheless, it results in dynamic amplifications and therefore, an increase of the fatigue failure risk. Due to this, the failure risk $E[C_f]$

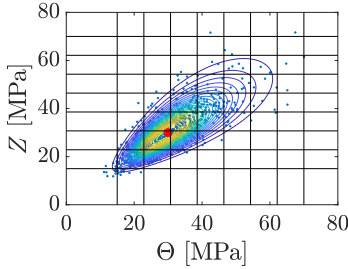


Figure 2: Likelihood function $L(\theta)$ between the outcome of the soil test Z and the true state of the soil modulus of elasticity Θ .

is studied through a fatigue limit state by using Eq. (3) (JCSS, 2001). Note that g_{fat} is the limit state function, P_f is the probability of failure and Δ is the uncertain Miner's sum at failure, defined by a Log-Normal with parameters $\mu_\Delta = 1$ and $\sigma_\Delta = 0.3$. The soil is represented, given prior knowledge, by a single sand stratum with modulus of elasticity E_{soil} following a Log-Normal with expected value equal to 30 MPa and coefficient of variation of 0.3. A multiplicative model uncertainty X , associated to the uncertainty in the soil-structure interaction model used to estimate the first natural frequency f_{n1} , is applied. X is represented by a Log-Normal with parameters $\mu_X = 1$ and $\mu_X = 0.05$. The other basic variables are represented deterministically.

$$P_f = \Pr[g_{fat} \leq 0] = \Pr[\Delta - FLD(f_{n1}) \leq 0] \quad (3)$$

A value of information (VoI) analysis (Raiffa and Schlaifer, 1961) is performed in order to quantify the economic value of testing the soil site-specific characteristics. Two testing options are considered $\mathbf{e} = \{e_0, e_1\}$: (e_0) To not invest in acquiring new information, and (e_1) To test the soil site-specific conditions in order to reduce the epistemic uncertainties associated to E_{soil} . The net VoI V^* is computed using Eq. (4), where $E[C_T|e_1, \mathbf{d}_s]$ is the preposterior expected total cost.

$$V^* = E[C_T|e_0, d_{opt}] - E[C_T|e_1, \mathbf{d}_s] \quad (4)$$

In order to compute $E[C_T|e_1, \mathbf{d}_s]$, a likelihood $L(\theta)$ of the test outcomes Z is formulated, see

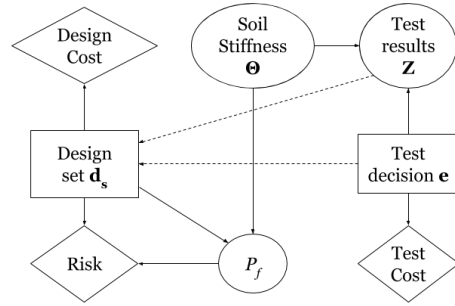


Figure 3: Influence Diagram used for the VoI analysis.

Eq. (5). Note that θ refers to the true state of the soil modulus of elasticity. In this example, due to the absence of empirical data, $L(\theta)$ is defined by a multivariate Log-Normal with mean value vector $\mu_{\theta,Z} = [30, 30]^T$ [MPa], a correlation $\rho_{\theta,Z} = 0.8$ and standard deviations $\sigma_\theta = \sigma_Z = 9$ MPa.

$$L(\theta) = \Pr[Z|\Theta = \theta] \quad (5)$$

The influence diagram (ID) illustrated in Figure 3 is implemented in GeNIe[®] to evaluate V^* . All the nodes are discretized. $L(\theta)$ is discretized to 9 test outcome intervals.

3. DESCRIPTION OF THE NUMERICAL MODEL

A simplified numerical model is developed to estimate the fatigue damage given a realization of the first natural frequency of the structure. This is later used to estimate the probability of failure and ultimately, the risk. The risk is employed as a decision ranking metric, taking basis on utility theory. Therefore, it is not pursued to develop a complex, computationally expensive model that captures the detailed behaviour of the structure. On the contrary, a sufficiently complete model that enables the assessment of the structural behavior that affects the considered design decisions is preferred. The dynamic behaviour of the OWT is to be modelled in the time domain in order to evaluate the cumulative fatigue damage. In the following, the parametric definition of the design and the employed numerical model are documented.

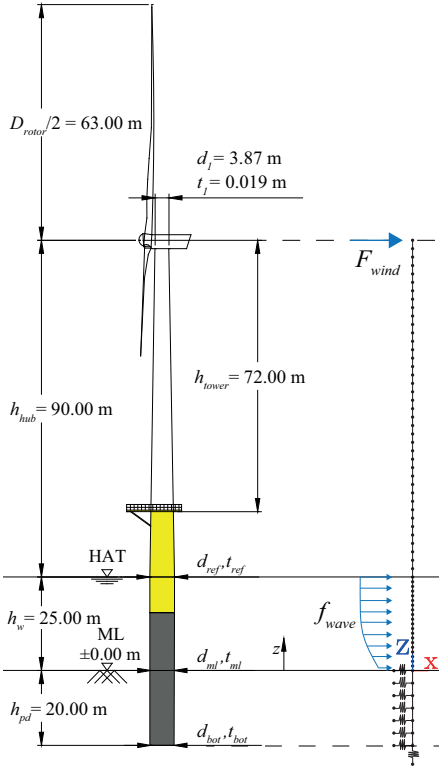


Figure 4: Illustration of the parametric description of the design and the numerical model.

3.1. Design set

A set \mathbf{d}_s of 12 designs is built based on a parametric definition of an OWT. A design is given by the specification of two design parameters, the diameter d_{ref} and the thickness t_{ref} at a reference location. The Matlab[®] FE toolbox StaBIL2.0 is used to develop a numerical model of the OWT structure. The 5-MW NREL reference wind turbine is employed (Jonkman et al., 2009). For this turbine, the cut-in and rated rotor speeds are $\Omega_0 = 0.1150$ Hz and $\Omega_r = 0.2017$ Hz, respectively. A sketch of the OWT parametric definition and the numerical model is presented in Figure 4. The following should be noticed. A linear transition of both the diameter and thickness is set between the two mentioned cross-sections. The connection between the tower and the

Table 1: Definition of the reference diameter d_{ref} and thickness t_{ref} for the design set \mathbf{d}_s used in this study.

Design #	d_{ref}	t_{ref}
d_{s1}	5.50 m	0.055 m
d_{s2}	5.80 m	0.058 m
d_{s3}	6.25 m	0.063 m
d_{s4}	6.60 m	0.067 m
d_{s5}	7.00 m	0.070 m
d_{s6}	7.20 m	0.072 m
d_{s7}	5.50 m	0.058 m
d_{s8}	5.80 m	0.061 m
d_{s9}	6.25 m	0.066 m
d_{s10}	6.60 m	0.069 m
d_{s11}	7.00 m	0.073 m
d_{s12}	7.20 m	0.075 m

monopile is assumed to be perfect. Secondary steel components, such as boat landing, are not explicitly included in the analysis. The added mass of the secondary steel is taken into account by setting the steel density to 8500 kg/m^3 . The cross-section of the monopile is kept constant from h_w up to the penetration depth, i.e. h_{pd} . The design set is defined in Table 1.

The soil-structure interaction is modelled by a set of linear springs with stiffness equal to the modulus of subgrade reaction k_s . The formulation of this simple model was firstly proposed in Winkler (1867). There is no agreement in the literature regarding the relation between k_s and the soil modulus of elasticity E_{soil} . This issue is investigated by comparing the 1-D model with more sophisticated 3-D FE models in Rani and Prashant (2014). It is concluded that the relation $k_s = 2E_{soil}$, proposed in Muschelišvili (1953), gives reasonable results. Due to that and its simplicity, this relation is used in this study. The relation between realizations of E_{soil} and the first natural frequency of the structure f_{n1} is mapped using the numerical model, see Figure 5.

3.2. Environmental loading

The dynamic analysis performed in this study is carried out in the time domain. The environmental loading is computed for eleven fatigue load cases (FLCs) from 1-hour time series of the sea state.

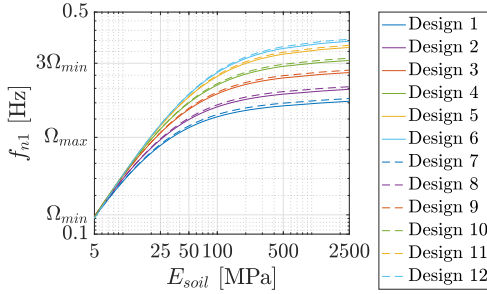


Figure 5: Relation between the soil modulus of elasticity E_{soil} and the first natural frequency f_{n1} for the considered designs.

The FLCs are taken from the K13 shallow water site (Fischer et al., 2010), where the stochastic wind was fitted to a Weibull distribution with parameters $A = 11.31$ m/s and $k = 1.97$. The lumped sea states are defined by four parameters: the 10-min average wind speed at hub height V_{10} , the turbulence intensity I , the significant wave height H_s and the peak period T_p . The wind bins are set to 2 m/s. The probability of occurrence of the wind bins $f_V(v)$ is scaled to fit the cut-in and cut-out wind speeds of the 5-MW NREL wind turbine. Since the purpose of the dynamic analysis is to estimate the fatigue damage, the load effects induced by non-cyclic sources, such as currents, are neglected.

The wind time series are generated by inverse Fourier transform of the wind spectrum, which is chosen to be the Karman spectrum (von Karman, 1948). The Karman spectrum is modified to account for rotational sampling. This is done in order to model the 1P and 3P excitations in a simplified manner, so that computationally expensive aero-elastic simulations are avoided. The modified Karman spectrum $S_w(f)$ is the Fourier transform of the autocorrelation function $R_{11}(\tau)$ derived in Connell (1982), cf. Eqs. (6) and (7). Note that D_{Rotor} is the rotor diameter, L_u is the turbulence length, which is set to 340.2 m, Γ is the gamma function and K_v is the modified Bessel function of the second kind of order v .

$$S_w(f) = 4 \int_0^{\infty} R_{11}(\tau) \cos(2\pi f \tau) d\tau \quad (6)$$

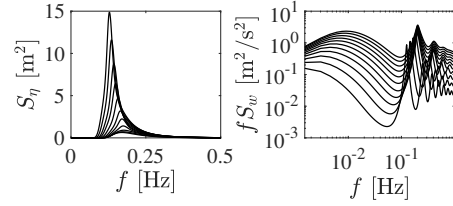


Figure 6: Spectra used to generate the environmental loading: JONSWAP spectra S_η and Karman spectra S_w accounting for rotational sampling.

$$R_{11}(\tau) = \frac{2(V_{10}I)^2}{\Gamma(1/3)} (\kappa/2)^{1/3} \cdot \left[K_{1/3}(\kappa) - \kappa/2 \cdot K_{2/3}(\kappa) \left(\frac{4D_{Rotor} \sin(\Omega\tau/2)}{5s} \right)^2 \right] \quad (7)$$

With κ and s defined as:

$$\kappa = \frac{s}{1.34L_u} \quad (8)$$

$$s = \sqrt{V_{10}^2 \tau^2 + \frac{16}{25} D_{Rotor}^2 \sin^2(\Omega\tau/2)}$$

The JONSWAP spectrum is used to generate the wave time series. The different wind and wave spectrums used to generate the 11 lumped sea states are illustrated in Figure 6.

3.3. Dynamic response

The dynamic model takes basis on the simplified numerical model in Schløer et al. (2018). Only the in-plane deflections are considered. The dynamic response of the system is assumed to be represented accurately enough by the first mode of vibration. Hence, the dynamic horizontal displacement u is approximated by $u \approx \alpha_1 \phi_1$, with ϕ_1 and α_1 being the first mode shape and the generalized coordinate of the first mode of vibration, respectively. The equation of motion of the system can then be described by Eq. (9). The generalized mass GM_1 , stiffness GK_1 , damping GD_1 and force GF_1 are defined in Eqs. (10) to (13); where ζ is the damping ratio and \mathbf{M} and \mathbf{K} are the mass and stiffness matrices, respectively.

$$GM_1 \ddot{\alpha}_1 + GD_1 \dot{\alpha}_1 + GK_1 \alpha_1 = GF_1 \quad (9)$$

$$GM_1 = \phi_1^T \mathbf{M} \phi_1 \quad (10)$$

$$GK_1 = \phi_1^T \mathbf{K} \phi_1 \quad (11)$$

$$GD_1 = \frac{\zeta GK_1}{\pi f_{n1}} + 2\zeta \sqrt{GM_1 \cdot GK_1} \quad (12)$$

$$GF_1 = \phi_1(z_{hub}) F_{wind} + \int_{z_{ml}}^{z_{hub}} f_{wave} \phi_1 dz \quad (13)$$

The stress at mudline S is used as a proxy of the maximum stress of the monopile, which in general occurs at a cross-section embedded in the soil. S is computed from the bending moment at mudline $M_y(z_{ml})$ defined in Eq. (14), assuming linear-elastic behaviour of the steel. The shear induced stress is neglected.

$$M_y(z_{ml}) = F_{wind} \cdot (h_{hub} + h_w) + \int_{z_{ml}}^{z_0} f_{wave}(z) z dz - \int_{z_{ml}}^{z_{hub}} \rho \ddot{\alpha}_1 \phi_1 z dz \quad (14)$$

3.4. Fatigue resistance

The fatigue resistance is computed following the SN-curve methodology as described in DNV-GL (2016a). The relation between a certain stress range and the number of cycles to failure is given by Eq. (15). The parameters $\log \bar{a}_i$, m_i and k are set as for the D-curve. The sub-index i refers to the first ($i = 1$) or second part ($i = 2$) of the two sloped piece-wise SN-curve definition. Eq. (15) can be reorganized as in Eq. (16) to account for stress amplitudes $\sigma/2$. This is required since the rainflow counting algorithm is used to identify and group stress amplitudes into cycles and semi-cycles.

$$\log N = \log \bar{a}_i - m_i \log \left(S \left(\frac{t}{t_{ref}} \right)^k \right) \quad (15)$$

$$N \left(\frac{\sigma}{2} \right)^{m_i} = 10^{\log \bar{a}_i} \cdot 2^{-m_i} \cdot \left(\frac{t}{t_{ref}} \right)^{-k \cdot m_i} \quad (16)$$

The fatigue damage caused by each loading cycle or semi-cycle is defined as the ratio in Eq. (17). The Palmgren-Miner superposition is adopted (Miner,

1945). The life-time fatigue damage FLD is computed using Eq. (18), in which the fatigue damage estimated from the 1-hour simulations T_{sim} is weighed with the probability of occurrence of each of the eleven FLCs $f_V(v_{j2})$ and scaled to the 20-year service life T_{life} .

$$D_{j1} = \frac{n_{j1} S_{j1}^{m_i}}{N \left(\frac{\sigma}{2} \right)^{m_i}} = \frac{1}{10^{\log \bar{a}_i}} \cdot 2^{m_i} \cdot \left(\frac{t}{t_{ref}} \right)^{k \cdot m_i} \quad (17)$$

$$FLD = \frac{T_{life}}{T_{sim}} \sum_{j2=1}^{11} \left(\sum_{j1 \in I_h} D_{j1, j2} \right) f_V(v_{j2}) \quad (18)$$

4. RESULTS AND DISCUSSION

The probability density functions of the first natural frequency $f_{F_{n1}}(f_{n1})$ are plotted in Figure 7. Note that the relation between f_{n1} and E_{soil} presented in Figure 5 and the model uncertainty X are used for their computation.

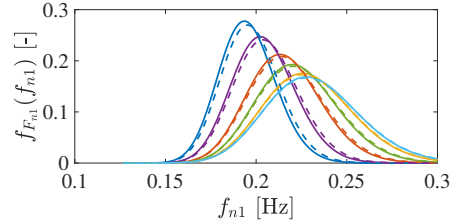


Figure 7: Probability density function of the first natural frequency $f_{F_{n1}}(f_{n1})$ based on prior soil parameters. The colour scheme corresponds to Figure 5.

The results of the estimation of the fatigue life damage FLD are presented in Figure 8. An increase of the FLD can be observed within the 1P region, having its maximum value when $f_{n1} \approx \Omega_r$. This reflects the importance of the effect of the resonance on the fatigue life. Considering e.g. d_{s1} , a realization of $f_{n1} \approx 0.2$ Hz results in double the FLD as a realization of $f_{n1} \approx 0.26$ Hz; or in other words the design is expected to fail at half the time, since FLD is inversely proportional to the fatigue life. Furthermore, it is observed that the resonance effect influences a large frequency range within the soft-stiff region.

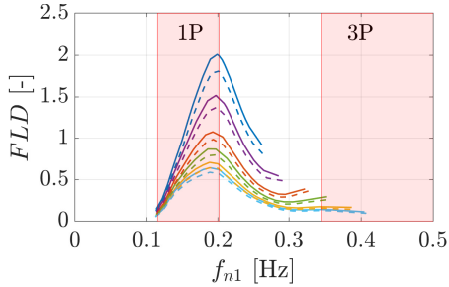


Figure 8: Fatigue life damage (FLD) for each realization of f_{n1} of the tested design set. The colour scheme corresponds to Figure 5.

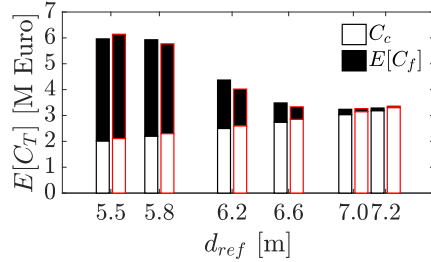


Figure 10: Expected prior total cost $E[C_T]$. Black-edged bars correspond to designs with reference thickness $t_{ref} = d_{ref}/100$, i.e. d_{s1} to d_{s6} ; and red-edged bars to $t_{ref} = d_{ref}/100 + 0.003$ m, i.e. d_{s7} to d_{s12} .

The expected fatigue life damage $E[FLD]$ and the probability of failure P_f given prior knowledge are plotted in Figure 9 as a function of d_{ref} . The expected total cost $E[C_T]$ is plotted in Figure 10. It can be seen that $P_f \approx 1$ for the designs d_{s1} and d_{s7} . This was expected since the expected value of f_{n1} for these designs is ca. 0.197 Hz, i.e. it lies in the 1P region. Furthermore, it can be observed that the additional investment needed to realize the design d_{s2} in comparison to d_{s1} does not compensate the risk reduction, since the expected cost remains almost constant. The optimum design given prior knowledge is found to be the design d_{s5} , which is defined by $d_{ref} = 7.00$ m and $t_{ref} = 0.07$ m. The minimum prior expected cost is then computed to be $E[C_T|e_0, d_{s5}] = 3.239$ M€.

The preposterior expected total cost $E[C_T|e_1, \mathbf{d}_s]$ is computed using the likelihood function of the soil testing technology, see Figure 2. The minimum value of $E[C_T|e_1, \mathbf{d}_s]$ results in 3.198M€. The net VoI follows then from Eq. (4), resulting in $V^* = 41000$ €. This value is significantly smaller

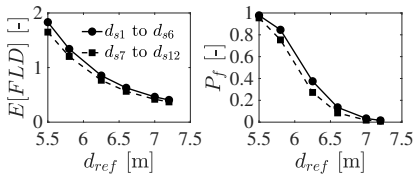


Figure 9: Expected fatigue life damage $E[FLD]$ and Probability of failure P_f given prior soil parameters.

than what it would be required for testing the soil in offshore conditions. Nevertheless, the system effects associated to considering the complete wind farm and the added value provided by informing decisions that regard other failure modes are not included in this study. This is further discussed in the following section.

5. CONCLUSIONS

A risk-based framework to inform decisions for the design phase of OWTs was presented in this paper. In particular, the study focuses on quantifying the risk due to the resonance hazard with the rotor and blade-passing excitations. The risk was quantified by defining a fatigue limit state. A simplified case study was regarded to showcase the methodology.

First, the optimum design was assessed utilizing available prior information. Insight regarding the optimum dimensions of the monopile support structure was provided. These results were then used to estimate the value of information of testing the site-specific soil conditions. The obtained net value of information is significantly smaller than the cost of a typical offshore soil testing campaign. Nevertheless, this study considered a single OWT rather than an offshore wind farm. Taking into account the wind farm system effects may have a significant impact in the results. Information could be used to update the spacial variability of the soil properties and the estimated prior correlation between the soil characteristics at different locations within the wind farm. Additionally, the comparison of the

computed value of information and the costs of performing a soil campaign could be compared in a fair manner. It should be noted that the benefit of inspecting the soil conditions are broader than just updating the knowledge regarding the soil parameters. For instance, the value of hazard identification on the seabed should be included in the analysis.

Further research regarding the application of the value of information analysis to design decisions should follow this study. Future investigations may include the collection of empirical soil data to build the likelihood function and the modelling of the system effects to compute the value of information. The studies should address the sensitivity of the analysis regarding the cost model and the modelling of the uncertainty.

6. REFERENCES

- Connell, J. R. (1982). "Spectrum of wind speed fluctuations encountered by a rotating blade of a wind energy conversion system: observations and theory." *Solar Energy*, 29(5), 363–375.
- De Vries, W. E., Vemula, N. K., Passon, P., Fischer, T., Kaufer, D., Matha, D., et al. (2011). "Final report WP 4.2: support structure concepts for deep water sites: deliverable D4. 2.8." *Report no.*, WP4: offshore foundations and support structures.
- DNV-GL (2016a). "Fatigue design of offshore steel structures." *Standard DNVGL-RP-C203*, DNV-GL.
- DNV-GL (2016b). "Support structures for wind turbines." *Standard DNVGL-ST-0126*, DNV-GL.
- Fischer, T., De Vries, W. E., and Schmidt, B. (2010). "UpWind design basis (WP4: Offshore foundations and support structures)." *resreport*, UpWind project.
- Hu, W.-H., Thöns, S., Said, S., and Rücker, W. (2014). "Resonance phenomenon in a wind turbine system under operational conditions." *structural health monitoring*, 12, 14.
- JCSS (2001). "Probabilistic model code. part 3: Resistance models." *Standard*, Joint Committee of Structural Safety.
- Jonkman, J., Butterfield, S., Musial, W., and Scott, G. (2009). "Definition of a 5-MW reference wind turbine for offshore system development." *National Renewable Energy Laboratory, Golden, CO, Technical Report No. NREL/TP-500-38060*.
- McAuliffe, F. D., Murphy, J., Lynch, K., Desmond, C., Norbeck, J. A., Nonås, L. M., Attari, Y., Doherty, P., Sorensen, J. D., et al. (2017). "Driving cost reductions in offshore wind." *Report no.*, Leanwind.
- Mendoza, J. and Köhler, J. (2019). "Value of site-specific information for the design of offshore wind-farms." *IABSE Symposium 2019 Guimarães*.
- Miner, M. A. (1945). "Cumulative damage in fatigue." *Journal of Applied Mechanics*, 12(3), 159–164.
- Muschelišvili, N. I. (1953). *Some basic problems of the mathematical theory of elasticity: fundamental equations, plane theory of elasticity, torsion and bending*. Springer.
- Raiffa, H. and Schlaifer, R. (1961). *Applied statistical decision theory*. Cambridge University Press.
- Rani, S. and Prashant, A. (2014). "Estimation of the linear spring constant for a laterally loaded monopile embedded in nonlinear soil." *International Journal of Geomechanics*, 15(6), 04014090.
- Remy, T. and Mbistrova, A. (2018). "Offshore wind in Europe. Key trends and statistics 2017." *techreport*, Wind Europe.
- Schafhirt, S., Page, A., Eiksund, G. R., and Muskulus, M. (2016). "Influence of soil parameters on the fatigue lifetime of offshore wind turbines with monopile support structure." *Energy Procedia*, 94, 347–356.
- Schløer, S., Castillo, L. G., Fejerskov, M., Stroescu, E., and Bredmose, H. (2018). "A model for quick load analysis for monopile-type offshore wind turbine sub-structures." *Wind Energy Science*, 3, 57–73.
- von Karman, T. (1948). "Progress in the statistical theory of turbulence." *Proceedings of the National Academy of Sciences of the United States of America*, 34(11), 530.
- von Neumann, J. and Morgenstern, O. (1966). *Theory of games and economic behavior*. Princeton university press, third edition.
- Winkler, E. (1867). *Die Lehre von der Elasticitaet und Festigkeit*, Vol. 1. Dominicus.

**DEPARTMENT OF STRUCTURAL ENGINEERING
NORWEGIAN UNIVERSITY OF SCIENCE AND TECHNOLOGY**

N-7491 TRONDHEIM, NORWAY
Telephone: +47 73 59 47 00

"Reliability Analysis of Structural Systems using Nonlinear Finite Element Methods",
C. A. Holm, 1990:23, ISBN 82-7119-178-0.

"Uniform Stratified Flow Interaction with a Submerged Horizontal Cylinder",
Ø. Arntsen, 1990:32, ISBN 82-7119-188-8.

"Large Displacement Analysis of Flexible and Rigid Systems Considering
Displacement-Dependent Loads and Nonlinear Constraints",
K. M. Mathisen, 1990:33, ISBN 82-7119-189-6.

"Solid Mechanics and Material Models including Large Deformations",
E. Levold, 1990:56, ISBN 82-7119-214-0, ISSN 0802-3271.

"Inelastic Deformation Capacity of Flexurally-Loaded Aluminium Alloy Structures",
T. Welo, 1990:62, ISBN 82-7119-220-5, ISSN 0802-3271.

"Visualization of Results from Mechanical Engineering Analysis",
K. Aamnes, 1990:63, ISBN 82-7119-221-3, ISSN 0802-3271.

"Object-Oriented Product Modeling for Structural Design",
S. I. Dale, 1991:6, ISBN 82-7119-258-2, ISSN 0802-3271.

"Parallel Techniques for Solving Finite Element Problems on Transputer Networks",
T. H. Hansen, 1991:19, ISBN 82-7119-273-6, ISSN 0802-3271.

"Statistical Description and Estimation of Ocean Drift Ice Environments",
R. Korsnes, 1991:24, ISBN 82-7119-278-7, ISSN 0802-3271.

"Properties of concrete related to fatigue damage: with emphasis on high strength
concrete",
G. Petkovic, 1991:35, ISBN 82-7119-290-6, ISSN 0802-3271.

"Turbidity Current Modelling",
B. Brørs, 1991:38, ISBN 82-7119-293-0, ISSN 0802-3271.

"Zero-Slump Concrete: Rheology, Degree of Compaction and Strength. Effects of
Fillers as Part Cement-Replacement",
C. Sørensen, 1992:8, ISBN 82-7119-357-0, ISSN 0802-3271.

"Nonlinear Analysis of Reinforced Concrete Structures Exposed to Transient Loading",
K. V. Høiseth, 1992:15, ISBN 82-7119-364-3, ISSN 0802-3271.

"Finite Element Formulations and Solution Algorithms for Buckling and Collapse
Analysis of Thin Shells",
R. O. Bjærum, 1992:30, ISBN 82-7119-380-5, ISSN 0802-3271.

"Response Statistics of Nonlinear Dynamic Systems",
J. M. Johnsen, 1992:42, ISBN 82-7119-393-7, ISSN 0802-3271.

"Digital Models in Engineering. A Study on why and how engineers build and operate
digital models for decision support",
J. Høyte, 1992:75, ISBN 82-7119-429-1, ISSN 0802-3271.

"Sparse Solution of Finite Element Equations",
A. C. Damhaug, 1992:76, ISBN 82-7119-430-5, ISSN 0802-3271.

"Some Aspects of Floating Ice Related to Sea Surface Operations in the Barents Sea",
S. Løset, 1992:95, ISBN 82-7119-452-6, ISSN 0802-3271.

"Modelling of Cyclic Plasticity with Application to Steel and Aluminium Structures",
O. S. Hopperstad, 1993:7, ISBN 82-7119-461-5, ISSN 0802-3271.

"The Free Formulation: Linear Theory and Extensions with Applications to Tetrahedral
Elements
with Rotational Freedoms",
G. Skeie, 1993:17, ISBN 82-7119-472-0, ISSN 0802-3271.

"Høyfast betongs motstand mot piggdekkslitasje. Analyse av resultater fra prøving i
Veisliter'n",
T. Tveter, 1993:62, ISBN 82-7119-522-0, ISSN 0802-3271.

"A Nonlinear Finite Element Based on Free Formulation Theory for Analysis of
Sandwich Structures",
O. Aamlid, 1993:72, ISBN 82-7119-534-4, ISSN 0802-3271.

"The Effect of Curing Temperature and Silica Fume on Chloride Migration and Pore
Structure of High Strength Concrete",
C. J. Hauck, 1993:90, ISBN 82-7119-553-0, ISSN 0802-3271.

"Failure of Concrete under Compressive Strain Gradients",
G. Markeset, 1993:110, ISBN 82-7119-575-1, ISSN 0802-3271.

"An experimental study of internal tidal amphidromes in Vestfjorden",
J. H. Nilsen, 1994:39, ISBN 82-7119-640-5, ISSN 0802-3271.

"Structural analysis of oil wells with emphasis on conductor design",
H. Larsen, 1994:46, ISBN 82-7119-648-0, ISSN 0802-3271.

"Adaptive methods for non-linear finite element analysis of shell structures",
K. M. Okstad, 1994:66, ISBN 82-7119-670-7, ISSN 0802-3271.

"On constitutive modelling in nonlinear analysis of concrete structures",
O. Fyrileiv, 1994:115, ISBN 82-7119-725-8, ISSN 0802-3271.

"Fluctuating wind load and response of a line-like engineering structure with emphasis on motion-induced wind forces",
J. Bogunovic Jakobsen, 1995:62, ISBN 82-7119-809-2, ISSN 0802-3271.

"An experimental study of beam-columns subjected to combined torsion, bending and axial actions",
A. Aalberg, 1995:66, ISBN 82-7119-813-0, ISSN 0802-3271.

"Scaling and cracking in unsealed freeze/thaw testing of Portland cement and silica fume concretes",
S. Jacobsen, 1995:101, ISBN 82-7119-851-3, ISSN 0802-3271.

"Damping of water waves by submerged vegetation. A case study of laminaria hyperborea",
A. M. Dubi, 1995:108, ISBN 82-7119-859-9, ISSN 0802-3271.

"The dynamics of a slope current in the Barents Sea",
Sheng Li, 1995:109, ISBN 82-7119-860-2, ISSN 0802-3271.

"Modellering av delmaterialenes betydning for betongens konsistens",
Ernst Mørtsell, 1996:12, ISBN 82-7119-894-7, ISSN 0802-3271.

"Bending of thin-walled aluminium extrusions",
Birgit Søvik Opheim, 1996:60, ISBN 82-7119-947-1, ISSN 0802-3271.

"Material modelling of aluminium for crashworthiness analysis",
Torodd Berstad, 1996:89, ISBN 82-7119-980-3, ISSN 0802-3271.

"Estimation of structural parameters from response measurements on submerged floating tunnels",
Rolf Magne Larssen, 1996:119, ISBN 82-471-0014-2, ISSN 0802-3271.

"Numerical modelling of plain and reinforced concrete by damage mechanics",
Mario A. Polanco-Loria, 1997:20, ISBN 82-471-0049-5, ISSN 0802-3271.

"Nonlinear random vibrations - numerical analysis by path integration methods",
Vibeke Moe, 1997:26, ISBN 82-471-0056-8, ISSN 0802-3271.

“Numerical prediction of vortex-induced vibration by the finite element method”,
Joar Martin Dalheim, 1997:63, ISBN 82-471-0096-7, ISSN 0802-3271.

“Time domain calculations of buffeting response for wind sensitive structures”,
Ketil Aas-Jakobsen, 1997:148, ISBN 82-471-0189-0, ISSN 0802-3271.

"A numerical study of flow about fixed and flexibly mounted circular cylinders",
Trond Stokka Meling, 1998:48, ISBN 82-471-0244-7, ISSN 0802-3271.

“Estimation of chloride penetration into concrete bridges in coastal areas”,
Per Egil Steen, 1998:89, ISBN 82-471-0290-0, ISSN 0802-3271.

“Stress-resultant material models for reinforced concrete plates and shells”,
Jan Arve Øverli, 1998:95, ISBN 82-471-0297-8, ISSN 0802-3271.

“Chloride binding in concrete. Effect of surrounding environment and concrete composition”,
Claus Kenneth Larsen, 1998:101, ISBN 82-471-0337-0, ISSN 0802-3271.

“Rotational capacity of aluminium alloy beams”,
Lars A. Moen, 1999:1, ISBN 82-471-0365-6, ISSN 0802-3271.

“Stretch Bending of Aluminium Extrusions”,
Arild H. Clausen, 1999:29, ISBN 82-471-0396-6, ISSN 0802-3271.

“Aluminium and Steel Beams under Concentrated Loading”,
Tore Tryland, 1999:30, ISBN 82-471-0397-4, ISSN 0802-3271.

"Engineering Models of Elastoplasticity and Fracture for Aluminium Alloys",
Odd-Geir Lademo, 1999:39, ISBN 82-471-0406-7, ISSN 0802-3271.

"Kapasitet og duktilitet av dybelforbindelser i trekonstruksjoner",
Jan Siem, 1999:46, ISBN 82-471-0414-8, ISSN 0802-3271.

“Etablering av distribuert ingeniørarbeid; Teknologiske og organisatoriske erfaringer fra en norsk ingeniørbedrift”,
Lars Line, 1999:52, ISBN 82-471-0420-2, ISSN 0802-3271.

“Estimation of Earthquake-Induced Response”,
Simon Ólafsson, 1999:73, ISBN 82-471-0443-1, ISSN 0802-3271.

“Coastal Concrete Bridges: Moisture State, Chloride Permeability and Aging Effects”
Ragnhild Holen Relling, 1999:74, ISBN 82-471-0445-8, ISSN 0802-3271.

”Capacity Assessment of Titanium Pipes Subjected to Bending and External Pressure”,
Arve Bjørset, 1999:100, ISBN 82-471-0473-3, ISSN 0802-3271.

“Validation of Numerical Collapse Behaviour of Thin-Walled Corrugated Panels”,
Håvar Ilstad, 1999:101, ISBN 82-471-0474-1, ISSN 0802-3271.

“Strength and Ductility of Welded Structures in Aluminium Alloys”,
Mirosław Matusiak, 1999:113, ISBN 82-471-0487-3, ISSN 0802-3271.

“Thermal Dilation and Autogenous Deformation as Driving Forces to Self-Induced Stresses in High Performance Concrete”,
Øyvind Bjøntegaard, 1999:121, ISBN 82-7984-002-8, ISSN 0802-3271.

“Some Aspects of Ski Base Sliding Friction and Ski Base Structure”,
Dag Anders Moldestad, 1999:137, ISBN 82-7984-019-2, ISSN 0802-3271.

"Electrode reactions and corrosion resistance for steel in mortar and concrete",
Roy Antonsen, 2000:10, ISBN 82-7984-030-3, ISSN 0802-3271.

"Hydro-Physical Conditions in Kelp Forests and the Effect on Wave Damping and Dune Erosion. A case study on Laminaria Hyperborea",
Stig Magnar Løvås, 2000:28, ISBN 82-7984-050-8, ISSN 0802-3271.

"Random Vibration and the Path Integral Method",
Christian Skaug, 2000:39, ISBN 82-7984-061-3, ISSN 0802-3271.

"Buckling and geometrical nonlinear beam-type analyses of timber structures",
Trond Even Eggen, 2000:56, ISBN 82-7984-081-8, ISSN 0802-3271.

”Structural Crashworthiness of Aluminium Foam-Based Components”,
Arve Grønsund Hanssen, 2000:76, ISBN 82-7984-102-4, ISSN 0809-103X.

“Measurements and simulations of the consolidation in first-year sea ice ridges, and some aspects of mechanical behaviour”,
Knut V. Høyland, 2000:94, ISBN 82-7984-121-0, ISSN 0809-103X.

”Kinematics in Regular and Irregular Waves based on a Lagrangian Formulation”,
Svein Helge Gjøvsund, 2000-86, ISBN 82-7984-112-1, ISSN 0809-103X.

”Self-Induced Cracking Problems in Hardening Concrete Structures”,
Daniela Bosnjak, 2000-121, ISBN 82-7984-151-2, ISSN 0809-103X.

"Ballistic Penetration and Perforation of Steel Plates",
Tore Børvik, 2000:124, ISBN 82-7984-154-7, ISSN 0809-103X.

"Freeze-Thaw resistance of Concrete. Effect of: Curing Conditions, Moisture Exchange and Materials",
Terje Finnerup Rønning, 2001:14, ISBN 82-7984-165-2, ISSN 0809-103X

"Structural behaviour of post tensioned concrete structures. Flat slab. Slabs on ground",
Steinar Trygstad, 2001:52, ISBN 82-471-5314-9, ISSN 0809-103X.

"Slipforming of Vertical Concrete Structures. Friction between concrete and slipform panel",
Kjell Tore Fosså, 2001:61, ISBN 82-471-5325-4, ISSN 0809-103X.

"Some numerical methods for the simulation of laminar and turbulent incompressible flows",
Jens Holmen, 2002:6, ISBN 82-471-5396-3, ISSN 0809-103X.

"Improved Fatigue Performance of Threaded Drillstring Connections by Cold Rolling",
Steinar Kristoffersen, 2002:11, ISBN: 82-421-5402-1, ISSN 0809-103X.

"Deformations in Concrete Cantilever Bridges: Observations and Theoretical Modelling",
Peter F. Takács, 2002:23, ISBN 82-471-5415-3, ISSN 0809-103X.

"Stiffened aluminium plates subjected to impact loading",
Hilde Giæver Hildrum, 2002:69, ISBN 82-471-5467-6, ISSN 0809-103X.

"Full- and model scale study of wind effects on a medium-rise building in a built up area",
Jónas Thór Snæbjörnsson, 2002:95, ISBN82-471-5495-1, ISSN 0809-103X.

"Evaluation of Concepts for Loading of Hydrocarbons in Ice-infested water",
Arnor Jensen, 2002:114, ISBN 82-417-5506-0, ISSN 0809-103X.

"Numerical and Physical Modelling of Oil Spreading in Broken Ice",
Janne K. Økland Gjølsteen, 2002:130, ISBN 82-471-5523-0, ISSN 0809-103X.

"Diagnosis and protection of corroding steel in concrete",
Franz Pruckner, 20002:140, ISBN 82-471-5555-4, ISSN 0809-103X.

"Tensile and Compressive Creep of Young Concrete: Testing and Modelling",
Dawood Atrushi, 2003:17, ISBN 82-471-5565-6, ISSN 0809-103X.

"Rheology of Particle Suspensions. Fresh Concrete, Mortar and Cement Paste with Various Types of Lignosulfonates",
Jon Elvar Wallevik, 2003:18, ISBN 82-471-5566-4, ISSN 0809-103X.

"Oblique Loading of Aluminium Crash Components",
Aase Reyes, 2003:15, ISBN 82-471-5562-1, ISSN 0809-103X.

"Utilization of Ethiopian Natural Pozzolans",
Surafel Ketema Desta, 2003:26, ISSN 82-471-5574-5, ISSN:0809-103X.

“Behaviour and strength prediction of reinforced concrete structures with discontinuity regions”, Helge Brå, 2004:11, ISBN 82-471-6222-9, ISSN 1503-8181.

“High-strength steel plates subjected to projectile impact. An experimental and numerical study”, Sumita Dey, 2004:38, ISBN 82-471-6282-2 (printed version), ISBN 82-471-6281-4 (electronic version), ISSN 1503-8181.

“Alkali-reactive and inert fillers in concrete. Rheology of fresh mixtures and expansive reactions.”

Bård M. Pedersen, 2004:92, ISBN 82-471-6401-9 (printed version), ISBN 82-471-6400-0 (electronic version), ISSN 1503-8181.

“On the Shear Capacity of Steel Girders with Large Web Openings”.

Nils Christian Hagen, 2005:9 ISBN 82-471-6878-2 (printed version), ISBN 82-471-6877-4 (electronic version), ISSN 1503-8181.

”Behaviour of aluminium extrusions subjected to axial loading”.

Østen Jensen, 2005:7, ISBN 82-471-6873-1 (printed version), ISBN 82-471-6872-3 (electronic version), ISSN 1503-8181.

”Thermal Aspects of corrosion of Steel in Concrete”.

Jan-Magnus Østvik, 2005:5, ISBN 82-471-6869-3 (printed version), ISBN 82-471-6868 (electronic version), ISSN 1503-8181.

”Mechanical and adaptive behaviour of bone in relation to hip replacement.” A study of bone remodelling and bone grafting.

Sébastien Muller, 2005:34, ISBN 82-471-6933-9 (printed version), ISBN 82-471-6932-0 (electronic version), ISSN 1503-8181.

“Analysis of geometrical nonlinearities with applications to timber structures”.

Lars Wollebæk, 2005:74, ISBN 82-471-7050-5 (printed version), ISBN 82-471-7019-1 (electronic version), ISSN 1503-8181.

“Pedestrian induced lateral vibrations of slender footbridges”.

Anders Rönnquist, 2005:102, ISBN 82-471-7082-5 (printed version), ISBN 82-471-7081-7 (electronic version), ISSN 1503-8181.

“Initial Strength Development of Fly Ash and Limestone Blended Cements at Various Temperatures Predicted by Ultrasonic Pulse Velocity”.

Tom Ivar Fredvik, 2005:112, ISBN 82-471-7105-8 (printed version), ISBN 82-471-7103-1 (electronic version), ISSN 1503-8181.

“Behaviour and modelling of thin-walled cast components”.

Cato Dørum, 2005:128, ISBN 82-471-7140-6 (printed version), ISBN 82-471-7139-2 (electronic version), ISSN 1503-8181.

- “Behaviour and modelling of selfpiercing riveted connections”,
Raffaele Porcaro, 2005:165, ISBN 82-471-7219-4 (printed version), ISBN 82-471-7218-6 (electronic version), ISSN 1503-8181.
- ”Behaviour and Modelling of Aluminium Plates subjected to Compressive Load”,
Lars Rønning, 2005:154, ISBN 82-471-7169-1 (printed version), ISBN 82-471-7195-3 (electronic version), ISSN 1503-8181.
- ”Bumper beam-longitudinal system subjected to offset impact loading”,
Satyanarayana Kokkula, 2005:193, ISBN 82-471-7280-1 (printed version), ISBN 82-471-7279-8 (electronic version), ISSN 1503-8181.
- “Control of Chloride Penetration into Concrete Structures at Early Age”,
Guofei Liu, 2006:46, ISBN 82-471-7838-9 (printed version), ISBN 82-471-7837-0 (electronic version), ISSN 1503-8181.
- “Modelling of Welded Thin-Walled Aluminium Structures”,
Ting Wang, 2006:78, ISBN 82-471-7907-5 (printed version), ISBN 82-471-7906-7 (electronic version), ISSN 1503-8181.
- ”Time-variant reliability of dynamic systems by importance sampling and probabilistic analysis of ice loads”,
Anna Ivanova Olsen, 2006:139, ISBN 82-471-8041-3 (printed version), ISBN 82-471-8040-5 (electronic version), ISSN 1503-8181.
- “Fatigue life prediction of an aluminium alloy automotive component using finite element analysis of surface topography”,
Sigmund Kyrre Ås, 2006:25, ISBN 82-471-7791-9 (printed version), ISBN 82-471-7791-9 (electronic version), ISSN 1503-8181.
- ”Constitutive models of elastoplasticity and fracture for aluminium alloys under strain path change”,
Dasharatha Achani, 2006:76, ISBN 82-471-7903-2 (printed version), ISBN 82-471-7902-4 (electronic version), ISSN 1503-8181.
- “Simulations of 2D dynamic brittle fracture by the Element-free Galerkin method and linear fracture mechanics”,
Tommy Karlsson, 2006:125, ISBN 82-471-8011-1 (printed version), ISBN 82-471-8010-3 (electronic version), ISSN 1503-8181.
- “Penetration and Perforation of Granite Targets by Hard Projectiles”,
Chong Chiang Seah, 2006:188, ISBN 82-471-8150-9 (printed version), ISBN 82-471-8149-5 (electronic version), ISSN 1503-8181.

“Deformations, strain capacity and cracking of concrete in plastic and early hardening phases”,

Tor Arne Hammer, 2007:234, ISBN 978-82-471-5191-4 (printed version), ISBN 978-82-471-5207-2 (electronic version), ISSN 1503-8181.

“Crashworthiness of dual-phase high-strength steel: Material and Component behaviour”, Venkatapathi Tarigopula, 2007:230, ISBN 82-471-5076-4 (printed version), ISBN 82-471-5093-1 (electronic version), ISSN 1503-8181.

“Fibre reinforcement in load carrying concrete structures”,

Åse Lyslo Døssland, 2008:50, ISBN 978-82-471-6910-0 (printed version), ISBN 978-82-471-6924-7 (electronic version), ISSN 1503-8181.

“Low-velocity penetration of aluminium plates”,

Frode Grytten, 2008:46, ISBN 978-82-471-6826-4 (printed version), ISBN 978-82-471-6843-1 (electronic version), ISSN 1503-8181.

“Robustness studies of structures subjected to large deformations”,

Ørjan Fyllingen, 2008:24, ISBN 978-82-471-6339-9 (printed version), ISBN 978-82-471-6342-9 (electronic version), ISSN 1503-8181.

“Constitutive modelling of morsellised bone”,

Knut Birger Lunde, 2008:92, ISBN 978-82-471-7829-4 (printed version), ISBN 978-82-471-7832-4 (electronic version), ISSN 1503-8181.

“Experimental Investigations of Wind Loading on a Suspension Bridge Girder”,

Bjørn Isaksen, 2008:131, ISBN 978-82-471-8656-5 (printed version), ISBN 978-82-471-8673-2 (electronic version), ISSN 1503-8181.

“Cracking Risk of Concrete Structures in The Hardening Phase”,

Guomin Ji, 2008:198, ISBN 978-82-471-1079-9 (printed version), ISBN 978-82-471-1080-5 (electronic version), ISSN 1503-8181.

“Modelling and numerical analysis of the porcine and human mitral apparatus”,

Victorien Emile Prot, 2008:249, ISBN 978-82-471-1192-5 (printed version), ISBN 978-82-471-1193-2 (electronic version), ISSN 1503-8181.

“Strength analysis of net structures”,

Heidi Moe, 2009:48, ISBN 978-82-471-1468-1 (printed version), ISBN 978-82-471-1469-8 (electronic version), ISSN 1503-8181.

“Numerical analysis of ductile fracture in surface cracked shells”,

Espen Berg, 2009:80, ISBN 978-82-471-1537-4 (printed version), ISBN 978-82-471-1538-1 (electronic version), ISSN 1503-8181.

“Subject specific finite element analysis of bone – for evaluation of the healing of a leg lengthening and evaluation of femoral stem design”,
Sune Hansborg Pettersen, 2009:99, ISBN 978-82-471-1579-4 (printed version), ISBN 978-82-471-1580-0 (electronic version), ISSN 1503-8181.

“Evaluation of fracture parameters for notched multi-layered structures”,
Lingyun Shang, 2009:137, ISBN 978-82-471-1662-3 (printed version), ISBN 978-82-471-1663-0 (electronic version), ISSN 1503-8181.

“Modelling of Dynamic Material Behaviour and Fracture of Aluminium Alloys for Structural Applications”
Yan Chen, 2009:69, ISBN 978-82-471-1515-2 (printed version), ISBN 978-82-471-1516-9 (electronic version), ISSN 1503-8181.

“Nanomechanics of polymer and composite particles”
Jianying He 2009:213, ISBN 978-82-471-1828-3 (printed version), ISBN 978-82-471-1829-0 (electronic version), ISSN 1503-8181.

“Mechanical properties of clear wood from Norway spruce”
Kristian Berbohm Dahl 2009:250, ISBN 978-82-471-1911-2 (printed version) ISBN 978-82-471-1912-9 (electronic version), ISSN 1503-8181.

“Modeling of the degradation of TiB₂ mechanical properties by residual stresses and liquid Al penetration along grain boundaries”
Micol Pezzotta 2009:254, ISBN 978-82-471-1923-5 (printed version) ISBN 978-82-471-1924-2 (electronic version) ISSN 1503-8181.

“Effect of welding residual stress on fracture”
Xiabo Ren 2010:77, ISBN 978-82-471-2115-3 (printed version) ISBN 978-82-471-2116-0 (electronic version), ISSN 1503-8181.

“Pan-based carbon fiber as anode material in cathodic protection system for concrete structures”
Mahdi Chini 2010:122, ISBN 978-82-471-2210-5 (printed version) ISBN 978-82-471-2213-6 (electronic version), ISSN 1503-8181.

“Structural Behaviour of deteriorated and retrofitted concrete structures”
Irina Vasilijeva Sæther 2010:171, ISBN 978-82-471-2315-7 (printed version) ISBN 978-82-471-2316-4 (electronic version) ISSN 1503-8181.

“Prediction of local snow loads on roofs”
Vivian Meløysund 2010:247, ISBN 978-82-471-2490-1 (printed version) ISBN 978-82-471-2491-8 (electronic version) ISSN 1503-8181.

“Behaviour and modelling of polymers for crash applications”
Virgile Delhaye 2010:251, ISBN 978-82-471-2501-4 (printed version) ISBN 978-82-471-2502-1 (electronic version) ISSN 1503-8181.

“Blended cement with reduced CO₂ emission – Utilizing the Fly Ash-Limestone Synergy”,
Klaartje De Weerd 2011:32, ISBN 978-82-471-2584-7 (printed version) ISBN 978-82-471-2584-4 (electronic version) ISSN 1503-8181.

“Chloride induced reinforcement corrosion in concrete” Concept of critical chloride content – methods and mechanisms.
Ueli Angst 2011:113, ISBN 978-82-471-2769-9 (printed version) ISBN 978-82-471-2763-6 (electronic version) ISSN 1503-8181.

“A thermo-electric-Mechanical study of the carbon anode and contact interface for Energy savings in the production of aluminium”.
Dag Herman Andersen 2011:157, ISBN 978-82-471-2859-6 (printed version) ISBN 978-82-471-2860-2 (electronic version) ISSN 1503-8181.

“Structural Capacity of Anchorage Ties in Masonry Veneer Walls Subjected to Earthquake”. The implications of Eurocode 8 and Eurocode 6 on a typical Norwegian veneer wall.
Ahmed Mohamed Yousry Hamed 2011:181, ISBN 978-82-471-2911-1 (printed version) ISBN 978-82-471-2912-8 (electronic ver.) ISSN 1503-8181.

“Work-hardening behaviour in age-hardenable Al-Zn-Mg(-Cu) alloys”.
Ida Westermann , 2011:247, ISBN 978-82-471-3056-8 (printed ver.) ISBN 978-82-471-3057-5 (electronic ver.) ISSN 1503-8181.

“Behaviour and modelling of selfpiercing riveted connections using aluminium rivets”.
Nguyen-Hieu Hoang, 2011:266, ISBN 978-82-471-3097-1 (printed ver.) ISBN 978-82-471-3099-5 (electronic ver.) ISSN 1503-8181.

“Fibre reinforced concrete”.
Sindre Sandbakk, 2011:297, ISBN 978-82-471-3167-1 (printed ver.) ISBN 978-82-471-3168-8 (electronic ver) ISSN 1503:8181.

“Dynamic behaviour of cablesupported bridges subjected to strong natural wind”.
Ole Andre Øiseth, 2011:315, ISBN 978-82-471-3209-8 (printed ver.) ISBN 978-82-471-3210-4 (electronic ver.) ISSN 1503-8181.

“Constitutive modeling of solargrade silicon materials”
Julien Cochard, 2011:307, ISBN 978-82-471-3189-3 (printed ver). ISBN 978-82-471-3190-9 (electronic ver.) ISSN 1503-8181.

“Constitutive behavior and fracture of shape memory alloys”
Jim Stian Olsen, 2012:57, ISBN 978-82-471-3382-8 (printed ver.) ISBN 978-82-471-3383-5 (electronic ver.) ISSN 1503-8181.

“Field measurements in mechanical testing using close-range photogrammetry and digital image analysis”

Egil Fagerholt, 2012:95, ISBN 978-82-471-3466-5 (printed ver.) ISBN 978-82-471-3467-2 (electronic ver.) ISSN 1503-8181.

“Towards a better understanding of the ultimate behaviour of lightweight aggregate concrete in compression and bending”

Håvard Nedrelid, 2012:123, ISBN 978-82-471-3527-3 (printed ver.) ISBN 978-82-471-3528-0 (electronic ver.) ISSN 1503-8181.

“Numerical simulations of blood flow in the left side of the heart”

Sigrid Kaarstad Dahl, 2012:135, ISBN 978-82-471-3553-2 (printed ver.) ISBN 978-82-471-3555-6 (electronic ver.) ISSN 1503-8181.

“Moisture induced stresses in glulam”

Vanessa Angst-Nicollier, 2012:139, ISBN 978-82-471-3562-4 (printed ver.) ISBN 978-82-471-3563-1 (electronic ver.) ISSN 1503-8181.

“Biomechanical aspects of distraction osteogenesis”

Valentina La Russa, 2012:250, ISBN 978-82-471-3807-6 (printed ver.) ISBN 978-82-471-3808-3 (electronic ver.) ISSN 1503-8181.

“Ductile fracture in dual-phase steel. Theoretical, experimental and numerical study”

Gaute Gruben, 2012:257, ISBN 978-82-471-3822-9 (printed ver.) ISBN 978-82-471-3823-6 (electronic ver.) ISSN 1503-8181.

“Damping in Timber Structures”

Nathalie Labonnote, 2012:263, ISBN 978-82-471-3836-6 (printed ver.) ISBN 978-82-471-3837-3 (electronic ver.) ISSN 1503-8181.

“Biomechanical modeling of fetal veins: The umbilical vein and ductus venosus bifurcation”

Paul Roger Leinan, 2012:299, ISBN 978-82-471-3915-8 (printed ver.) ISBN 978-82-471-3916-5 (electronic ver.) ISSN 1503-8181.

“Large-Deformation behaviour of thermoplastics at various stress states”

Anne Serine Ognedal, 2012:298, ISBN 978-82-471-3913-4 (printed ver.) ISBN 978-82-471-3914-1 (electronic ver.) ISSN 1503-8181.

“Hardening accelerator for fly ash blended cement”

Kien Dinh Hoang, 2012:366, ISBN 978-82-471-4063-5 (printed ver.) ISBN 978-82-471-4064-2 (electronic ver.) ISSN 1503-8181.

“From molecular structure to mechanical properties”

Jiayang Wu, 2013:186, ISBN 978-82-471-4485-5 (printed ver.) ISBN 978-82-471-4486-2 (electronic ver.) ISSN 1503-8181.

“Experimental and numerical study of hybrid concrete structures”

Linn Grepstad Nes, 2013:259, ISBN 978-82-471-4644-6 (printed ver.) ISBN 978-82-471-4645-3 (electronic ver.) ISSN 1503-8181.

“Mechanics of ultra-thin multi crystalline silicon wafers”

Saber Saffar, 2013:199, ISBN 978-82-471-4511-1 (printed ver.) ISBN 978-82-471-4513-5 (electronic ver.) ISSN 1503-8181.

“Through process modelling of welded aluminium structures”

Anizahyati Alisibramulisi, 2013:325, ISBN 978-82-471-4788-7 (printed ver.) ISBN 978-82-471-4789-4 (electronic ver.) ISSN 1503-8181.

“Combined blast and fragment loading on steel plates”

Knut Gaarder Rakvåg, 2013:361, ISBN 978-82-471-4872-3 (printed ver.) ISBN 978-82-4873-0 (electronic ver.) ISSN 1503-8181.

“Characterization and modelling of the anisotropic behaviour of high-strength aluminium alloy”

Marion Fourmeau, 2014:37, ISBN 978-82-326-0008-3 (printed ver.) ISBN 978-82-326-0009-0 (electronic ver.) ISSN 1503-8181.

“Behaviour of threaded steel fasteners at elevated deformation rates”

Henning Fransplass, 2014:65, ISBN 978-82-326-0054-0 (printed ver.) ISBN 978-82-326-0055-7 (electronic ver.) ISSN 1503-8181.

“Sedimentation and Bleeding”

Ya Peng, 2014:89, ISBN 978-82-326-0102-8 (printed ver.) ISBN 978-82-326-0103-5 (electronic ver.) ISSN 1503-8181.

“Impact against X65 offshore pipelines”

Martin Kristoffersen, 2014:362, ISBN 978-82-326-0636-8 (printed ver.) ISBN 978-82-326-0637-5 (electronic ver.) ISSN 1503-8181.

“Formability of aluminium alloy subjected to prestrain by rolling”

Dmitry Vysochinskiy, 2014:363, ISBN 978-82-326-0638-2 (printed ver.) ISBN 978-82-326-0639-9 (electronic ver.) ISSN 1503-8181.

“Experimental and numerical study of Yielding, Work-Hardening and anisotropy in textured AA6xxx alloys using crystal plasticity models”

Mikhail Khadyko, 2015:28, ISBN 978-82-326-0724-2 (printed ver.) ISBN 978-82-326-0725-9 (electronic ver.) ISSN 1503-8181.

“Behaviour and Modelling of AA6xxx Aluminium Alloys Under a Wide Range of Temperatures and Strain Rates”

Vincent Vilamosa, 2015:63, ISBN 978-82-326-0786-0 (printed ver.) ISBN 978-82-326-0787-7 (electronic ver.) ISSN 1503-8181.

“A Probabilistic Approach in Failure Modelling of Aluminium High Pressure Die-Castings”

Octavian Knoll, 2015:137, ISBN 978-82-326-0930-7 (printed ver.) ISBN 978-82-326-0931-4 (electronic ver.) ISSN 1503-8181.

“Ice Abrasion on Marine Concrete Structures”

Egil Møen, 2015:189, ISBN 978-82-326-1034-1 (printed ver.) ISBN 978-82-326-1035-8 (electronic ver.) ISSN 1503-8181.

“Fibre Orientation in Steel-Fibre-Reinforced Concrete”

Giedrius Zirgulis, 2015:229, ISBN 978-82-326-1114-0 (printed ver.) ISBN 978-82-326-1115-7 (electronic ver.) ISSN 1503-8181.

“Effect of spatial variation and possible interference of localised corrosion on the residual capacity of a reinforced concrete beam”

Mohammad Mahdi Kioumars, 2015:282, ISBN 978-82-326-1220-8 (printed ver.) ISBN 978-82-1221-5 (electronic ver.) ISSN 1503-8181.

“The role of concrete resistivity in chloride-induced macro-cell corrosion”

Karla Horbostel, 2015:324, ISBN 978-82-326-1304-5 (printed ver.) ISBN 978-82-326-1305-2 (electronic ver.) ISSN 1503-8181.

“Flowable fibre-reinforced concrete for structural applications”

Elena Vidal Sarmiento, 2015:335, ISBN 978-82-326-1324-3 (printed ver.) ISBN 978-82-326-1325-0 (electronic ver.) ISSN 1503-8181.

“Development of chushed sand for concrete production with microproportioning”

Rolands Cepuritis, 2016:19, ISBN 978-82-326-1382-3 (printed ver.) ISBN 978-82-326-1383-0 (electronic ver.) ISSN 1503-8181.

“Withdrawal properties of threaded rods embedded in glued-laminated timber elements”

Haris Stamatopoulos, 2016:48, ISBN 978-82-326-1436-3 (printed ver.) ISBN 978-82-326-1437-0 (electronic ver.) ISSN 1503-8181.

“An Experimental and numerical study of thermoplastics at large deformation”

Marius Andersen, 2016:191, ISBN 978-82-326-1720-3 (printed ver.) ISBN 978-82-326-1721-0 (electronic ver.) ISSN 1503-8181.

“Modeling and Simulation of Ballistic Impact”

Jens Kristian Holmen, 2016:240, ISBN 978-82-326-1818-7 (printed ver.) ISBN 978-82-326-1819-4 (electronic ver.) ISSN 1503-8181.

“Early age crack assessment of concrete structures”

Anja B. Estensen Klausen, 2016:256, ISBN 978-82-326-1850-7 (printed ver.) ISBN 978-82-326-1851-4 (electronic ver.) ISSN 1503-8181.

- “Uncertainty quantification and sensitivity analysis for cardiovascular models”
Vinzencz Gregor Eck, 2016:234, ISBN 978-82-326-1806-4 (printed ver.) ISBN 978-82-326-1807-1 (electronic ver.) ISSN 1503-8181.
- “Dynamic behaviour of existing and new railway catenary systems under Norwegian conditions”
Petter Røe Nàvik, 2016:298, ISBN 978-82-326-1935-1 (printed ver.) ISBN 978-82-326-1934-4 (electronic ver.) ISSN 1503-8181.
- “Mechanical behaviour of particle-filled elastomers at various temperatures”
Arne IIseng, 2016:295, ISBN 978-82-326-1928-3 (printed ver.) ISBN 978-82-326-1929-0 (electronic ver.) ISSN 1503-8181.
- “Nanotechnology for Anti-Icing Application”
Zhiwei He, 2016:348, ISBN 978-82-326-2038-8 (printed ver.) ISBN 978-82-326-2019-5 (electronic ver.) ISSN 1503-8181.
- “Conduction Mechanisms in Conductive Adhesives with Metal-Coated Polymer Spheres”
Sigurd Rolland Pettersen, 2016:349, ISBN 978-82-326-2040-1 (printed ver.) ISBN 978-82-326-2041-8 (electronic ver.) ISSN 1503-8181.
- “The interaction between calcium lignosulfonate and cement”
Alessia Colombo, 2017:20, ISBN 978-82-326-2122-4 (printed ver.) ISBN 978-82-326-2123-1 (electronic ver.) ISSN 1503-8181.
- “Behaviour and Modelling of Flexible Structures Subjected to Blast Loading”
Vegard Aune, 2017:101, ISBN 978-82-326-2274-0 (printed ver.) ISBN 978-82-326-2275-7 (electronic ver.) ISSN 1503-8181.
- “Behaviour of steel connections under quasi-static and impact loading”
Erik Løhre Grimsmo, 2017:159, ISBN 978-82-326-2390-7 (printed ver.) ISBN 978-82-326-2391-4 (electronic ver.) ISSN 1503-8181.
- “An experimental and numerical study of cortical bone at the macro and Nano-scale”
Masoud Ramenzanzadehkoldeh, 2017:208, ISBN 978-82-326-2488-1 (printed ver.) ISBN 978-82-326-2489-8 (electronic ver.) ISSN 1503-8181.
- “Optoelectrical Properties of a Novel Organic Semiconductor: 6,13-Dichloropentacene”
Mao Wang, 2017:130, ISBN 978-82-326-2332-7 (printed ver.) ISBN 978-82-326-2333-4 (electronic ver.) ISSN 1503-8181.
- “Core-shell structured microgels and their behavior at oil and water interface”
Yi Gong, 2017:182, ISBN 978-82-326-2436-2 (printed ver.) ISBN 978-82-326-2437-9 (electronic ver.) ISSN 1503-8181.

“Aspects of design of reinforced concrete structures using nonlinear finite element analyses”

Morten Engen, 2017:149, ISBN 978-82-326-2370-9 (printed ver.) ISBN 978-82-326-2371-6 (electronic ver.) ISSN 1503-8181.

“Numerical studies on ductile failure of aluminium alloys”

Lars Edvard Dæhli, 2017:284, ISBN 978-82-326-2636-6 (printed ver.) ISBN 978-82-326-2637-3 (electronic ver.) ISSN 1503-8181.

“Modelling and Assessment of Hydrogen Embrittlement in Steels and Nickel Alloys”

Haiyang Yu, 2017:278, ISBN 978-82-326-2624-3 (printed. ver.) ISBN 978-82-326-2625-0 (electronic ver.) ISSN 1503-8181.

“Network arch timber bridges with light timber deck on transverse crossbeams”

Anna Weronika Ostrycharczyk, 2017:318, ISBN 978-82-326-2704-2 (printed ver.) ISBN 978-82-326-2705-9 (electronic ver.) ISSN 1503-8181.

“Splicing of Large Glued Laminated Timber Elements by Use of Long Threaded Rods”

Martin Cepelka, 2017:320, ISBN 978-82-326-2708-0 (printed ver.) ISBN 978-82-326-2709-7 (electronic ver.) ISSN 1503-8181.

“Thermomechanical behaviour of semi-crystalline polymers: experiments, modelling and simulation”

Joakim Johnsen, 2017-317, ISBN 978-82-326-2702-8 (printed ver.) ISBN 978-82-326-2703-5 (electronic ver.) ISSN 1503-8181.

“Small-Scale Plasticity under Hydrogen Environment”

Kai Zhao, 2017:356, ISBN 978-82-326-2782-0 (printed ver.) ISBN 978-82-326-2783-7 (electronic er.) ISSN 1503-8181.

“Risk and Reliability Based Calibration of Structural Design Codes”

Michele Baravalle, 2017:342, ISBN 978-82-326-2752-3 (printed ver.) ISBN 978-82-326-2753-0 (electronic ver.) ISSN 1503-8181.

“Dynamic behaviour of floating bridges exposed to wave excitation”

Knut Andreas Kvåle, 2017:365, ISBN 978-82-326-2800-1 (printed ver.) ISBN 978-82-326-2801-8 (electronic ver.) ISSN 1503-8181.

“Dolomite calcined clay composite cement – hydration and durability”

Alisa Lydia Machner, 2018:39, ISBN 978-82-326-2872-8 (printed ver.). ISBN 978-82-326-2873-5 (electronic ver.) ISSN 1503-8181.

“Modelling of the self-excited forces for bridge decks subjected to random motions: an experimental study”

Bartosz Siedziako, 2018:52, ISBN 978-82-326-2896-4 (printed ver.). ISBN 978-82-326-2897-1 (electronic ver.) ISSN 1503-8181.

“A probabilistic-based methodology for evaluation of timber facade constructions”
Klodian Gradeci, 2018:69, ISBN 978-82-326-2928-2 (printed ver.) ISBN 978-82-326-2929-9 (electronic ver.) ISSN 1503-8181.

“Behaviour and modelling of flow-drill screw connections”
Johan Kolstø Sønstabø, 2018:73, ISBN 978-82-326-2936-7 (printed ver.) ISBN 978-82-326-2937-4 (electronic ver.) ISSN 1503-8181.

“Full-scale investigation of the effects of wind turbulence characteristics on dynamic behavior of long-span cable-supported bridges in complex terrain”
Aksel Fenerci, 2018:100, ISBN 978-82-326-2990-9 (printed ver.) ISBN 978-82-326-2991-6 (electronic ver.) ISSN 1503-8181.

“Modeling and simulation of the soft palate for improved understanding of the obstructive sleep apnea syndrome”
Hongliang Liu, 2018:101, ISBN 978-82-326-2992-3 (printed ver.) ISBN 978-82-326-2993-0 (electronic ver.) ISSN 1503-8181.

“Long-term extreme response analysis of cable-supported bridges with floating pylons subjected to wind and wave loads”
Yuwang Xu, 2018:229, ISBN 978-82-326-3248-0 (printed ver.) ISBN 978-82-326-3249-7 (electronic ver.) ISSN 1503-8181.

“Reinforcement corrosion in carbonated fly ash concrete”
Andres Belda Revert, 2018:230, ISBN 978-82-326-3250-3 (printed ver.) ISBN 978-82-326-3251-0 (electronic ver.) ISSN 1503-8181.

“Direct finite element method for nonlinear earthquake analysis of concrete dams including dam-water-foundation rock interaction”
Arnkjell Løkke, 2018:252, ISBN 978-82-326-3294-7 (printed ver.) ISBN 978-82-326-3295-4 (electronic ver.) ISSN 1503-8181.

“Electromechanical characterization of metal-coated polymer spheres for conductive adhesives”
Molly Strimbeck Bazilchuk, 2018:295, ISBN 978-82-326-3380-7 (printed. ver.) ISBN 978-82-326-3381-4 (electrical ver.) ISSN 1503-8181.

“Determining the tensile properties of Arctic materials and modelling their effects on fracture”
Shengwen Tu, 2018:269, ISBN 978-82-326-3328-9 (printed ver.) ISBN 978-82-326-3329-6 (electronic ver.) ISSN 1503-8181.

“Atomistic Insight into Transportation of Nanofluid in Ultra-confined Channel”
Xiao Wang, 2018:334, ISBN 978-82-326-3456-9 (printed ver.) ISBN 978-82-326-3457-6 (electronic ver.) ISSN 1503-8181.

“An experimental and numerical study of the mechanical behaviour of short glass-fibre reinforced thermoplastics”.

Jens Petter Henrik Holmstrøm, 2019:79, ISBN 978-82-326-3760-7 (printed ver.) ISBN 978-82-326-3761-4 (electronic ver.) ISSN 1503-8181.

“Uncertainty quantification and sensitivity analysis informed modeling of physical systems”

Jacob Sturdy, 2019:115, ISBN 978-82-326-3828-4 (printed ver.) ISBN 978-82-326-3829-1 (electronic ver.) ISSN 1503-8181.

“Load model of historic traffic for fatigue life estimation of Norwegian railway bridges”

Gunnstein T. Frøseth, 2019:73, ISBN 978-82-326-3748-5 (printed ver.) ISBN 978-82-326-3749-2 (electronic ver.) ISSN 1503-8181.

“Force identification and response estimation in floating and suspension bridges using measured dynamic response”

Øyvind Wiig Petersen, 2019:88, ISBN 978-82-326-3778-2 (printed ver.) ISBN 978-82-326-3779-9 (electronic ver.) ISSN 1503-8181.

“Consistent crack width calculation methods for reinforced concrete elements subjected to 1D and 2D stress states”

Reignard Tan, 2019:147, ISBN 978-82-326-3892-5 (printed ver.) ISBN 978-82-326-3893-2 (electronic ver.) ISSN 1503-8181.

“Nonlinear static and dynamic isogeometric analysis of slender spatial and beam type structures”

Siv Bente Raknes, 2019:181, ISBN 978-82-326-3958-8 (printed ver.) ISBN 978-82-326-3959-5 (electronic ver.) ISSN 1503-8181.

“Experimental study of concrete-ice abrasion and concrete surface topography modification”

Guzel Shamsutdinova, 2019:182, ISBN 978-82-326-3960-1 (printed ver.) ISBN 978-82-326-3961-8 (electronic ver.) ISSN 1503-8181.

“Wind forces on bridge decks using state-of-the art FSI methods”

Tore Andreas Helgedagsrud, 2019:180, ISBN 978-82-326-3956-4 (printed ver.) ISBN 978-82-326-3957-1 (electronic ver.) ISSN 1503-8181.

“Numerical Study on Ductile-to-Brittle Transition of Steel and its Behavior under Residual Stresses”

Yang Li, 2019:227, ISBN 978-82-326-4050-8 (printed ver.) ISBN 978-82-326-4015-5 (electronic ver.) ISSN 1503-8181.

“Micromechanical modelling of ductile fracture in aluminium alloys”

Bjørn Håkon Frodal, 2019:253, ISBN 978-82-326-4102-4 (printed ver.) ISBN 978-82-326-4103-1 (electronic ver.) ISSN 1503-8181.

“Monolithic and laminated glass under extreme loading: Experiments, modelling and simulations”

Karoline Osnes, 2019:304, ISBN 978-82-326-4204-5 (printed ver.) ISBN 978-82-326-4205-2 (electronic ver.) ISSN 1503-8181.

“Plastic flow and fracture of isotropic and anisotropic 6000-series aluminium alloys: Experiments and numerical simulations “

Susanne Thomesen, 2019:312, ISBN 978-82-326-4220-5 (printed ver.), ISBN 978-82-326-4221-2 (electronic ver.) ISSN 1503-8181

“Stress-laminated timber decks in bridges”

Francesco Mirko Massaro, 2019:346, ISBN 978-82-326-4288-5 (printed ver.), ISBN 978-82-326-4289-2 (electronic ver.) ISSN 1503-8181

“Connections between steel and aluminium using adhesive bonding combined with self-piercing riveting: Testing, modelling and analysis”

Matthias Reil, 2019:319, ISBN 978-82-326-4234-2 (printed ver.), ISBN 978-82-326-4235-9 (electronic ver.) ISSN 1503-8181

“Designing Polymeric Icephobic Materials”

Yizhi Zhuo, 2019:345, ISBN 978-82-326-4286-1 (printed ver.), ISBN 978-82-326-4287-8 (electronic ver.) ISSN 1503-8181

“Fundamental Mechanisms of Ice Adhesion”

Rønneberg, Sigrid 2020:87, ISBN 978-82-326-4527-8 (printed version) ISBN 978-82-326-4524-5 (electronic version) ISSN 1503-8181

“Mechanical modeling of the polymeric coating on a subsea pipeline” Vestrum, Ole 2020:105, ISBN 978-82-326-4562-6 (printed version) ISBN 978-82-4563-3 (electronic version) ISSN 1503-8181

“Conceptual form-finding in structural engineering” Marcin Luczkowski 2020: “Self-assembled superstructures of magnetic nanoparticles: advanced nanofabrication and enhanced mechanical properties”

“Self-assembled superstructures of magnetic nanoparticles: advanced nanofabrication and enhanced mechanical properties” Verner Håkonsen 2020:271, ISBN 978-82-326-4890-0 (printed version) ISBN 978-82-326-4891-7 (electronic version) ISSN 1503-8181

“Micromechanical modelling of fracture in ductile alloys with applications to high-strength steel”

Sondre Bergo 2020:313, ISBN 978-82-326-4974-7 (printed version) ISBN 978-82-326-4975-4 (electronic version) ISSN 1503-8181

“Fracture in wood of Norway spruce - Experimental and numerical study”
Katarzyna Ostapska 2020:314, ISBN 978-82-326-4976-1 (printed version) ISBN 978- 82-326-4977-8 (electronic version) ISSN 1503-8181

“Dynamic anti-icing surfaces (DAIS)” Feng Wang 2020:330 ISBN 978-82-326-5006-4 (printed version) ISBN 978-82-326-5007-1 (electronic version) ISSN 1503-8181

“«Multiaxial Fatigue analysis of offshore mooring chains, considering the effects of residual stresses and corrosion pits» Ershad P. Zarandi 2020:337 ISBN 978-82-326-5020-0 (printed version) ISBN 978-82-326-5021-7 (electronic version) ISSN 1503-8181

“Production and documentation of frost durable high-volume fly ash concrete: air entrainment, cracking and scaling in performance testing” Andrei Shpak 2020:366 ISBN 978-82-326-5078-1 (printed version) ISBN 978-82-326-5079-8 (electronic version) ISSN 1503-8181

“Physics-based and data-driven reduced-order blood flow models: Applications to coronary artery disease diagnostics” Fredrik Eikeland Fossan 2020:362 ISBN 978-82-326-5070-5 (printed version) ISBN 978-82-326-5071-2 (electronic version) ISSN 1503-8181

“Multi-scale modelling and simulation of ductile failure in aluminium structures” Henrik Granum 2020:374 ISBN 978-82-326-5094-1 (printed version) ISBN 978-82-326-5095-8 (electronic version) ISSN 1503-8181

“Testing and modelling of multi-material joints” Jon Fredrick Berntsen 2020:368 ISBN 978-82-326-5082-8 (printed version) ISBN 978-82-326-5083-5 ISSN 1503-8181

“Heuristic models for wear prediction and dynamic-based condition monitoring techniques in pantograph-catenary interaction” Stefano Derosa 2020:381 ISBN 978-82-326-5108-5 (printed version) ISBN 978-82-326-5109-2 (electronic version) ISSN 1503-8181

“Experimental and numerical study of dilation in mineral filled PVC” Sindre Nordmark Olufsen 2020:388 ISBN 978-82-326-5122-1 (printed version) ISBN 978-82-326-5123-8 (electronic version) ISSN 1503-8181

“Residual stresses and dimensional deviation in metal additive manufacturing: prediction and mitigation methods” Li Sun 2020:411 ISBN 978-82-471-9600-7 (printed version) ISBN 978-82-471-9581-9 (electronic version) ISSN 1503-8181 (printed version) ISSN 2703-8084 (online version)

“Moment-resisting timber frames with semi-rigid connections” Aivars Vilguts 2021:88 ISBN 978-82-326-6987 (printed version) ISBN 978-82-326-5737-7 (electronic version) ISSN 2703-8084 (online version)

“Thermal transport in metal-polymer systems” Susanne Sandell 2021:63 ISBN 978-82-326-5304-1 (printed version) ISBN 978-82-326-6278-4 (electronic version) ISSN 2703-8084 (online version)

“Competitive timber floors” Sveinung Ørjan Nesheim 2021:134 ISBN 978-82-326-6481-8 (printed version) ISBN 978-82-326-5399-7 (electronic version) ISSN 2703-8084

“Thermodynamics of Nanoscale Films and Fluid Volumes” Bjørn Andre Strøm 2021:166 ISBN 978-82-326-6778-9 (printed version) ISBN 978-82-326-5900-5 (electronic version) ISSN 2703-8084 (online version)

“Characterization and modeling of the mechanical behavior of polymer foam” Daniel Thor Morton 2021:173 ISBN 978-82-326-6245-6 (printed version) ISBN 978-82-326-5699-8 (electronic version) ISSN 2703-8084 (online version)

“Atomistic Insights to Interfacial Dynamics” Yuequn Fu 2021:233 ISBN 978-82-326-5530-4 (printed version) ISBN 978-82-326-6894-6 (electronic version) ISSN 2703-8084 (online version)

“Mechanisms and enhancement of CO₂ condensation heat transfer” Ingrid Snustad 2021:236 ISBN 978-82-326-5606-6 ISBN 978-82-236-6715-4 (electronic version) ISSN 2703-8084

“Experimental study of reinforced concrete slabs subjected to fire exposure and blast loading” Assis Arano Barenys 2021:239 ISBN 978-82-326-5289-1 ISBN 978-82-326-5876-3 (electronic version) ISSN 2703-8084 (online version)

“Long-term extreme buffeting response investigations for long-span bridges considering uncertain turbulence parameters based on field measurements” Tor Martin Lystad 2021:216 ISBN 978-82-326-5797-1 (printed version) ISBN 978-82-326-6154-1 (electronic version) ISSN 2703-8084 (online version)

“Development and Application of a Vision-Based System for Structural Monitoring of Railway Catenary System” Tengjiao Jiang 2021:280 ISBN 978-82-326-6866-3 (printed ver.) ISBN 978-82-326-5778-0 (electronic ver.) ISSN 1503-8181 (online ver.)

ISBN 978-82-326-6608-9 (printed ver.)
ISBN 978-82-326-6954-7 (electronic ver.)
ISSN 1503-8181 (printed ver.)
ISSN 2703-8084 (online ver.)



NTNU

Norwegian University of
Science and Technology